

# **BSIM-BULK106.2.0 MOSFET Compact Model**

## **Technical Manual**

### **Authors:**

**Harshit Agarwal, Chetan Gupta, Huan-Lin Chang,  
Sourabh Khandelwal, Juan Pablo Duarte,  
Yogesh Singh Chauhan, Sayeef Salahuddin and Chenming Hu**

### **Project Director:**

**Prof. Sayeef Salahuddin and Prof. Chenming Hu**

**Department of Electrical Engineering and Computer Sciences  
University of California, Berkeley, CA 94720**

**Copyright 2017**

**The Regents of University of California  
All Right Reserved**

## **Past Developers :**

Aditya Medury, UC Berkeley  
Navid Paydavosi, UC Berkeley  
Sriramkumar Venugopalan, UC Berkeley  
Pankaj Thakur, UC Berkeley  
Mohammed A. Karim, UC Berkeley

# Contents

<b>1</b>	<b>RELEASE NOTES</b>	<b>9</b>
1.1	Updates made in BSIM-BULK106.2.0 . . . . .	9
<b>2</b>	<b>BSIM-BULK Model Equations</b>	<b>12</b>
2.1	Physical constants . . . . .	12
2.2	Effective Channel Length & Width . . . . .	13
2.3	Binning Calculations . . . . .	13
2.4	Global geometrical scaling . . . . .	14
2.5	Terminal Voltages . . . . .	19
2.6	Pinch-off Potential and Normalized Charge Calculation . . . . .	20
2.6.1	Pinch-off Potential with Poly Depletion . . . . .	20
2.6.2	Normalized Charge Density . . . . .	22
2.7	Short Channel Effects . . . . .	26
2.8	Drain Saturation Voltage . . . . .	28
2.9	Mobility degradation with vertical field . . . . .	29
2.10	Parasitic series resistance . . . . .	30
2.10.1	Bias Independent External Series Resistance, Bias Dependent Internal Resistance (RDSMOD=0) . . . . .	30
2.10.2	Bias Dependent External Series Resistance ( $R_s(V)$ & $R_d(V)$ ) . . . . .	31
2.10.3	Bias Dependent Internal Resistance (RDSMOD=2) . . . . .	31
2.10.4	Sheet resistance model . . . . .	32
2.11	Output Conductance . . . . .	32
2.12	Velocity Saturation . . . . .	34
2.13	Effective Mobility . . . . .	35
2.14	Drain Current Model . . . . .	35
2.14.1	Without Velocity Saturation . . . . .	35
2.14.2	Including Velocity Saturation . . . . .	36

2.15	Threshold Voltage Model . . . . .	38
2.15.1	Long Channel Threshold Voltage . . . . .	38
2.16	MNUD model to increase Fitting Flexibility . . . . .	39
2.17	Subthreshold Hump Module . . . . .	39
2.18	Modeling of Sub-Surface Leakage Drain Current . . . . .	40
2.19	Impact Ionization Model . . . . .	40
2.20	GIDL/GISL Current Model . . . . .	40
2.21	Gate Tunneling Current Model . . . . .	41
2.21.1	Model Selectors . . . . .	41
2.21.2	Equations for Tunneling Currents . . . . .	42
2.22	Gate resistance and Body resistance network Model . . . . .	45
2.22.1	Gate Electrode Electrode and Intrinsic-Input Resistance (IIR) Model . . . . .	45
2.22.2	Substrate Resistance Network . . . . .	47
2.23	Noise Modeling . . . . .	51
2.23.1	Flicker Noise Models . . . . .	51
2.23.2	Channel Thermal Noise . . . . .	54
2.23.3	Gate Current Shot Noise . . . . .	56
2.23.4	Resistor Noise . . . . .	57
2.24	Self Heating Model . . . . .	57
<b>3</b>	<b>Asymmetric MOS Junction Diode Models</b>	<b>57</b>
3.1	Junction Diode IV Model . . . . .	57
3.2	Junction Diode CV Model . . . . .	60
<b>4</b>	<b>Layout dependent Parasitics Models</b>	<b>62</b>
4.1	Layout-Dependent Parasitics Models . . . . .	62
4.1.1	Geometry Definition . . . . .	62
4.1.2	Model Formulation and Options . . . . .	63

<b>5</b>	<b>Temperature dependence Models</b>	<b>66</b>
5.1	Temperature Dependence Model . . . . .	66
5.1.1	Length Scaling of Temperature parameters . . . . .	66
5.1.2	Temperature Dependence of Threshold Voltage . . . . .	67
5.1.3	Temperature Dependence of Mobility . . . . .	67
5.1.4	Temperature Dependence of Saturation Velocity . . . . .	67
5.1.5	Temperature Dependence of LDD Resistance . . . . .	67
5.1.6	Temperature Dependence of Junction Diode IV . . . . .	68
5.1.7	Temperature Dependence of Junction Diode CV . . . . .	69
5.1.8	Temperature Dependences of $E_g$ and $n_i$ . . . . .	72
<b>6</b>	<b>Stress effect Model Development</b>	<b>72</b>
6.1	Stress Effect Model . . . . .	72
6.1.1	Stress Effect Model Development . . . . .	73
6.1.2	Effective SA and SB for Irregular LOD . . . . .	76
<b>7</b>	<b>Well Proximity Effect Model</b>	<b>77</b>
<b>8</b>	<b>Well Proximity Effect Model</b>	<b>77</b>
8.1	Well Proximity Effect Model . . . . .	78
<b>9</b>	<b>C-V Model</b>	<b>80</b>
<b>10</b>	<b>Parameter Extraction Procedure</b>	<b>86</b>
10.1	Extraction of Geometry Independent Parameters . . . . .	87
10.1.1	Gate Capacitance $C_{GG}$ vs. $V_G$ Analysis @ $V_S = 0 V$ , $V_D = 0 V$ & $V_B = 0 V$ . . . . .	87
10.1.2	Drain Current $I_D$ vs. $V_G$ Analysis @ $V_D = [V_{D,lin}, V_{D,sat}]$ , $V_S = 0 V$ & $V_B = 0 V$ . . . . .	88
10.1.3	Gate Current $I_G$ vs. $V_G$ Analysis @ various $V_D$ , $V_S = 0 V$ & $V_B = 0 V$	89

10.1.4	Drain Current $I_D$ vs. $V_D$ Analysis @ various $V_G$ , $V_S = 0 V$ & $V_B = 0 V$ . . . . .	90
10.1.5	Gate Capacitance $C_{GG}$ vs. $V_G$ Analysis @ $V_{DS} \neq 0 V$ & $V_B = 0 V$ . . . . .	90
10.1.6	Drain Current $I_D$ vs. $V_G$ Analysis @ $V_D = [V_{D,lin}, V_{D,sat}]$ & various $V_B$ . . . . .	90
10.1.7	Fitting Verification . . . . .	91
10.2	Extraction of Short Channel Effects & Length Scaling Parameters . . . . .	91
10.2.1	Gate Capacitance $C_{GG}$ vs. $V_G$ Analysis @ $V_S = 0 V$ , $V_D = 0 V$ & $V_B = 0 V$ . . . . .	92
10.2.2	Drain Current $I_D$ vs. $V_G$ Analysis @ $V_D = [V_{D,lin}, V_{D,sat}]$ , $V_S = 0 V$ & $V_B = 0 V$ . . . . .	92
10.2.3	$I_G$ vs. $V_G$ Analysis @ various $V_D$ , $V_S = 0 V$ & $V_B = 0 V$ . . . . .	94
10.2.4	$I_D$ vs. $V_D$ Analysis @ various $V_G$ , $V_S = 0 V$ & $V_B = 0 V$ . . . . .	94
10.2.5	$C_{GG}$ vs. $V_G$ Analysis @ $V_{DS} \neq 0 V$ & $V_B = 0 V$ . . . . .	94
10.2.6	$I_D$ vs. $V_G$ Analysis @ $V_D = [V_{D,lin}, V_{D,sat}]$ & various $V_B$ (or various $V_S$ ) . . . . .	95
10.2.7	Fitting Verification . . . . .	95
10.3	Extraction of Narrow Channel Effects & Width Scaling Parameters . . . . .	96
10.3.1	Gate Capacitance $C_{GG}$ vs. $V_G$ Analysis @ $V_S = 0 V$ , $V_D = 0 V$ & $V_B = 0 V$ . . . . .	96
10.3.2	Drain Current $I_D$ vs. $V_G$ Analysis @ $V_D = [V_{D,lin}, V_{D,sat}]$ , $V_S = 0 V$ & $V_B = 0 V$ . . . . .	96
10.3.3	Gate Current $I_G$ vs. $V_G$ Analysis @ various $V_D$ , $V_S = 0 V$ & $V_B = 0 V$ . . . . .	97
10.3.4	Gate Capacitance $C_{GG}$ vs. $V_G$ Analysis @ $V_{DS} \neq 0 V$ & $V_B = 0 V$ . . . . .	98
10.3.5	Drain Current $I_D$ vs. $V_G$ Analysis @ $V_D = [V_{D,lin}, V_{D,sat}]$ & various $V_B$ (or various $V_S$ ) . . . . .	98
10.3.6	Fitting Verification . . . . .	98
10.4	Extraction of Parameters for Narrow/Short Channel Devices . . . . .	98
10.4.1	Gate Capacitance $C_{GG}$ vs. $V_G$ Analysis @ $V_S = 0 V$ , $V_D = 0 V$ & $V_B = 0 V$ . . . . .	99

10.4.2	Drain Current $I_D$ vs. $V_G$ Analysis @ $V_D = [V_{D,lin}, V_{D,sat}]$ , $V_S = 0 V$ & $V_B = 0 V$ . . . . .	99
10.4.3	$C_{GG}$ vs. $V_G$ Analysis @ $V_{DS} \neq 0 V$ & $V_B = 0 V$ . . . . .	100
10.4.4	Drain Current $I_D$ vs. $V_G$ Analysis @ $V_D = [V_{D,lin}, V_{D,sat}]$ & various $V_B$ (or various $V_S$ ) . . . . .	100
10.4.5	Fitting Verification . . . . .	101
10.5	Extraction of Temperature Dependence Parameters . . . . .	101
10.5.1	Wide & Long Channel Devices . . . . .	101
10.5.2	Length Scaling of Wide Channel Devices . . . . .	103
<b>11</b>	<b>Instance Parameters</b>	<b>105</b>
<b>12</b>	<b>Model Controllers and Process Parameters</b>	<b>106</b>
<b>13</b>	<b>Basic Model Parameters</b>	<b>109</b>
<b>14</b>	<b>Both model and instance parameters</b>	<b>117</b>
<b>15</b>	<b>High-Speed/RF Model Parameters</b>	<b>117</b>
<b>16</b>	<b>Flicker and Thermal Noise Model Parameters</b>	<b>120</b>
<b>17</b>	<b>Layout-Dependent Parasitic Model Parameters</b>	<b>122</b>
<b>18</b>	<b>Asymmetric Source/Drain Junction Diode Model Parameters</b>	<b>123</b>
<b>19</b>	<b>Temperature Dependence and Self Heating Parameters</b>	<b>126</b>
<b>20</b>	<b>Stress Effect Model Parameters</b>	<b>128</b>
<b>21</b>	<b>Well-Proximity Effect Parameters</b>	<b>130</b>
<b>22</b>	<b>Parameters for Edge FET and Sub-Surface Leakage Current</b>	<b>131</b>

<b>23</b>	<b>Parameter equivalence between BSIM-BULK &amp; BSIM4</b>	<b>133</b>
<b>24</b>	<b>Appendix A : Smoothing Function</b>	<b>137</b>
24.1	Polynomial Smoothing . . . . .	137
<b>25</b>	<b>Acknowledgements</b>	<b>143</b>



# 1 RELEASE NOTES

## 1.1 Updates made in BSIM-BULK106.2.0

- Modified Flicker noise model which can also model the flicker noise trends for Halo transistors.
- Added modified function of  $VDSX$  to avoid negative  $G_{DS}$  issue.
- $MNUD$  model to increase flexibility in  $I_{DS} - V_{DS}$  fitting.
- Removed kink around  $V_{DS} = 0$  for  $GIDLMOD = 1$ .
- Improved Gamma behaviour in the linear Region for  $TNOIMOD = 1$ .
- Model for Sub-Surface leakage (between drain and source) added.  $FLAG - SSLMOD$ .
- Stress model added to  $EDGEFET$ .
- Added parameters for  $EDGEFET$  to control threshold voltage shift  $KVTH0EDGE$ ,  $STK2EDGE$  and  $STETA0EDGE$  while keeping their length and width parameters same as main BSIM-BULK.
- Sign correction in charge calculations.
- Parameters  $EDGEFET$  and  $DELVT0$  are made instance parameter.
- $EDGEFET$  SCE model made similar to main BSIM6 to avoid convergence at large L.
- Protection on  $DLCIG$  and  $DLCIGD$  from going negative.
- Hidden states during  $PSS$  have been resolved.

- Variables - *LOCALSCA*, *LOCALSCB* and *LOCALSCC* are initialized to avoid warnings.
- Removed clamping from *UCR*.
- Added protection to the following parameters: *LP1*, *LP2*, *NJS*, *NJD*, *XJBVS* and *XJBVD*.
- Added description for all the parameters in the Verilog-A code.
- Added *K2EDGE* parameter for  $V_{TH}$  shift with body bias for *EDGEFET*.
- Default values of Stress parameters for *EDGEFET* are set same as main parameters.
- Use limited log in fringe Capacitance Module.
- Removed hidden states in *EDGEFET* variables : *K2\_EDGE*, *ETA0\_EDGE*, *Eta\_Stress\_EDGE*.
- Added type="instance" for all instance parameters declaration in the macros definition just like in *BSIM-CMG* and *BSIM-IMG*.
- Modified Thermal noise model to tune *NF50* in Sub-threshold region and to achieve ideal trend of gamma for long channel transistors.
- Added Clamping in  $I_{GD}$  and  $I_{GS}$ .
- Added Self-Heating output variables.
- Deactivated node "T" when *RTH0* or *SHMOD* or both are zero.
- Used *SRCFLAG* as the formal argument of *BSIM6RdsEndSha* and *BSIM6RdseffGeo* in place of *TYPE*.

- Modified Calculations of Geometry-dependent source/drain resistance.
- Multiplied with  $DEVSIGN$  in the Operating point  $V_{TH}$  expression.
- Limit  $(W_{eff} + W_{TH0})$  to  $(W_{eff} + W_{TH0}) > 0$  in Self Heating module.
- Module name has changed from  $bsim6$  to  $bsimbulk$ .
- Added  $CLM$  and Velocity Saturation terms of the Charge Expressions in manual.
- Added binning in the  $EDGEFET$  parameters.
- Removed all the "ifdef" statements from the code.
- Node collapsing has been done for " $SHMOD = 0$ " and " $TNOIMOD = 0$ ". Since we had removed 'define\_TNOISW\_' and 'define\_SHMOD\_' .
- Every "IF" and "ELSE" statement starts with "begin" and ends with the "end" statement.
- Modified the name of the parameter " $MULUO$ " to " $MULU0$ ".
- Align the Stress module conditioning similar to  $BSIM4$ .
- $SCA, SCB, SCC$  and  $SC$  are allowed to take real number, instead of integer.
- $DTEMP, MULU0, DELVTO$  and  $IDS0MULT$  have modified to both instance and model parameters.
- Added units for all the parameters of  $BSIM - BULK106.2.0$  Verilog-A code and manual.

## 2 BSIM-BULK Model Equations

### 2.1 Physical constants

Physical quantities are in M.K.S units unless specified otherwise.

$$q = 1.6 \times 10^{-19} C \quad (2.1)$$

$$\epsilon_0 = 8.8542 \times 10^{-12} \frac{F}{m} \quad (2.2)$$

$$\epsilon_{sub} = EPSRSUB \cdot \epsilon_0 \frac{F}{m} \quad (2.3)$$

$$\epsilon_{ox} = EPSROX \cdot \epsilon_0 \frac{F}{m} \quad (2.4)$$

$$C_{ox} = \frac{3.9 \cdot \epsilon_0}{TOXE} \frac{F}{m^2} \quad (2.5)$$

$$\epsilon_{ratio} = \frac{EPSRSUB}{3.9} \quad (2.6)$$

$$(2.7)$$

## 2.2 Effective Channel Length & Width

$$\Delta L = LINT + \frac{LL}{(L_{new})^{LLN}} + \frac{LW}{(W_{new})^{LWN}} + \frac{LWL}{(L_{new})^{LLN} \cdot (W_{new})^{LWN}} \quad (2.8)$$

$$\Delta W = WINT + \frac{WL}{(L_{new})^{WLN}} + \frac{WW}{(W_{new})^{WWN}} + \frac{WWL}{L_{new}^{WLN} \cdot (W_{new})^{WWN}} \quad (2.9)$$

$$\Delta L_1 = LINT + \frac{LL}{(L_{new} + DLBIN)^{LLN}} + \frac{LW}{(W_{new} + DWBIN)^{LWN}} + \quad (2.10)$$

$$\frac{LWL}{(L_{new} + DLBIN)^{LLN} \cdot (W_{new} + DWBIN)^{LWN}} \quad (2.11)$$

$$\Delta W_1 = WINT + \frac{WL}{(L_{new} + DLBIN)^{WLN}} + \frac{WW}{(W_{new} + DWBIN)^{WWN}} + \quad (2.12)$$

$$\frac{WWL}{(L_{new} + DLBIN)^{WLN} \cdot (W_{new} + DWBIN)^{WWN}} \quad (2.13)$$

$$L_{new} = L * LMLT + XL; \quad (2.14)$$

$$W_{new} = \frac{W}{NF} * WMLT + XW; \quad (2.15)$$

$$\Delta L_{CV} = DLC \quad (2.16)$$

$$\Delta W_{CV} = DWC \quad (2.17)$$

$$L_{eff} = L * LMLT + XL - 2\Delta L \quad (2.18)$$

$$W_{eff} = W * WMLT + XW - 2\Delta W \quad (2.19)$$

$$L_{eff,CV} = L * LMLT + XL - 2\Delta L_{CV} \quad (2.20)$$

$$W_{eff,CV} = W * WMLT + XW - 2\Delta W_{CV} \quad (2.21)$$

$$L_{eff,Bin} = L * LMLT + XL - 2\Delta L_1 \quad (2.22)$$

$$W_{eff,Bin} = W * WMLT + XW - 2\Delta W_1 \quad (2.23)$$

## 2.3 Binning Calculations

For a given L and W, each model parameter  $PARAM_i$  is calculated as a function of PARAM, and length dependent term, LPARAM, width dependent term, WPARAM, area

dependent term, PPARAM:

$$PARAM_i = PARAM + LPARAM \cdot BINL + WPARAM \cdot BINW + PPARAM \cdot BINWL \quad (2.24)$$

BINUNIT is the binning unit selector. When BINUNIT=1,

$$BINL = \frac{1e^{-6}}{L_{eff} + DLBIN} \quad (2.25)$$

$$BINW = \frac{1e^{-6}}{W_{eff} + DWBIN} \quad (2.26)$$

when BINUNIT=0,

$$BINL = \frac{1.0}{L_{eff} + DLBIN} \quad (2.27)$$

$$BINW = \frac{1.0}{W_{eff} + DWBIN} \quad (2.28)$$

and

$$BINWL = BINL \cdot BINW \quad (2.29)$$

For the list of binable parameters, please refer to the complete parameter list at the end of this technical note.

## 2.4 Global geometrical scaling

Following scaling formulation is used in global scaling -

$$\begin{aligned} PARAM[L] = & PARAM \cdot \left[ 1 + PARAML \cdot \left( \frac{1}{L_{eff}^{PARAMLEXP}} - \frac{1}{LLONG^{PARAMLEXP}} \right) \right. \\ & + PARAMW \cdot \left( \frac{1}{W_{eff}^{PARAMWEXP}} - \frac{1}{WWIDE^{PARAMWEXP}} \right) \\ & \left. + PARAMWL \cdot \left( \frac{1}{(L_{eff} \cdot W_{eff})^{PARAMWLEXP}} \right) \right] \quad (2.30) \end{aligned}$$

LLONG is the length of extracted long channel device and WWIDE is the width for extracted wide device. They are used to ensure that scaling parameters do not affect long-wide fitting. We will not mention LLONG and WWIDE part again but all of the following scaling equation use above kind of formulation.

$$\begin{aligned}
 NDEP[L] = NDEP \cdot & \left[ 1 + NDEPL1 \cdot \frac{1}{L_{eff}^{NDEPLEXP1}} + NDEPL2 \cdot \frac{1}{L_{eff}^{NDEPLEXP2}} \right. \\
 & \left. + NDEPW \cdot \frac{1}{W_{eff}^{NDEPWEXP}} + NDEPWL \cdot \frac{1}{(L_{eff} \cdot W_{eff})^{NDEPWLEXP}} \right]
 \end{aligned}
 \tag{2.31}$$

$$\begin{aligned}
NFACTOR[L] = NFACTOR \cdot & \left[ 1 + NFACTORL \cdot \frac{1}{L_{eff}^{NFACTORLEXP}} \right. \\
& \left. + NFACTORW \cdot \frac{1}{W_{eff}^{NFACTORWEXP}} + NFACTORWL \cdot \frac{1}{(L_{eff} \cdot W_{eff})^{NFACTORWLEXP}} \right]
\end{aligned} \tag{2.32}$$

$$CDSCD[L] = CDSCD \cdot \left[ 1 + CDSCDL \cdot \frac{1}{L_{eff}^{CDSCDLEXP}} \right] \tag{2.33}$$

$$CDSCB[L] = CDSCB \cdot \left[ 1 + CDSCBL \cdot \frac{1}{L_{eff}^{CDSCBLEXP}} \right] \tag{2.34}$$

$$\text{if (MOBSCALE=0)} \tag{2.35}$$

$$U_0[L] = \begin{cases} U_0 \cdot \left[ 1 - U_0L \cdot \frac{1}{L_{eff}^{U_0LEXP}} \right] & U_0LEXP > 0 \\ U_0 \cdot [1 - U_0L] & \text{Otherwise} \end{cases} \tag{2.36}$$

$$\text{else} \tag{2.37}$$

$$U_0[L] = U_0 \cdot [1 - UP1 \cdot \exp^{-\frac{L_{eff}}{LP1}} - UP2 \cdot \exp^{-\frac{L_{eff}}{LP2}}] \tag{2.38}$$

$$UA[L] = UA \cdot \left[ 1 + UAL \cdot \frac{1}{L_{eff}^{UALEXP}} + UAW \cdot \frac{1}{W_{eff}^{UAWEXP}} + UAWL \cdot \frac{1}{(L_{eff} \cdot W_{eff})^{UAWLEXP}} \right] \tag{2.39}$$

$$EU[L] = EU \cdot \left[ 1 + EUL \cdot \frac{1}{L_{eff}^{EULEXP}} + EUW \cdot \frac{1}{W_{eff}^{EUWEXP}} + EUWL \cdot \frac{1}{(L_{eff} \cdot W_{eff})^{EUWLEXP}} \right] \tag{2.40}$$

$$UD[L] = UD \cdot \left[ 1 + UDL \cdot \frac{1}{L_{eff}^{UDLEXP}} \right] \tag{2.41}$$

$$UC[L] = UC \cdot \left[ 1 + UCL \cdot \frac{1}{L_{eff}^{UCLEXP}} + UCW \cdot \frac{1}{W_{eff}^{UCWEXP}} + UCWL \cdot \frac{1}{(L_{eff} \cdot W_{eff})^{UCWLEXP}} \right] \tag{2.42}$$

$$ETA0[L] = ETA0 \cdot \left[ \frac{1}{L_{eff}^{DSUB}} \right] \tag{2.43}$$

$$ETAB[L] = ETAB \cdot \left[ \frac{1}{L_{eff}^{ETABEXP}} \right] \tag{2.44}$$

$$PDIBLC[L] = PDIBLC \cdot \left[ 1 + PDIBLCL \cdot \frac{1}{L_{eff}^{PDIBLCLEXP}} \right] \tag{2.45}$$

$$DELTA[L] = DELTA \cdot \left[ 1 + DELTAL \cdot \frac{1}{L_{eff}^{DELTALEXP}} \right] \tag{2.46}$$



$$FPROUT[L] = FPROUT \cdot \left[ 1 + FPROUTL \cdot \frac{1}{L_{eff}^{FPROUTLEXP}} \right] \quad (2.47)$$

$$PCLM[L] = PCLM \cdot \left[ 1 + PCLML \cdot \frac{1}{L_{eff}^{PCLMLEXP}} \right] \quad (2.48)$$

$$VSAT[L] = VSAT \cdot \left[ 1 + VSATL \cdot \frac{1}{L_{eff}^{VSATLEXP}} + VSATW \cdot \frac{1}{W_{eff}^{VSATWEXP}} \right. \\ \left. + VSATWL \cdot \frac{1}{(L_{eff} \cdot W_{eff})^{VSATWLEXP}} \right] \quad (2.49)$$

$$PSAT[L] = PSAT \cdot \left[ 1 + PSATL \cdot \frac{1}{L_{eff}^{PSATLEXP}} \right] \quad (2.50)$$

$$PTWG[L] = PTWG \cdot \left[ 1 + PTWGL \cdot \frac{1}{L_{eff}^{PTWGLEXP}} \right] \quad (2.51)$$

$$ALPHA0[L] = ALPHA0 \cdot \left[ 1 + ALPHA0L \cdot \frac{1}{L_{eff}^{ALPHA0LEXP}} \right] \quad (2.52)$$

$$AGIDL[L] = AGIDL \cdot \left[ 1 + AGIDLL \cdot \frac{1}{L_{eff}} + AGIDLW \cdot \frac{1}{W_{eff}} \right] \quad (2.53)$$

$$AGISL[L] = AGISL \cdot \left[ 1 + AGISLL \cdot \frac{1}{L_{eff}} + AGISLW \cdot \frac{1}{W_{eff}} \right] \quad (2.54)$$

$$AIGC[L] = AIGC \cdot \left[ 1 + AIGCL \cdot \frac{1}{L_{eff}} + AIGCW \cdot \frac{1}{W_{eff}} \right] \quad (2.55)$$

$$AIGS[L] = AIGS \cdot \left[ 1 + AIGSL \cdot \frac{1}{L_{eff}} + AIGSW \cdot \frac{1}{W_{eff}} \right] \quad (2.56)$$

$$AIGD[L] = AIGD \cdot \left[ 1 + AIGDL \cdot \frac{1}{L_{eff}} + AIGDW \cdot \frac{1}{W_{eff}} \right] \quad (2.57)$$

$$PIGCD[L] = PIGCD \cdot \left[ 1 + PIGCDL \cdot \frac{1}{L_{eff}} \right] \quad (2.58)$$

$$NDEPCV[L] = NDEPCV \cdot \left[ 1 + NDEPCVL1 \cdot \frac{1}{L_{eff}^{NDEPCVLEXP1}} \right. \\ \left. + NDEPCVL2 \cdot \frac{1}{L_{eff}^{NDEPCVLEXP2}} + NDEPCVW \cdot \frac{1}{W_{eff}^{NDEPCVWEXP}} \right. \\ \left. + NDEPCVWL \cdot \frac{171}{(L_{eff} \cdot W_{eff})^{NDEPCVWLEXP}} \right] \quad (2.59)$$

$$\begin{aligned}
VFBCV[L] = VFBCV \cdot & \left[ 1 + VFBCVL \cdot \frac{1}{L_{eff}^{VFBCVLEXP}} \right. \\
& \left. + VFBCVW \cdot \frac{1}{W_{eff}^{VFBCVWEXP}} + VFBCVWL \cdot \frac{1}{(L_{eff} \cdot W_{eff})^{VFBCVWLEXP}} \right]
\end{aligned} \tag{2.60}$$

$$\begin{aligned}
VSATCV[L] = VSATCV \cdot & \left[ 1 + VSATCVL \cdot \frac{1}{L_{eff}^{VSATCVLEXP}} \right. \\
& \left. + VSATCVW \cdot \frac{1}{W_{eff}^{VSATCVWEXP}} + VSATCVWL \cdot \frac{1}{(L_{eff} \cdot W_{eff})^{VSATCVWLEXP}} \right]
\end{aligned} \tag{2.61}$$

$$PCLMCV[L] = PCLMCV \cdot \left[ 1 + PCLMCVL \cdot \frac{1}{L_{eff}^{PCLMCVLEXP}} \right] \tag{2.62}$$

$$\begin{aligned}
K2[L] = K2 \cdot & \left[ 1 + K2L \cdot \frac{1}{L_{eff}^{K2LEXP}} + K2W \cdot \frac{1}{W_{eff}^{K2WEXP}} + K2WL \cdot \frac{1}{(L_{eff} \cdot W_{eff})^{K2WLEXP}} \right]
\end{aligned} \tag{2.63}$$

$$PRWB[L] = PRWB \cdot \left[ 1 + PRWBL \cdot \frac{1}{L_{eff}^{PRWBLEXP}} \right] \tag{2.64}$$

$$RSW[L] = RSW \cdot \left[ 1 + RSWL \cdot \frac{1}{L_{eff}^{RSWLEXP}} \right] \tag{2.65}$$

$$RDW[L] = RDW \cdot \left[ 1 + RDWL \cdot \frac{1}{L_{eff}^{RDWLEXP}} \right] \tag{2.66}$$

$$RDSW[L] = RDSW \cdot \left[ 1 + RDSWL \cdot \frac{1}{L_{eff}^{RDSWLEXP}} \right] \tag{2.67}$$

## 2.5 Terminal Voltages

BSIM6 is a body referenced model [1].

$$V_t = \frac{K.T}{q} \quad (2.68)$$

$$V_g = V_g - V_b \quad (2.69)$$

$$V_d = V_d - V_b \quad (2.70)$$

$$V_s = V_s - V_b \quad (2.71)$$

$$V_{gs} = V_g - V_s \quad (2.72)$$

$$V_{gd} = V_g - V_d \quad (2.73)$$

$$V_{gb} = V_g - V_b \quad (2.74)$$

$$V_{ds} = V_d - V_s \quad (2.75)$$

$$V_{dsx} = \left[ \frac{2}{AVDSX} \cdot \ln(1 + \exp^{AVDSX \cdot V_{DS}}) - V_{DS} - \frac{2}{AVDSX} \cdot \ln(2) \right] \quad (2.76)$$

$$V_{bsx} = - \left[ V_s + \frac{1}{2}(V_{ds} - V_{dsx}) \right] \quad (2.77)$$

## 2.6 Pinch-off Potential and Normalized Charge Calculation

### 2.6.1 Pinch-off Potential with Poly Depletion

$$\phi_b = \ln \left( \frac{n_{body}}{n_i} \right) \quad (2.78)$$

$$\gamma_0 = \frac{\sqrt{2 \cdot q \cdot \epsilon_{si} \cdot NDEP}}{C_{ox} \sqrt{nV_t}} \quad (2.79)$$

$$\gamma_g = \frac{\sqrt{2 \cdot q \cdot \epsilon_{si} \cdot NGATE}}{C_{ox} \sqrt{nV_t}} \quad (2.80)$$

$$\gamma' = \gamma_0 \cdot \sqrt{nV_t} \quad (2.81)$$

$$\gamma'_g = \gamma_g \cdot \sqrt{nV_t} \quad (2.82)$$

$$\delta_{PD} = \frac{NDEP}{NGATE} \quad (2.83)$$

$$\left( \frac{\gamma_0}{\gamma_g} \right)^2 = \left( \frac{\frac{\sqrt{2 \cdot q \cdot \epsilon_{si} \cdot NDEP}}{C_{ox} \sqrt{nV_t}}}{\frac{\sqrt{2 \cdot q \cdot \epsilon_{si} \cdot NGATE}}{C_{ox} \sqrt{nV_t}}} \right)^2 = \frac{NDEP}{NGATE} = \delta_{PD} \quad (2.84)$$

$$\gamma = \frac{\gamma_0}{1 + \delta_{PD}} \quad (2.85)$$

In accumulation and inversion under depletion approximation, the bulk charge is given as [2]

$$Q_b = -sign(\psi_s) \cdot \gamma' \cdot C_{ox} \cdot \sqrt{V_t \cdot (e^{-\frac{\psi_s}{V_t}} - 1) + \psi_s} \quad (2.86)$$

From potential balance equation including poly depletion,

$$V_G = V_{FB} + \psi_S - \frac{Q_i + Q_b}{C_{ox}} + \left( \frac{Q_i + Q_b}{\gamma'_g \cdot C_{ox}} \right)^2 \quad (2.87)$$

At pinch off,  $\psi_S = \psi_P$  and  $Q_i = 0$ . Substituting in (2.86) and (2.87),

$$V_G - V_{FB} = \psi_P + \gamma' \cdot \sqrt{V_t \cdot (e^{-\frac{\psi_P}{V_t}} - 1) + \psi_P} + \left( \frac{\gamma'}{\gamma'_g} \right)^2 \left( V_t \cdot (e^{-\frac{\psi_P}{V_t}} - 1) + \psi_P \right) \quad (2.88)$$

$$= \psi_P + \gamma' \cdot \sqrt{V_t \cdot (e^{-\frac{\psi_P}{V_t}} - 1) + \psi_P} + \delta_{PD} \left( V_t \cdot (e^{-\frac{\psi_P}{V_t}} - 1) + \psi_P \right) \quad (2.89)$$

Normalizing it,

$$v_g - v_{fb} = \psi_p + \gamma_0 \cdot \sqrt{e^{-\psi_p} + \psi_p - 1 + \delta_{PD}} \left( e^{-\psi_p} - 1 + \psi_p \right) \quad (2.90)$$

Explicit expression for  $\psi_p$  can be derived from above relation in the asymptotic form by inspecting the behavior in three different regions. First consider the depletion and inversion region of operation where  $\psi_p \gg 0$  so that  $e^{-\psi_p}$  is very small. Let  $\zeta_1 = e^{-\psi_p}$

$$v_g - v_{fb} = \psi_p + \gamma_0 \cdot \sqrt{\psi_p + \zeta_1 - 1 + \delta_{PD}} \left( \zeta_1 - 1 + \psi_p \right) \quad (2.91)$$

Let

$$\sqrt{\psi_p + \zeta_1 - 1} = x \quad (2.92)$$

or

$$\psi_p = x^2 + 1 - \zeta_1 \quad (2.93)$$

Thus

$$v_g - v_{fb} = x^2 + 1 - \zeta_1 + \gamma_0 \cdot x + \delta_{PD} \cdot x^2 \quad (2.94)$$

or

$$x^2 + \frac{\gamma_0}{1 + \delta_{PD}} \cdot x + \frac{1 - \zeta_1}{1 + \delta_{PD}} - \frac{v_g - v_{fb}}{1 + \delta_{PD}} = 0 \quad (2.95)$$

This gives

$$x = \left[ \sqrt{\frac{v_g - v_{fb} - 1 + \zeta_1}{1 + \delta_{PD}} + \left( \frac{\gamma_0}{2 \cdot (1 + \delta_{PD})} \right)^2} - \frac{\gamma_0}{2 \cdot (1 + \delta_{PD})} \right] \quad (2.96)$$

$$\psi_p = x^2 + 1 - \zeta_1 = \left[ \sqrt{\frac{v_g - v_{fb} - 1 + \zeta_1}{1 + \delta_{PD}} + \left( \frac{\gamma_0}{2 \cdot (1 + \delta_{PD})} \right)^2} - \frac{\gamma_0}{2 \cdot (1 + \delta_{PD})} \right]^2 + 1 - \zeta_1 \quad (2.97)$$

$$= \left[ \sqrt{\frac{v_g - v_{fb} - 1 + \zeta_1}{1 + \delta_{PD}} + \left( \frac{\gamma}{2} \right)^2} - \frac{\gamma}{2} \right]^2 + 1 - \zeta_1 \quad (2.98)$$

where  $\gamma = \frac{\gamma_0}{1+\delta_{PD}}$

Similarly,

when  $\psi_p$  is close to 0

$$\psi_{p0} = \left[ \frac{v_g - v_{fb}}{2} - 3\left(1 + \frac{\gamma}{\sqrt{2}}\right) \right] + \sqrt{\left[ \frac{v_g - v_{fb}}{2} - 3\left(1 + \frac{\gamma}{\sqrt{2}}\right) \right]^2 + 6(v_g - v_{fb})} \quad (2.99)$$

and in accumulation where  $\psi_p \ll 0$  ( $\zeta_2 = \psi_p$ ),

$$\psi_p = -\ln \left[ 1 - \zeta_2 + \left( \frac{v_g - v_{fb} - \zeta_2}{\gamma} \right)^2 \right] \quad (2.100)$$

Thus the pinch off potential is expressed as

$$\psi_p = \begin{cases} -\ln \left[ 1 - \psi_{p0} + \left( \frac{v_g - v_{fb} - \psi_{p0}}{\gamma} \right)^2 \right] & \text{if } v_g - v_{fb} < 0 \\ 1 - e^{-\psi_{p0}} + \left[ \sqrt{v_g - v_{fb} - 1 + e^{-\psi_{p0}} + \left( \frac{\gamma}{2} \right)^2} - \frac{\gamma}{2} \right]^2 & \text{otherwise} \end{cases} \quad (2.101)$$

Note : Derivatives of  $\psi_p$  are continuous in all regions.

## 2.6.2 Normalized Charge Density

**Inversion Charge** [3], [4] : Normalized inversion charge density at source/drain is newly derived for BSIM6 and can be obtained as follows.

Charge sheet model approximates inversion charge density as

$$Q_i = -\gamma' \cdot C_{ox} \cdot \sqrt{V_t} \left[ \sqrt{\frac{\psi_S}{V_t} + e^{\frac{\psi_S - 2 \cdot \phi_F - V_{ch}}{V_t}}} - \sqrt{\frac{\psi_S}{V_t}} \right] \quad (2.102)$$

Using inversion charge linearization [4],

$$Q_i = n_q \cdot C_{ox} \cdot (\psi_S - \psi_P) \quad (2.103)$$

or

$$\psi_S = \psi_P + \frac{Q_i}{n_q \cdot C_{ox}} \quad (2.104)$$

Substituting  $\psi_S$  from (2.104) in (2.102),

$$-\frac{Q_i}{\gamma' \cdot C_{ox} \cdot \sqrt{V_t}} = \left[ \sqrt{\frac{\psi_P + \frac{Q_i}{n_q \cdot C_{ox}}}{V_t} + e^{\frac{\psi_P + \frac{Q_i}{n_q \cdot C_{ox}} - 2 \cdot \phi_F - V_{ch}}{V_t}}} - \sqrt{\frac{\psi_P + \frac{Q_i}{n_q \cdot C_{ox}}}{V_t}} \right] \quad (2.105)$$

rearranging,

$$\left[ -\frac{Q_i}{\gamma' \cdot C_{ox} \cdot \sqrt{V_t}} + \sqrt{\frac{\psi_P + \frac{Q_i}{n_q \cdot C_{ox}}}{V_t}} \right]^2 = \left[ \sqrt{\frac{\psi_P + \frac{Q_i}{n_q \cdot C_{ox}}}{V_t} + e^{\frac{\psi_P + \frac{Q_i}{n_q \cdot C_{ox}} - 2 \cdot \phi_F - V_{ch}}{V_t}}} \right]^2 \quad (2.106)$$

$$e^{\frac{\psi_P + \frac{Q_i}{n_q \cdot C_{ox}} - 2 \cdot \phi_F - V_{ch}}{V_t}} = \left( -\frac{Q_i}{\gamma' \cdot C_{ox} \cdot \sqrt{V_t}} \right)^2 - 2 \cdot \left( \frac{Q_i}{\gamma' \cdot C_{ox} \cdot \sqrt{V_t}} \right) \cdot \sqrt{\frac{\psi_P + \frac{Q_i}{n_q \cdot C_{ox}}}{V_t}} \quad (2.107)$$

This reduces to

$$\frac{\psi_P + \frac{Q_i}{n_q \cdot C_{ox}} - 2 \cdot \phi_F - V_{ch}}{V_t} = \ln \left[ \left( -\frac{Q_i}{\gamma' \cdot C_{ox} \cdot \sqrt{V_t}} \right)^2 - 2 \cdot \left( \frac{Q_i}{\gamma' \cdot C_{ox} \cdot \sqrt{V_t}} \right) \cdot \sqrt{\frac{\psi_P + \frac{Q_i}{n_q \cdot C_{ox}}}{V_t}} \right] \quad (2.108)$$

$$= \ln \left[ -\frac{Q_i}{\gamma' \cdot C_{ox} \cdot \sqrt{V_t}} \left( -\frac{Q_i}{\gamma' \cdot C_{ox} \cdot \sqrt{V_t}} + 2 \cdot \sqrt{\frac{\psi_P + \frac{Q_i}{n_q \cdot C_{ox}}}{V_t}} \right) \right] \quad (2.109)$$

Normalizing inversion charge to  $-2V_t \cdot n_q \cdot C_{ox}$ , all voltages to  $V_t$ ,

$$\psi_p - 2 \cdot q_i - 2 \cdot \phi_f - v_{ch} = \ln \left[ \frac{2n_q \cdot q_i}{\gamma_0} \left( \frac{2 \cdot n_q \cdot q_i}{\gamma_0} + 2 \cdot \sqrt{\psi_p - 2q_i} \right) \right] \quad (2.110)$$

which gives

$$\ln(q_i) + \ln \left[ \frac{2n_q}{\gamma_0} \left( q_i \frac{2n_q}{\gamma_0} + 2 \sqrt{\psi_p - 2q_i} \right) \right] + 2q_i = \psi_p - 2\phi_f - v_{ch} \quad (2.111)$$

This is a general equation which can be solved to give normalized inversion charge density. The procedure of obtaining initial guess for the solution of above equation for weak inversion is described below [5]. Note that to generalized the process, subscript "i" is dropped from the term  $q_i$

Let  $v = \psi_p - 2\phi_f - v_{ch} - \ln\left(\frac{4n_q\sqrt{\psi_p}}{\gamma}\right) = \ln q + 2q$

$$v = \ln q + 2q \quad (2.112)$$

$$= \ln q + 2e^{\ln q} \quad (2.113)$$

$$= \ln q + \frac{1}{F(\ln q)} \quad (2.114)$$

Here in second term  $q$  has been used as  $\ln(e^q)$ . The function  $F$  is defined as

$$F = \frac{1}{2e^{\ln q}} \quad (2.115)$$

$$= \frac{1}{2e^{(\ln q + \ln q_t - \ln q_t)}} \quad (2.116)$$

$$= \frac{1}{2q_t e^{\ln \frac{q}{q_t}}} \quad (2.117)$$

$$= \frac{1}{2q_t} e^{-\Delta} \quad (2.118)$$

Where  $\Delta = \ln \frac{q}{q_t}$ . Expanding (2.118) around  $\Delta = 0$  using Taylor series expansion (as  $|2q| \ll |\ln q|$ ),

$$F = \frac{1}{2q_t} \cdot [1 - e^{-\Delta}] \quad (2.119)$$

$$= \frac{1}{2q_t} \left(1 - \ln \frac{q}{q_t}\right) \quad (2.120)$$

substituting in (2.114),

$$v = \ln q + \frac{2q_t}{1 - \ln q + \ln q_t} \quad (2.121)$$

This equation is solved for  $q$ . Let,

$$\ln q = x \quad (2.122)$$

$$v = x + \frac{2q_t}{1 + \ln q_t - x} \quad (2.123)$$

$$v(1 + \ln q_t) - vx - x(1 + \ln q_t) + x^2 - 2q_t = 0 \quad (2.124)$$

$$x = \frac{v + (1 + \ln q_t) - \sqrt{(v + (1 + \ln q_t))^2 - 4v(1 + \ln q_t) + 8q_t}}{2} \quad (2.125)$$



For subthreshold region, normalized inversion charge density will be  $|q| \ll 1$  and  $|\ln q| \gg |2q|$ . The initial value is taken at a point where  $|\ln q| = 2 \cdot |2q|$  which gives

$$q_t = 0.301 \quad (2.126)$$

$$1 + \ln q_t = -0.201491 \quad (2.127)$$

substituting in (2.125),

$$x = \frac{v - 0.201491 - \sqrt{(v - 0.201491)^2 - 4v(-0.201491) + 8(0.301)}}{2} \quad (2.128)$$

$$x = \ln q = \frac{v - 0.201491 - \sqrt{(v + 0.402982)v + 2.446562}}{2} \quad (2.129)$$

Once the initial guess is known, the final value is obtained by using analytical method as shown below

$$n_{q0} = 1 + \frac{\gamma}{2\sqrt{\psi_p}} \quad (2.130)$$

$$v = \psi_p - 2\phi - v_{ch} - \ln \left( 4.0 \cdot \frac{n_{q0}}{\gamma} \cdot \sqrt{\psi_p} \right) \quad (2.131)$$

$$\ln q_0 = \frac{1}{2} \left[ v - 0.201491 - \sqrt{v \cdot (v + 0.402982) + 2.446562} \right] \quad (2.132)$$

$$q_0 = e^{\ln q_0} \quad (2.133)$$

if  $\ln q_0 \leq -80.0$

$$q_{s/d} = f = q_0 \cdot \left[ 1 + \psi_p - 2\phi - v_{ch} - \ln q_0 - \ln \left( 2 \cdot \frac{n_{q0}}{\gamma} \left( 2 \cdot q_0 \cdot \frac{n_{q0}}{\gamma} + 2 \cdot \sqrt{\psi_p} \right) \right) \right] \quad (2.134)$$

In this equation, if  $\ln q_0$  becomes very large and negative then  $q_0 = e^{\ln q_0}$  may be out of range of precision limit of the simulator. Therefore it is approximated as follows

if  $\ln q_0 < -110$ ,  $q_0 = e^{-100}$

if  $\ln q_0 > -90$ ,  $q_0 = e^{\ln q_0}$

else  $q_0 = \exp(-100 + 20(\frac{5}{64} + \frac{z}{2} + z^2(\frac{15}{16} - z^2(1.25 - z^2))))$

where  $z = \frac{\ln q_0 + 100}{20}$ .

The above polynomial provides smooth derivatives for  $q$ . For the derivation of polynomial coefficients, refer to Appendix A.

For  $\ln q_0 > -80$

$$f = 2q_0 + \ln \left( 2q_0 \frac{n_q}{\gamma} (2q_0 \frac{n_q}{\gamma} + 2\sqrt{\psi_p}) - (v_p - 2\phi_f - v_{ch}) \right) \quad (2.135)$$

$$f' = 2 + \frac{1}{q_0} + \frac{\frac{n_{q0}}{\gamma} - \frac{1}{\sqrt{\psi_p}}}{\frac{n_{q0}}{\gamma} \cdot q_0 + \sqrt{\psi_p}} \quad (2.136)$$

$$q_1 = q_0 - \frac{f}{f'} \quad (2.137)$$

The accuracy of this initial guess is further improved by following procedure

$$f = 2q_1 + \ln \left( 2q_1 \frac{n_q}{\gamma} (2q_1 \frac{n_q}{\gamma} + 2\sqrt{\psi_p}) - (v_p - 2\phi_f - v_{ch}) \right) \quad (2.138)$$

$$f' = 2 + \frac{1}{q_1} + \frac{\frac{n_{q1}}{\gamma} - \frac{1}{\sqrt{\psi_p}}}{\frac{n_{q1}}{\gamma} \cdot q_1 + \sqrt{\psi_p}} \quad (2.139)$$

Applying Halley's method,

$$f'' = -\frac{1}{q_1^2} - \frac{1}{\left[ (\psi_p)^{\frac{3}{2}} \right] \cdot \left[ \frac{n_{q0}}{\gamma} \cdot q_1 + \sqrt{\psi_p} \right]} - \left[ \frac{\frac{n_{q0}}{\gamma} - \frac{1}{\sqrt{\psi_p}}}{\frac{n_{q0}}{\gamma} \cdot q_1 + \sqrt{\psi_p}} \right]^2 \quad (2.140)$$

$$q_{s/d} = q_1 - \frac{f}{f'} \cdot \left( 1 + \frac{f \cdot f''}{2 \cdot f'^2} \right) \quad (2.141)$$

## 2.7 Short Channel Effects

### Asymmetry Mode

There are some devices with asymmetric drain and source structures. This is modeled as follows:

### Weighting Function for forward and reverse modes

$$T_0 = \tanh(0.6 * q * Vds_{noswap} / K \cdot T); \quad (2.142)$$

$$wf = 0.5 + 0.5 * T_0; \quad (2.143)$$

$$wr = 1.0 - wf; \quad (2.144)$$

$$if(ASYMMOD! = 0) \quad (2.145)$$

$$PARAM_A = PARAM_I * wr + PARAM_I * wf \quad (2.146)$$

$$else \quad (2.147)$$

$$PARAM_A = PARAM_I \quad (2.148)$$

$$(2.149)$$

Asymmetry mode affect following parameters: CDSCD, ETA0, PDIBLC, PCLM, PSAT, VSAT, PTWG, U0, UA, UC, UD, UCS

### Vt Roll-off, DIBL, and Subthreshold Slope Degradation (Ref.: BSIM4 Model)

$$\psi_{st} = 0.4 + PHIN + \frac{kT}{q} \cdot \ln \frac{NDEP}{n_i} \quad (2.150)$$

$$PhistVbs = \psi_{st} - V_{bsx} \quad (2.151)$$

$$X_{dep} = \sqrt{\frac{2 \cdot \epsilon_{sub} \cdot PhistVbs}{q \cdot NDEP}} \quad (2.152)$$

$$n = 1 + \frac{CIT + NFACTOR + CDSCD \cdot V_{dsx} - CDSCB \cdot V_{bsx}}{C_{ox}} \quad (2.153)$$

$$V_t = \frac{k_b \cdot T}{q} \quad (2.154)$$

$$nV_t = n \cdot V_t \quad (2.155)$$

$$\Delta V_{th,VDNUD} = K1 \cdot (\sqrt{\phi_{st} - V_{bs}} - \sqrt{\phi_{st}}) - K2 \cdot V_{bsx} \quad (2.156)$$

$$\Delta V_{th,DIBL} = -(ETA0 + ETAB \cdot V_{bsx}) \cdot V_{dsx} \quad (2.157)$$

$$\Delta V_{th,DITS} = -n \frac{KT}{q} \cdot \ln \left( \frac{L_{eff}}{L_{eff} + DVTP0 \cdot (1 + \exp(-DVTP1 \cdot V_{ds}))} \right) - \left( DVTP5 + \frac{DVTP2}{L_{eff}^{DVTP3}} \right) \cdot \tanh(DVTP4 \cdot V_{dsx}) \quad (2.158)$$

$$\Delta V_{th,all} = \Delta V_{th,VNUD} + \Delta V_{th,DIBL} + \Delta V_{th,DITS} \quad (2.159)$$

$$V_{gfb} = V_g - V_{fb} - \Delta V_{th,all} \quad (2.160)$$

Note: Short channel effect and Reverse short channel effect are modeled using NDEPL1, NDELEXP1, NDEPL2 and NDEPLEXP2 parameters. Width scaling of  $V_{th}$  is modeled using NDEPW and NDEPWEXP parameters.

## 2.8 Drain Saturation Voltage

The drain saturation voltage model is calculated after the source-side charge ( $q_s$ ) has been calculated.  $V_{dseff}$  is subsequently used to compute the drain-side charge ( $q_d$ ).

### Electric Field Calculations

Electric Field is in  $MV/cm$

$$\eta = \begin{cases} \frac{1}{2} \cdot ETAMOB & \text{for NMOS} \\ \frac{1}{3} \cdot ETAMOB & \text{for PMOS} \end{cases} \quad (2.161)$$

$$E_{effs} = 10^{-8} \cdot \left( \frac{q_{bs} + \eta \cdot q_{is}}{\epsilon_{ratio} \cdot TOXE} \right) \quad (2.162)$$

**Drain Saturation Voltage ( $V_{dsat}$ ) Calculations** (Ref. BSIM4 & EKV Model)

$$D_{mobs} = 1 + (UA + UC \cdot V_{bsx}) \cdot (E_{effs})^{EU} + \frac{UD}{\left[ \frac{1}{2} \cdot \left( 1 + \frac{q_{is}}{q_{bs}} \right) \right]^{UCS}} \quad (2.163)$$

$$T_0 = \begin{cases} \frac{1}{1 + PSATB \cdot V_{bsx}} & PSATB \geq 0 \\ 1 - PSATB \cdot V_{bsx} & PSATB < 0 \end{cases} \quad (2.164)$$

$$\lambda_C = \frac{2 \cdot U0 \cdot nV_t}{(D_{mobs})^{PSAT} \cdot VSAT \cdot L_{eff}} \cdot \left[ 1 + PTWG \cdot \frac{10 \cdot PSATX \cdot q_s \cdot T_0}{10 \cdot PSATX + q_s \cdot T_0} \right] \quad (2.165)$$

$$q_{dsat} = \frac{\lambda_C}{2} \cdot \frac{q_s^2 + q_s}{1 + \frac{\lambda_C}{2} \cdot (1 + q_s)} \quad (2.166)$$

$$v_{dsat} = \psi_p - \frac{2\phi_b}{n} - 2q_{dsat} - \ln \left[ \frac{2q_{dsat} \cdot n_q}{gam} \cdot \left( \frac{2q_{dsat} \cdot n_q}{gam} + \frac{gam}{n_q - 1} \right) \right] \quad (2.167)$$

$$V_{dsat} = v_{dsat} \cdot nV_t \quad (2.168)$$

$$V_{dssat} = V_{dsat} - V_s \quad (2.169)$$

$$V_{dseff} = \frac{V_{ds}}{\left[ 1 + \left( \frac{V_{ds}}{V_{dssat}} \right)^{1/DELTA} \right]^{DELTA}} \quad (2.170)$$

$$v_{deff} = \frac{V_{dseff} + V_s}{nV_t} \quad (2.171)$$

## 2.9 Mobility degradation with vertical field

(Ref. BSIM4 Model)

$$E_{effm} = 10^{-8} \cdot \left( \frac{q_{ba} + \eta \cdot q_{ia}}{\epsilon_{ratio} \cdot TOXE} \right) \quad (2.172)$$

Where  $q_{ia}$  and  $q_{ba}$  are the average inversion charge and bulk charge densities respectively.

$$D_{mob} = 1 + (UA + UC \cdot V_{bsx}) \cdot (E_{effm})^{EU} + \frac{UD}{\left[\frac{1}{2} \cdot \left(1 + \frac{q_{ia}}{q_{ba}}\right)\right]^{UCS}} \quad (2.173)$$

The  $D_{mob}$  goes into denominator of mobility expression.

## 2.10 Parasitic series resistance

BSIM6 offers three ways to model parasitic resistance of the MOSFET as shown below

(a) RDSMOD=0, External resistance are bias independent while internal resistance is bias dependent.

(b) RDSMOD=1, No internal resistance. Both bias dependent and independent resistor are kept externally.

(c) RDSMOD=2, No external resistance. Both bias dependent and independent resistor are kept internally.

### 2.10.1 Bias Independent External Series Resistance, Bias Dependent Internal Resistance (RDSMOD=0)

$$T_0 = 1 + PRWG \cdot q_{ia} \quad (2.174)$$

$$T_1 = PRWB \cdot (\sqrt{\phi_s - V_{bs}} - \sqrt{\phi_s}) \quad (2.175)$$

$$T_2 = \frac{1}{T_0} + T_1 \quad (2.176)$$

$$T_3 = \frac{1}{2} [T_2 + \sqrt{T_2^2 + 0.01}] \quad (2.177)$$

$$R_{ds}(V) = NF \cdot \left( W_{eff}^{WR} \left[ RDSWMIN + RDSW \cdot T_3 \right] \right) \quad (2.178)$$

$$D_r = 1.0 + \frac{\mu_0}{D_{mob} \cdot D_{vsat}} \cdot C_{ox} \cdot \frac{W_{eff}}{L_{eff}} \cdot q_{ia} \cdot R_{ds} \quad (2.179)$$

$$R_{source} = R_{s,geo} \quad (2.180)$$

$$R_{drain} = R_{d,geo} \quad (2.181)$$

$R_{s,geo}$  and  $R_{d,geo}$  are the source and drain diffusion resistances, which are described later. And,  $D_r$  goes into the denominator of the final  $I_{ds}$  expression.

### 2.10.2 Bias Dependent External Series Resistance ( $R_s(V)$ & $R_d(V)$ )

The bias-dependent external resistance model is adopted from BSIM4 and can be invoked by setting model selector RDSMOD=1. BSIM4 and BSIM6 allow the source extension resistance  $R_s(V)$  and the drain extension resistance  $R_d(V)$  to be external and asymmetric (i.e.  $R_s(V)$  and  $R_d(V)$  can be connected between the external and internal source and drain nodes, respectively; furthermore,  $R_s(V)$  does not have to be equal to  $R_d(V)$ ). This feature makes accurate RF CMOS simulation possible.

The source/drain series resistance is the sum of a bias-independent component and a bias-dependent component.

$$\begin{aligned} V_{gs,eff} &= \frac{1}{2} \left[ V_{gs} - V_{fbsdr} + \sqrt{(V_{gs} - V_{fbsdr})^2 + 10^{-2}} \right] \\ V_{gd,eff} &= \frac{1}{2} \left[ V_{gd} - V_{fbsdr} + \sqrt{(V_{gd} - V_{fbsdr})^2 + 10^{-2}} \right] \end{aligned} \quad (2.182)$$

$$\begin{aligned} R_{source} &= \frac{1}{W_{eff}^{WR} \cdot NF} \cdot \left( RSWMIN + RSW \cdot \left[ -PRWB \cdot V_{bs} + \frac{1}{1 + PRWG_i \cdot V_{gs,eff}} \right] \right) \\ &+ R_{s,geo} \end{aligned} \quad (2.183)$$

$$\begin{aligned} R_{drain} &= \frac{1}{W_{eff}^{WR} \cdot NF} \cdot \left( RDWMIN + RDW \cdot \left[ -PRWB \cdot V_{bd} + \frac{1}{1 + PRWG_i \cdot V_{gd,eff}} \right] \right) \\ &+ R_{d,geo} \end{aligned} \quad (2.184)$$

$R_{s,geo}$  and  $R_{d,geo}$  are the source and drain diffusion resistances.

### 2.10.3 Bias Dependent Internal Resistance (RDSMOD=2)

$$R_{ds}(V) = R_{s,geo} + NF \cdot \left( W_{eff}^{WR} \left[ RDSWMIN + RDSW \cdot T_3 \right] \right) + R_{d,geo} \quad (2.185)$$

$$D_r = 1.0 + \frac{\mu_0}{D_{mob} \cdot D_{vsat}} \cdot C_{ox} \cdot \frac{W_{eff}}{L_{eff}} \cdot q_{ia} \cdot R_{ds} \quad (2.186)$$

where T3 is given by (2.177).

### 2.10.4 Sheet resistance model

The resistances  $R_{s,geo}$  and  $R_{d,geo}$  are simply calculated as the sheet resistances ( $RSHS, RSHD$ ) times the number of squares ( $NRS, NRD$ ):

$$\begin{aligned} R_{s,geo} &= NRS \cdot RSHS \\ R_{d,geo} &= NRD \cdot RSHD \end{aligned} \quad (2.187)$$

## 2.11 Output Conductance

The Output conductance model is taken from BSIM4 [6]

### Channel Length Modulation (CLM)

$$E_{sat} = \frac{2 \cdot VSAT}{\frac{U_0}{D_{mob}}} \quad (2.188)$$

$$F = \begin{cases} 1 & \text{for } FPROUT \leq 0 \\ \frac{1}{1 + \frac{FPROUT \cdot \sqrt{L_{eff}}}{q_{ia} + 2 \cdot nV_t}} & \text{for } FPROUT > 0 \end{cases} \quad (2.189)$$

$$C_{clm} = \begin{cases} PCLM \cdot \left(1 + PCLMG \cdot \frac{q_{ia}}{E_{sat} \cdot L_{eff}}\right)^{\frac{1}{F}} & \text{for } PCLMG > 0 \\ \frac{PCLM}{\left(1 - PCLMG \cdot \frac{q_{ia}}{E_{sat} \cdot L_{eff}}\right)^{\frac{1}{F}}} & \text{for } PCLMG < 0 \end{cases} \quad (2.190)$$

$$V_{asat} = V_{dssat} + E_{sat}L \quad (2.191)$$

$$M_{CLM} = 1 + C_{clm} \ln \left[ 1 + \frac{V_{ds} - V_{dseff}}{V_{asat}} \cdot \frac{1}{C_{clm}} \right] \quad (2.192)$$

### Drain Induced Barrier Lowering (DIBL)

$$PVAGfactor = \begin{cases} 1 + PVAG \cdot \frac{q_{im}}{E_{sat}L_{eff}} & \text{for } PVAG > 0 \\ \frac{1}{1 - PVAG \cdot \frac{q_{im}}{E_{sat}L_{eff}}} & \text{for } PVAG < 0 \end{cases} \quad (2.193)$$



$$\theta_{rout} = PDIBLC \quad (2.194)$$

$$V_{ADIBL} = \frac{q_{ia} + 2kT/q}{\theta_{rout}} \cdot \left(1 - \frac{V_{dssat}}{V_{dssat} + q_{ia} + 2kT/q}\right) \cdot PVAGfactor \cdot \frac{1}{1 + PDIBLCB \cdot V_{bsx}} \quad (2.195)$$

$$M_{DIBL} = \left(1 + \frac{V_{ds} - V_{dseff}}{V_{ADIBL}}\right) \quad (2.196)$$

Note: Length scaling parameters for PDIBLC are PDIBLCL and PDIBLCLEXP.

### Drain Induced Threshold Shift (DITS)

$$V_{ADITS} = \frac{1}{PDITS} \cdot F \cdot [1 + (1 + PDITSL \cdot L_{eff}) \exp(PDITSD \cdot V_{ds})] \quad (2.197)$$

$$M_{DITS} = \left(1 + \frac{V_{ds} - V_{dseff}}{V_{ADITS}}\right) \quad (2.198)$$

### Substrate Current induced Body Effect (SCBE)

$$litl = \sqrt{(\epsilon_{sub}/\epsilon_{ox}) \cdot TOXE \cdot XJ} \quad (2.199)$$

$$V_{ASCBE} = \frac{L_{eff}}{PSCBE2} \cdot \exp\left(\frac{PSCBE1 \cdot litl}{V_{ds} - V_{dseff}}\right) \quad (2.200)$$

$$M_{SCBE} = \left(1 + \frac{V_{ds} - V_{dseff}}{V_{ASCBE}}\right) \quad (2.201)$$

$$M_{oc} = M_{DIBL} \cdot M_{CLM} \cdot M_{DITS} \cdot M_{SCBE} \quad (2.202)$$

$M_{oc}$  is multiplied to  $I_{ds}$  in the final drain current expression.

## 2.12 Velocity Saturation

### Current Degradation Due to Velocity Saturation

$$T_1 = 2 \cdot \lambda_C \cdot (q_s - q_{def}) \quad (2.203)$$

$$\lambda_C = \frac{2 \cdot U_0 \cdot nV_t}{(D_{mobs})^{\frac{1}{PSAT}} \cdot VSAT \cdot L_{eff}} \cdot \left[ 1 + PTWG \cdot \frac{10 \cdot PSATX \cdot q_s \cdot T_0}{10 \cdot PSATX + q_s \cdot T_0} \right] \quad (2.204)$$

$$D_{vsat} = \frac{1}{2} \left[ \sqrt{1 + T_1^2} + \frac{1}{T_1} \cdot \ln(T_1 + \sqrt{1 + T_1^2}) \right] \quad (2.205)$$

$$D_{ptwg} = D_{vsat} \quad (2.206)$$

$$D_{tot} = D_{mob} \cdot D_{vsat} \cdot D_r \quad (2.207)$$

where  $D_r$  is the effect of internal resistance ( $R_{dsi}$ ) on current, defined as

$$D_r = \begin{cases} 1 & \text{if } RDSMOD = 1 \\ 1 + U_0 \cdot C_{ox} \cdot \frac{W_{eff}}{L_{eff}} \cdot q_{ia} \cdot R_{dsi} & \text{if } RDSMOD = 0 \end{cases} \quad (2.208)$$

**Non-Saturation Effect** Some devices do not exhibit prominent or abrupt velocity saturation. The parameters A1 and A2 are used to tune this non-saturation effect to better the  $I_{d,sat}$  or  $g_{m,sat}$  fitting.

$$T_0 = A_1 + A_2 / (q_{ia} + 2.0 * n * V_{tm}); \quad (2.209)$$

$$dq_i = q_s - q_{def}; \quad (2.210)$$

$$T_1 = T_0 * dq_i * dq_i; \quad (2.211)$$

$$T_2 = T_1 + 1.0 - 0.001; \quad (2.212)$$

$$T_3 = -1.0 + 0.5 * (T_2 + \sqrt{T_2 * T_2 + 0.004}); \quad (2.213)$$

$$N_{sat} = 0.5 * (1.0 + \sqrt{1.0 + T_3}); \quad (2.214)$$

$$I_{ds} = I_{ds} / N_{sat}; \quad (2.215)$$

## 2.13 Effective Mobility

$$\mu_{eff} = \frac{U0}{D_{tot}} \quad (2.216)$$

## 2.14 Drain Current Model

### 2.14.1 Without Velocity Saturation

The drain current expression is derived as follows,

$$I_{ds} = I_{drift} + I_{diff} \quad (2.217)$$

$$I_{ds} = -W_{eff} \cdot Q_i \cdot \mu_{eff} \frac{d\psi_s}{dx} + W \cdot \mu_{eff} \cdot V_t \frac{dQ_i}{dx} \quad (2.218)$$

from charge linearization,  $\psi_s = \psi_p + \frac{Q_i}{n_q \cdot C_{ox}}$ . Thus

$$I_{ds} = \mu_{eff} \cdot W_{eff} \cdot \left[ -\frac{Q_i}{n_q \cdot C_{ox}} + V_t \right] \frac{dQ_i}{dx} \quad (2.219)$$

normalizing inversion charge to  $-2n_q C_{ox} V_t$  and using  $\xi = \frac{x}{L}$ ,

$$I_{ds} = \mu_{eff} \cdot \frac{W_{eff}}{L_{eff}} \cdot \left[ -\frac{(-2 \cdot n_q \cdot C_{ox} \cdot V_t \cdot q)}{n_q \cdot C_{ox}} + V_t \right] \frac{d(-2 \cdot n_q \cdot C_{ox} \cdot V_t \cdot q)}{d\xi} \quad (2.220)$$

$$= -2 \cdot n_q \cdot \mu_{eff} \cdot \frac{W_{eff}}{L_{eff}} \cdot C_{ox} \cdot nV_t^2 \cdot (2q + 1) \frac{dq}{d\xi} \quad (2.221)$$

Total drain current,

$$I_{DS} = \int_0^1 I_{ds} d\xi = -2 \cdot n_q \cdot \mu_{eff} \cdot \frac{W_{eff}}{L_{eff}} \cdot C_{ox} \cdot nV_t^2 \cdot \int_{q_s}^{q_d} (2q + 1) dq \quad (2.222)$$

which gives

$$I_{DS} = 2 \cdot n_q \cdot \mu_{eff} \cdot \frac{W_{eff}}{L_{eff}} \cdot C_{ox} \cdot nV_t^2 \cdot [(q_s - q_{def}) (q_s + q_{def} + 1)] \quad (2.223)$$

$n_q$  is the slope factor in charge based model and  $nV_t$  is  $n \cdot \frac{KT}{q}$  with n given by (2.153).

### 2.14.2 Including Velocity Saturation

As the device is getting smaller and smaller, the lateral electric field strength and therefore kinetic energy of the carriers increases. On reaching optical phonon energy levels, they release optical phonon by virtue of reduction in kinetic energy and therefore lose velocity [7]. The effect of velocity saturation on mobility is captured as follows

$$\mu = \frac{\mu_{eff}}{\sqrt{1 + \left(\frac{E}{E_c}\right)^2}} \quad (2.224)$$

$$= \frac{\mu_{eff}}{\sqrt{1 + \left(\frac{1}{E_c} \cdot \frac{d\psi_s}{dx}\right)^2}} \quad (2.225)$$

from (2.221) and (2.225),

$$I_{ds} = -2 \cdot n_q \cdot \frac{\mu_{eff}}{\sqrt{1 + \left(\frac{1}{E_c} \cdot \frac{d\psi_s}{dx}\right)^2}} \cdot \frac{W_{eff}}{L_{eff}} \cdot C_{ox} \cdot nV_t^2 \cdot (2q + 1) \frac{dq}{d\xi} \quad (2.226)$$

$$= z \cdot \frac{(2q + 1) \frac{dq}{d\xi}}{\sqrt{1 + \left(\frac{1}{E_c} \cdot \frac{d\psi_s}{dx}\right)^2}} \quad (2.227)$$

with  $z = -2\mu_{eff} \cdot n_q \cdot \frac{W_{eff}}{L_{eff}} \cdot C_{ox} \cdot nV_t^2$

Total current,

$$I_{DS} = \int_0^1 I_{ds} d\xi = z \cdot \int_{q_s}^{q_d} \frac{(2q + 1)}{\sqrt{1 + \left(\frac{1}{E_c} \cdot \frac{d\psi_s}{dx}\right)^2}} dq \quad (2.228)$$

$$I_{DS} \int_0^1 \sqrt{1 + \left(\frac{1}{E_c} \cdot \frac{d\psi_s}{dx}\right)^2} d\xi = z \cdot \int_{q_s}^{q_d} (2q + 1) dq \quad (2.229)$$

from (2.223),

$$\int_{q_s}^{q_d} (2q + 1) dq = -(q_s - q_{def}) (q_s + q_{def} + 1) \quad (2.230)$$

Now consider the LHS of (2.229). Using charge linearization,  $\psi_s = \psi_p + \frac{Q_i}{n_q \cdot C_{ox}}$ ,

$$\frac{1}{E_c} \frac{d\psi_s}{dx} = \frac{1}{E_c \cdot n_q \cdot C_{ox}} \frac{Q_i}{dx} = -\frac{2V_t}{E_c \cdot L} \frac{dq}{d\xi} = -\lambda_c \cdot \frac{dq}{d\xi} \quad (2.231)$$

Let

$$D_{vsat} = \int \sqrt{1 + \left( \frac{1}{E_c} \cdot \frac{d\psi_s}{dx} \right)^2} d\xi$$

It is evaluated by assuming that lateral electric field  $(-\frac{d\psi_s}{d\xi})$  increases linearly from 0 at source to  $2 \cdot \left( \frac{\psi_{s,D} - \psi_{s,S}}{L} \right)$  at drain [8] i.e.

$$-\frac{d\psi_s}{dx} = 2 \cdot \frac{\psi_{s,D} - \psi_{s,S}}{L} \cdot \frac{x}{L} = 2 \cdot \frac{\psi_{s,D} - \psi_{s,S}}{L} \cdot \xi \quad (2.232)$$

From charge linearization (2.104),

$$\psi_{s,S} = \psi_P + \frac{Q_S}{n_q \cdot C_{ox}} = \psi_P - 2V_t \cdot q_s \quad (2.233)$$

$$\psi_{s,D} = \psi_P + \frac{Q_D}{n_q \cdot C_{ox}} = \psi_P - 2V_t \cdot q_d \quad (2.234)$$

$$\psi_{s,D} - \psi_{s,S} = 2 \cdot V_t (q_s - q_d) \quad (2.235)$$

substituting in (2.232),

$$-\frac{d\psi_s}{dx} = 2 \cdot \frac{2 \cdot V_t (q_s - q_d)}{L^2} \cdot x = 2 \cdot \frac{2 \cdot V_t (q_s - q_d)}{L} \cdot \xi \quad (2.236)$$

$$-\frac{1}{E_c} \frac{d\psi_s}{dx} = 2 \cdot \frac{2 \cdot V_t}{E_c L} \cdot (q_s - q_d) \xi = 2\lambda_c (q_s - q_d) \xi \quad (2.237)$$

where  $\lambda_c = \frac{2V_t}{E_c \cdot L}$ . Thus  $D_{vsat}$  can be given as

$$D_{vsat} = \int \sqrt{1 + \left( \frac{1}{E_c} \cdot \frac{d\psi_s}{dx} \right)^2} d\xi \quad (2.238)$$

$$= \int \sqrt{1 + (2\lambda_c (q_s - q_d) \xi)^2} d\xi = \int \sqrt{1 + (2\lambda_c \cdot \Delta q \cdot \xi)^2} d\xi \quad (2.239)$$

$$= \frac{1}{2} \left[ \sqrt{1 + (2 \cdot \lambda_c \cdot \Delta q)^2} + \frac{1}{2 \cdot \lambda_c \cdot \Delta q} \cdot \ln \left( 2 \cdot \lambda_c \cdot \Delta q + \sqrt{1 + (2 \cdot \lambda_c \cdot \Delta q)^2} \right) \right] \quad (2.240)$$

with  $\Delta q = q_s - q_d$ . From (2.229), (2.230) and (2.240),

$$I_{DS} = 2 \cdot n_q \cdot \mu_{eff} \cdot \frac{W_{eff}}{L_{eff}} \cdot C_{ox} \cdot nV_t^2 \cdot [(q_s - q_{def}) (q_s + q_{def} + 1)] \cdot M_{oc} \quad (2.241)$$

where  $\mu_{eff} = \frac{U_0}{D_{tot}}$  and  $D_{tot} = D_{mod} \cdot D_{vsat} \cdot D_r$

## 2.15 Threshold Voltage Model

### 2.15.1 Long Channel Threshold Voltage

The drain current under the standard drift-diffusion formalism can be represented as

$$I_{ds} = I_{drift} + I_{diff} \quad (2.242)$$

$$I_{ds} = -W \cdot Q_i \cdot \mu \frac{d\psi_s}{dx} + W \cdot \mu \cdot V_t \frac{dQ_i}{dx} \quad (2.243)$$

Defining threshold voltage as the gate voltage at which  $I_{drift} = I_{diff}$ , which leads to  $q_i = \frac{1}{2}$ . Here, we define threshold voltage as the gate voltage at which normalized inversion charge density at the source is  $q_s = \frac{1}{2}$ . Pinch-off potential corresponding to  $q_s = \frac{1}{2}$ ,  $\psi_{p,th}$ , is calculated using  $q_s = \frac{1}{2}$  in (2.111) leading to

$$\psi_{p,th} = \left[ \ln(0.5) + 1 \right] + \ln \left[ \frac{2n_q}{\gamma_0} \left( \frac{n_q}{\gamma_0} + 2\sqrt{\psi_{p,th} - 1} \right) \right] + 2\phi_f + v_s \quad (2.244)$$

To obtain  $\psi_{p,th}$  in explicit form, we make an assumption that at threshold voltage,

$$\psi_{p,th} - 1 = 2\phi_f + v_s \quad (2.245)$$

The other bias dependent term  $n_q$  is also approximated by

$$n_q = 1 + \frac{\gamma}{2\sqrt{2\phi_f}} \quad (2.246)$$

This gives,

$$\psi_{p,th} = \left[ \ln(0.5) + 1 \right] + \ln \left[ \frac{2n_q}{\gamma_0} \left( \frac{n_q}{\gamma_0} + 2\sqrt{2\phi_f - v_b} \right) \right] + 2\phi_f + v_s \quad (2.247)$$

After  $\psi_{p,th}$  is obtained, next step is to calculate threshold voltage. The potential balance equation in conjunction with Poisson's equation and Gauss law for the MOSFET is given as ()

$$V_G = V_{FB} + \psi_S - \frac{Q_{in} + Q_{dep}}{C_{ox}} \quad (2.248)$$

At pinch-off,  $\psi_S = \psi_P$ , and  $Q_{in} = 0$

$$V_G = V_{FB} + \psi_P + \gamma\sqrt{\psi_P} \quad (2.249)$$

Thus [9]

$$V_{TH,long} = V_{FB} + \psi_{p,th} \cdot V_t - \gamma\sqrt{\psi_{p,th} \cdot V_t} \quad (2.250)$$

### Short Channel Threshold Voltage

$$V_{TH} = V_{TH,long} - \Delta V_{th,all} \quad (2.251)$$

## 2.16 MNUD model to increase Fitting Flexibility

$$MNUD = 1 + K_0 \left[ \frac{(q_s - q_{def})}{(M_0 + q_s + q_{def})} \right]^2 \quad (2.252)$$

$$I_{DS} = 2 \cdot n_q \cdot \mu_{eff} \cdot \frac{W_{eff}}{L_{eff}} \cdot C_{ox} \cdot nV_t^2 \cdot [(q_s - q_{def})(q_s + q_{def} + 1)] \cdot M_{oc} / MNUD \quad (2.253)$$

## 2.17 Subthreshold Hump Module

The Edge FET Model current is added to the main current  $I_{ds}$ , when the parameter EDGEFET is 1 [10].

$$I_{ds,EDGE} = 2 \cdot NF \cdot nq \cdot \mu_{eff} \cdot WEDGE / L_{eff} \cdot C_{ox} \cdot nV_t \cdot ((q_s - q_{def}) \cdot (1 + q_s + q_{def})) \cdot M_{oc} \quad (2.254)$$

Now the total current will be  $I_{Total} = I_{dsEDGE} + I_{ds}$ . The parameters associated with subthreshold hump model are: WEDGE, DGAMMA, DGAMMAL, DGAMMALEXP, DVTEGE, NFACTOREDGE, CITEDGE, CDSCDEGE, CDSCBEDGE, ETA0EDGE, ETABEDGE, KT1EDGE, KT1LEGE, KT2EDGE, KT1EXPEDGE, TNFACTOREDGE, TETA0EDGE, DVT0EDGE, DVT1EDGE, DVT2EDGE.

## 2.18 Modeling of Sub-Surface Leakage Drain Current

The flag for the sub-surface leakage model is SSLMOD [11].

$$T1 = \left( \frac{NDEP}{1e23} \right)^{SSLEXP1} \quad T2 = \left( \frac{300}{T} \right)^{SSLEXP2} \quad (2.255)$$

$$T3 = SSL0.exp(-T1T2) \quad T4 = SSL1.T2.T1 \quad (2.256)$$

$$T5 = SSL3.tanh \left( exp(SSL4.(V_G - V_{TH})) \right) \quad (2.257)$$

$$I_{ssl} = T3.NF.W_{eff}.exp(-T4.L + \frac{T5}{V_t}) \left[ exp(SSL2.\frac{V_{dsx}}{V_t}) - 1 \right] \quad (2.258)$$

## 2.19 Impact Ionization Model

The impact ionization current model in BSIM6 is the same as that in BSIM4, and is modeled by

$$I_{ii} = ALPHA0 \cdot (V_{ds} - V_{dseff}) \cdot exp \left( - \frac{BETA0}{V_{ds} - V_{dseff}} \right) \cdot \frac{I_{ds}}{M_{SCBE}} \quad (2.259)$$

where parameters  $ALPHA0$  and  $BETA0$  are impact ionization coefficients.  $ALPHA0L$  and  $ALPHA0LEXP$  are length scaling parameters for  $ALPHA0$ .

Note: The order of  $ALPHA0$  in BSIM6 =  $10^6$  X order of  $ALPHA0$  in BSIM4

## 2.20 GIDL/GISL Current Model

GIDL/GISL currents are set using model selector GIDLMOD=1. The GIDL/GISL current and its body bias effect are modeled by

$$I_{GIDL} = AGIDL \cdot W_{eff} \cdot NF \cdot \frac{V_{ds} - V_{gse} - EGIDL}{3 \cdot T_{oxe}} \cdot exp \left( - \frac{3 \cdot T_{oxe} \cdot BGIDL}{V_{ds} - V_{gse} - EGIDL} \right) \cdot \frac{V_{db}^3}{CGIDL + V_{db}^3} \quad (2.260)$$



$$\begin{aligned}
I_{GISL} = & AGISL \cdot W_{eff} \cdot NF \cdot \frac{-V_{ds} - V_{gde} - EGISL}{3 \cdot T_{oxe}} \\
& \cdot \exp\left(-\frac{3 \cdot T_{oxe} \cdot BGISL}{-V_{ds} - V_{gde} - EGISL}\right) \cdot \frac{V_{sb}^3}{CGISL + V_{sb}^3}
\end{aligned} \tag{2.261}$$

where  $AGIDL$ ,  $BGIDL$ ,  $CGIDL$  and  $EGIDL$  are model parameters for the drain side and  $AGISL$ ,  $BGISL$ ,  $CGISL$  and  $EGISL$  are the model parameters for the source side.  $CGIDL$  and  $CGISL$  account for the body-bias dependence of  $I_{GIDL}$  and  $I_{GISL}$  respectively.  $W_{eff}$  and  $NF$  are the effective width of the source/drain diffusions and the number of fingers. Further explanation of  $W_{eff}$  and  $NF$  can be found in the chapter of the layout-dependence model. Check scaling parameters in the parameter list at the end.

$I_{GIDL}/I_{GISL}$  can be switched off by setting  $GIDL\text{MOD} = 0$ .

## 2.21 Gate Tunneling Current Model

As the gate oxide thickness is scaled down to  $3nm$  and below, gate leakage current due to carrier direct tunneling becomes important. This tunneling happens between the gate and silicon beneath the gate oxide. To reduce the tunneling current, high-k dielectrics are being used in place of gate oxide. In order to maintain a good interface with substrate, multi-layer dielectric stacks are being used. The BSIM6 gate tunneling model (taken from BSIM4) has been shown to work for multi-layer gate stacks as well. The tunneling carriers can be either electrons or holes, or both, either from the conduction band or valence band, depending on (the type of the gate and) the bias regime. In BSIM6, the gate tunneling current components include the tunneling current between gate and substrate ( $I_{gb}$ ), and the current between gate and channel ( $I_{gc}$ ), which is partitioned between the source and drain terminals by  $I_{gc} = I_{gcs} + I_{gcd}$ . The third component happens between gate and source/drain diffusion regions ( $I_{gs}$  and  $I_{gd}$ ). Figure 1 shows the schematic gate tunneling current flows.

### 2.21.1 Model Selectors

Two global selectors are provided to turn on or off the tunneling components. **IGCMOD** = 1 turns on  $I_{gc}$ ,  $I_{gs}$ , and  $I_{gd}$ ; **IGBMOD** = 1 turns on  $I_{gb}$ . When the

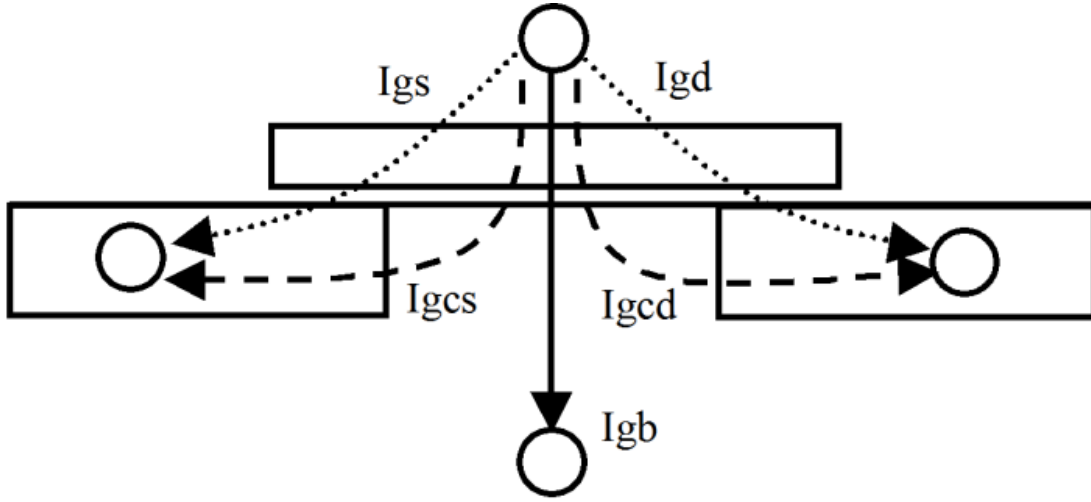


Figure 1: Schematic gate current components flowing between MOSFET terminals.

selectors are set to zero, no gate tunneling currents are modeled.

$$V_{ox} = nVt \cdot (v_g - v_{fb} - \psi_p + q_s + q_{def}) \quad (2.262)$$

$$V_{oxacc} = \frac{1}{2} \left( -V_{ox} + \sqrt{V_{ox}^2 + 10^{-4}} \right) \quad (2.263)$$

$$V_{oxdepinv} = \frac{1}{2} \left( V_{ox} + \sqrt{V_{ox}^2 + 10^{-4}} \right) \quad (2.264)$$

Eq. (2.263) and (2.264) are valid and continuous from accumulation through depletion to inversion.

### 2.21.2 Equations for Tunneling Currents

**Note:** All gate tunneling current equations use operating temperature in the calculations.

**Gate-to-Substrate Current** ( $I_{gb} = I_{gbacc} + I_{gbinv}$ ):  $I_{gbacc}$ , determined by ECB (Electron tunneling from Conduction Band), is significant in accumulation and given by

$$I_{gbacc} = NF \cdot W_{eff} L_{eff} \cdot A \cdot T_{oxRatio} \cdot V_{gb} \cdot V_{aux} \cdot i_{gtemp} \cdot \exp[-B \cdot TOXE(AIGBACC - BIGBACC \cdot V_{oxacc}) \cdot (1 + CIGBAC \cdot V_{oxacc})] \quad (2.265)$$

where the physical constants  $A = 4.97232e - 7 \text{ A/V}^2$ ,  $B = 7.45669e11(g/F - s^2)^{0.5}$ , and

$$T_{oxRatio} = \left( \frac{TOXREF}{TOXE} \right)^{NTOX} \cdot \frac{1}{TOXE^2} \quad (2.266)$$

$$V_{aux} = NIGBACC \cdot V_t \cdot \log \left( 1 + \exp \left( - \frac{V_{oxacc}}{NIGBACC \cdot V_t} \right) \right) \quad (2.267)$$

$I_{gbinv}$ , determined by EVB (Electron tunneling from Valence Band), is significant in inversion and given by

$$I_{gbinv} = NF \cdot W_{eff} L_{eff} \cdot A \cdot T_{oxRatio} \cdot V_{gb} \cdot V_{aux} \cdot i_{gtemp} \cdot \exp[-B \cdot TOXE(AIGBINV - BIGBINV \cdot V_{oxdepinv}) \cdot (1 + CIGBINV V_{oxdepinv})] \quad (2.268)$$

where  $A = 3.75956e-7 \text{ A/V}^2$ ,  $B = 9.82222e11 (g/F - s^2)^{0.5}$ , and

$$V_{aux} = NIGBINV \cdot V_t \cdot \log \left( 1 + \exp \left( \frac{V_{oxdepinv} - EIGBINV}{NIGBINV \cdot V_t} \right) \right) \quad (2.269)$$

$$I_{gb} = I_{gbacc} + I_{gbinv} \quad (2.270)$$

**Gate-to-Channel Current ( $I_{gc0}$ ) and Gate-to-S/D ( $I_{gs}$  and  $I_{gd}$ ):**  $I_{gc0}$ , determined by ECB for NMOS and HVB (Hole tunneling from Valence Band) for PMOS at  $V_{ds} = 0$ , is formulated as

$$I_{gc0} = NF \cdot W_{eff} L_{eff} \cdot A \cdot T_{oxRatio} \cdot V_{gse} \cdot V_{aux} \cdot i_{gtemp} \cdot \exp[-B \cdot TOXE(AIGC - BIGC \cdot V_{oxdepinv}) \cdot (1 + CIGCV_{oxdepinv})] \quad (2.271)$$

where  $A = 4.97232 A/V^2$  for NMOS and  $3.42537 A/V^2$  for PMOS,  $B = 7.45669e11 (g/F - s^2)^{0.5}$  for NMOS and  $1.16645e12 (g/F - s^2)^{0.5}$  for PMOS.

$$V_{aux} = n_q \cdot nVt \cdot (q_s + q_{def}) \quad (2.272)$$

**Partition of  $I_{gc}$ :** To consider the drain bias effect,  $I_{gc}$  is split into two components,  $I_{gcs}$  and  $I_{gcd}$ , that is  $I_{gc} = I_{gcs} + I_{gcd}$ , and

$$I_{gcs} = I_{gc0} \cdot \frac{PIGCD \cdot V_{dseffx} + \exp(-PIGCD \cdot V_{dseffx}) - 1 + 10^{-4}}{PIGCD \cdot V_{dseffx}^2 + 2 \cdot 10^{-4}} \quad (2.273)$$

and

$$I_{gcd} = I_{gc0} \cdot \frac{1 - (PIGCD \cdot V_{dseffx} + 1) \cdot \exp(-PIGCD \cdot V_{dseffx}) + 10^{-4}}{PIGCD \cdot V_{dseffx}^2 + 2 \cdot 10^{-4}} \quad (2.274)$$

where

$$V_{dseffx} = \sqrt{V_{dseff} + 0.01} - 0.1 \quad (2.275)$$

At  $V_{ds} = 0$ ,  $I_{gcs} = I_{gcd} = \frac{1}{2} I_{gc0}$ . Thus  $I_{gc0}$  is the gate to channel current  $I_{gc}$  at  $V_{ds} = 0$ .

**$I_{gs}$  and  $I_{gd}$ :**  $I_{gs}$  represents the gate tunneling current between the gate and the source diffusion region, while  $I_{gd}$  represents the gate tunneling current between the gate and the drain diffusion region.  $I_{gs}$  and  $I_{gd}$  are determined by ECB for NMOS and HVB for PMOS, respectively.

$$I_{gs} = NF \cdot W_{eff} DLCIG \cdot A \cdot T_{oxRatioEdge} \cdot V_{gs} \cdot V'_{gs} \cdot i_{gtemp} \cdot \exp[-B \cdot TOXE \cdot POXEDGE \cdot (AIGS - BIGS \cdot V'_{gs}) \cdot (1 + CIGSV'_{gs})] \quad (2.276)$$

and

$$I_{gd} = NF \cdot W_{eff} DLCIGD \cdot A \cdot T_{oxRatioEdge} \cdot V_{gd} \cdot V'_{gd} \cdot i_{gtemp} \cdot \exp[-B \cdot TOXE \cdot POXEDGE \cdot (AIGD - BIGD \cdot V'_{gd}) \cdot (1 + CIGDV'_{gd})] \quad (2.277)$$

where  $A = 4.97232 A/V^2$  for NMOS and  $3.42537 A/V^2$  for PMOS,  $B = 7.45669e11 (g/F - s^2)^{0.5}$  for NMOS and  $1.16645e12 (g/F - s^2)^{0.5}$  for PMOS, and

$$T_{oxRatioEdge} = \left( \frac{TOXREF}{TOXE \cdot POXEDGE} \right)^{NTOX} \cdot \frac{1}{(TOXE \cdot POXEDGE)^2} \quad (2.278)$$

$$V'_{gs} = \sqrt{(V_{gs} - V_{fbsd})^2 + 10^{-4}} \quad (2.279)$$

$$V'_{gd} = \sqrt{(V_{gd} - V_{fbsd})^2 + 10^{-4}} \quad (2.280)$$

$V_{fbsd}$  is the flat-band voltage between gate and S/D diffusions calculated as

If  $NGATE > 0.0$

$$V_{fbsd} = -devsign \cdot \frac{k_B T}{q} \log \left( \frac{NGATE}{NSD} \right) + VFBSDOFF \quad (2.281)$$

Else  $V_{fbsd} = 0.0$ .

## 2.22 Gate resistance and Body resistance network Model

### 2.22.1 Gate Electrode Electrode and Intrinsic-Input Resistance (IIR) Model

**General Description:** BSIM6 provides four options for modeling gate electrode resistance (bias-independent) and intrinsic-input resistance (IIR, bias-dependent). The IIR model considers the relaxation-time effect due to the distributive RC nature of the channel region, and therefore describes the first-order non-quasi-static effect. Thus, the IIR model should not be used together with the charge-deficit NQS model at the same time. The model selector RGATEMOD is used to choose different options.

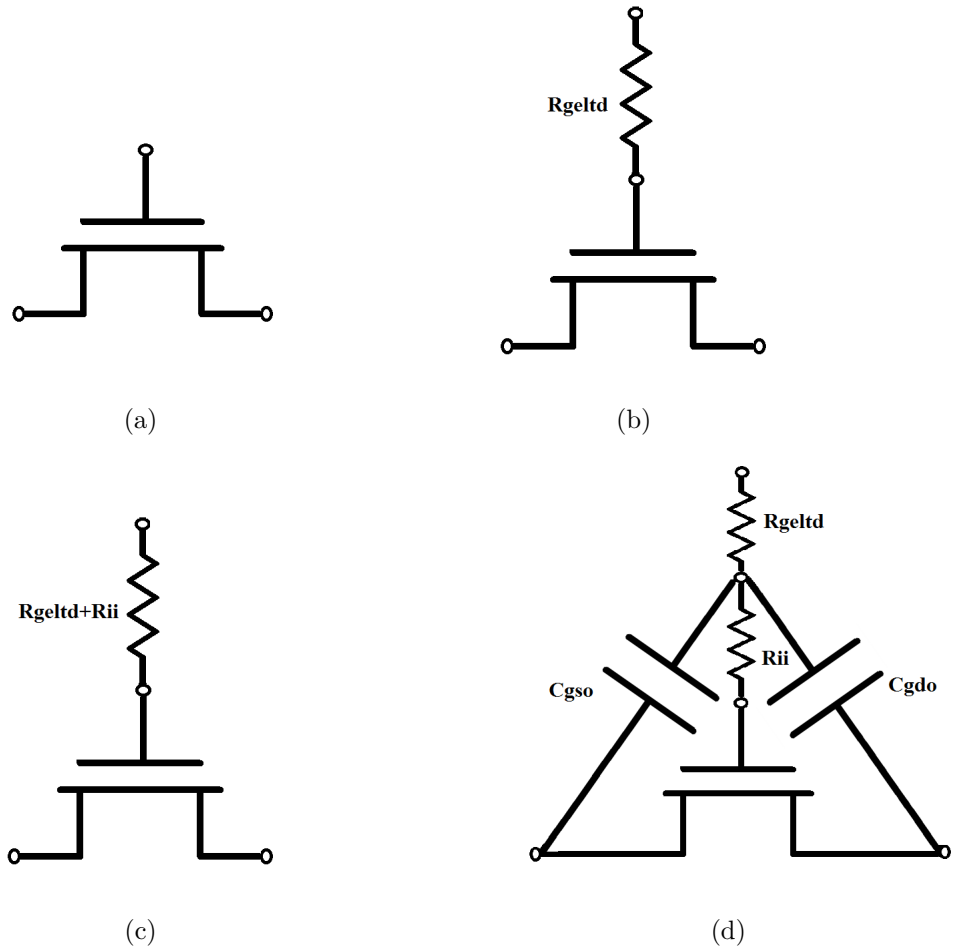


Figure 2: Gate resistance network for (a)  $RGATEMOD = 0$  (b)  $RGATEMOD = 1$  (c)  $RGATEMOD = 2$  (d)  $RGATEMOD = 3$  .

**Model Option and Schematic:** There are four model selectors for gate resistance network.

**RGATEMOD = 0** (zero-resistance): In this case, no gate resistance is generated (see Figure 2).

**RGATEMOD = 1** (constant-resistance): In this case, only the electrode gate resistance (bias-independent) is generated by adding an internal gate node.  $R_{geltd}$  is given by

$$R_{geltd} = \frac{RSHG \cdot (XGW + \frac{W_{effci}}{3 \cdot NGCON})}{NGCON \cdot (L_{drawn} - XGL) \cdot NF} \quad (2.282)$$

**RGATEMOD = 2** (IIR model with variable resistance): In this case, the gate resistance is the sum of the electrode gate resistance  $R_{geltd}$  (2.282) and the intrinsic-input resistance  $R_{ii}$  as given by (2.283). An internal gate node will be generated.

$$\frac{1}{R_{ii}} = XR CRG1 \cdot NF \cdot \left( \frac{I_{ds}}{V_{dseff}} + XR CRG2 \cdot \frac{W_{eff} \mu_{eff} C_{oxeff} V_t}{L_{eff}} \right)$$

or

$$\frac{1}{R_{ii}} \approx XR CRG1 \cdot NF \cdot \left( \mu_{eff} \left( \frac{W_{eff}}{L_{eff}} \right) C_{ox} \cdot q_{ia} + XR CRG2 \cdot \frac{W_{eff} \mu_{eff} C_{oxeff} V_t}{L_{eff}} \right) \quad (2.283)$$

**RGATEMOD = 3** (IIR model with two nodes): In this case, the gate electrode resistance  $R_{geltd}$  is in series with the intrinsic-input resistance  $R_{ii}$  through two internal gate nodes, so that the overlap capacitance current will not pass through the intrinsic-input resistance.

## 2.22.2 Substrate Resistance Network

**General Description:** For CMOS RF circuit simulation, it is essential to consider the high frequency coupling through the substrate. BSIM6 offers a flexible built-in substrate resistance network. This network is constructed such that little simulation efficiency penalty will result. Note that the substrate resistance parameters should be extracted for the total device, not on a per-finger basis.

**Model Selector and Topology** The model selector **RBODYMOD** can be used to turn on or turn off the resistance network.

**RBODYMOD** = 0 (Off):

No substrate resistance network is generated at all.

**RBODYMOD** = 1 (On):

All five resistances  $RBPS$ ,  $RBPD$ ,  $RBPB$ ,  $RBSB$ , and  $RBDB$  in the substrate network as shown schematically below are present simultaneously.

A minimum conductance,  $GBMIN$ , is introduced in parallel with each resistance and therefore to prevent infinite resistance values, which would otherwise cause poor convergence.  $GBMIN$  is merged into each resistance to simplify the representation of the model topology. Note that the intrinsic model substrate reference point in this case is the internal body node **bNodePrime**, into which the impact ionization current  $I_{ii}$  and the GIDL current  $I_{GIDL}$  flow.

**RBODYMOD** = 2 (On : Scalable Substrate Network):

The schematic is similar to **RBODYMOD** = 1 but all the five resistors in the substrate network are now scalable with a possibility of choosing either five resistors, three resistors or one resistor as the substrate network.

The resistors of the substrate network are scalable with respect to channel length (L), channel width (W) and number of fingers (NF). The scalable model allows to account for both horizontal and vertical contacts.

The scalable resistors  $RBPS$  and  $RBPD$  are evaluated through

$$RBPS = RBPS0 \cdot \left(\frac{L}{10^{-6}}\right)^{RBPSL} \cdot \left(\frac{W}{10^{-6}}\right)^{RBPSW} \cdot NF^{RBPSNF} \quad (2.284)$$

$$RBPD = RBPD0 \cdot \left(\frac{L}{10^{-6}}\right)^{RBPDL} \cdot \left(\frac{W}{10^{-6}}\right)^{RBPDW} \cdot NF^{RBPDNF} \quad (2.285)$$

The resistor  $RBPB$  consists of two parallel resistor paths, one to the horizontal contacts and other to the vertical contacts. These two resistances are scalable and  $RBPB$  is given



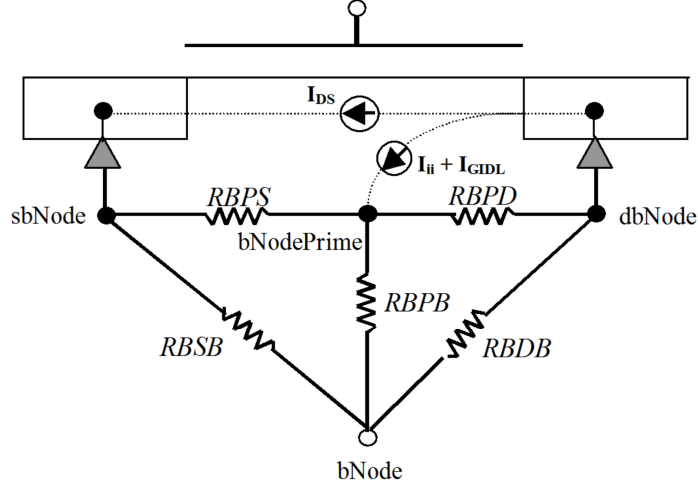


Figure 3: Topology with the substrate resistance network turned on.

by a parallel combination of these two resistances.

$$RBPBX = RBPBX0 \cdot \left(\frac{L}{10^{-6}}\right)^{RBPBXL} \cdot \left(\frac{W}{10^{-6}}\right)^{RBPBXW} \cdot NF^{RBPDN} \quad (2.286)$$

$$RBPBY = RBPBY0 \cdot \left(\frac{L}{10^{-6}}\right)^{RBPBYL} \cdot \left(\frac{W}{10^{-6}}\right)^{RBPBYW} \cdot NF^{RBPDN} \quad (2.287)$$

$$RBPB = \frac{RBPBX \cdot RBPBY}{RBPBX + RBPBY} \quad (2.288)$$

The resistors RBSB and RBDB share the same scaling parameters but have different scaling prefactors. These resistors are modeled in the same way as RBPB. The equations

for RBSB are shown below. The calculation for RBDB follows RBSB.

$$RBSBX = RBSBX0 \cdot \left(\frac{L}{10^{-6}}\right)^{RBSBXL} \cdot \left(\frac{W}{10^{-6}}\right)^{RBSBXW} \cdot NF^{RBSDNF} \quad (2.289)$$

$$RBSBY = RBSBY0 \cdot \left(\frac{L}{10^{-6}}\right)^{RBSBYL} \cdot \left(\frac{W}{10^{-6}}\right)^{RBSBYW} \cdot NF^{RBSDNF} \quad (2.290)$$

$$RBSB = \frac{RBSBX \cdot RBSBY}{RBSBX + RBSBY} \quad (2.291)$$

Similarly, the equations for RBDB is as follows

$$RBDBX = RBDBX0 \cdot \left(\frac{L}{10^{-6}}\right)^{RBDBXL} \cdot \left(\frac{L}{10^{-6}}\right)^{RBDBXW} \cdot (NF)^{RBDBXNF} \quad (2.292)$$

$$RBDBY = RBDBY0 \cdot \left(\frac{L}{10^{-6}}\right)^{RBDBYL} \cdot \left(\frac{L}{10^{-6}}\right)^{RBDBYW} \cdot (NF)^{RBDBYNF} \quad (2.293)$$

$$RBDB = \frac{RBDBX \times RBDBY}{RBDBX + RBDBY} \quad (2.294)$$

The implementation of **RBODYMOD** = 2 allows the user to chose between the 5-R network (with all five resistors), 3-R network (with RBPS, RBPD and RBPB) and 1-R network (with only RBPB).

If the user does not provide both the scaling parameters RBSBX0 and RBSBY0 for RBSB or both the scaling parameters RBDBX0 and RBDBY0 for RBDB, then the conductances for both RBSB and RBDB are set to GBMIN. This converts the 5-R schematic to 3-R schematic where the substrate network consists of the resistors RBPS, RBPD and RBPB. RBPS, RBPD and RBPB are then calculated using (2.284), (2.285), and (2.288).

If the user chooses not to provide either of RBPS0 or RBPD0, then the 5-R schematic is converted to 1-R network with only one resistor RBPB. The conductances for RBSB and RBDB are set to GBMIN. The resistances RBPS and RBPD are set to 1e-3 Ohm. The resistor RBPB is then calculated using (2.288).

In all other situations, 5-R network is used with the resistor values calculated from the equations aforementioned.

## 2.23 Noise Modeling

The following noise sources in MOSFETs are modeled in BSIM6 for SPICE noise analysis: flicker noise (also known as 1/f noise), channel thermal noise and induced gate noise and their correlation, thermal noise due to physical resistances such as the source/ drain, gate electrode, and substrate resistances, and shot noise due to the gate dielectric tunneling current.

Noise models in BSIM 6.0.0	Origin
Flicker noise model	BSIM4 Unified Model (FNOIMOD=1)
Thermal noise(TNOIMOD=0)	BSIM4 (TNOIMOD=0)
Thermal noise (TNOIMOD=1)	BSIM4 (TNOIMOD=2)
Gate current shot noise	BSIM4 gate current noise
Noise associated with parasitic resistances	BSIM4 parasitic resistance noise

### 2.23.1 Flicker Noise Models

**FNOIMOD = 1 (Flicker Noise Model):** BSIM6's flicker noise model for FNOIMOD =1 is same as FNOIMOD=1 in BSIM4. The unified physical flicker noise model is smooth over all bias regions.

The physical mechanism for the flicker noise is trapping/detrapping-related charge fluctuation in oxide traps, which results in fluctuations of both mobile carrier numbers and mobilities in the channel. The unified flicker noise model captures this physical process. In the inversion region, the noise density is expressed as [12]

$$S_{id,inv}(f) = \frac{kTq^2\mu_{eff}I_{ds}}{C_{oxe}L_{effNOI}^2f^{EF} \cdot 10^{10}} \left( NOIA \cdot \log \left( \frac{N_0 + N^*}{N_l + N^*} \right) \right. \\ \left. NOIB \cdot (N_0 - N_l) + \frac{NOIC}{2}(N_0^2 - N_l^2) \right) \\ \frac{kTI_{ds}^2\Delta L_{clm}}{W_{eff}L_{effNOI}^2f^{EF} \cdot 10^{10}} \left( \frac{NOIA + NOIB \cdot N_l + NOIC \cdot N_l^2}{(N_l + N^*)^2} \right) \quad (2.295)$$

where  $L_{effNOI} = L_{eff} - 2 \cdot LINTNOI$ ,  $\mu_{eff}$  is the effective mobility at the given bias condition, and  $L_{eff}$  and  $W_{eff}$  are the effective channel length and width, respectively.

The parameter  $N_0$  is the charge density at the source side given by

$$N_0 = \frac{2n_q C_{ox} V_t q_s}{q} \quad (2.296)$$

The parameter  $N_l$  is the charge density at the drain end given by

$$N_l = \frac{2n_q C_{ox} V_t q_{def}}{q} \quad (2.297)$$

and  $N^*$  is given by

$$N^* = \frac{V_t (C_{ox} + C_d + CIT)}{q} \quad (2.298)$$

where CIT is a model parameter from DC IV and  $C_d$  is the depletion capacitance.

$\Delta L_{clm}$  is the channel length reduction due to channel length modulation and given by

$$\begin{aligned} \Delta L_{clm} &= litl \cdot \log \left( \frac{V_{ds} - V_{dseff}}{litl} + EM \right) \\ E_{sat} &= \frac{2V_{SAT}}{\mu_{eff}} \end{aligned} \quad (2.299)$$

In the subthreshold region, the noise density is written as

$$S_{id,subVt}(f) = \frac{NOIA \cdot k \cdot T \cdot I_{ds}^2}{W_{eff} L_{eff} f^{EF} N^{*2} \cdot 10^{10}} \quad (2.300)$$

The total flicker noise density is

$$S_{id}(f) = \frac{S_{id,inv} \cdot S_{id,subVt}}{S_{id,inv} + S_{id,subVt}} \quad (2.301)$$

**FNOIMOD = 0 (Flicker Noise Model for Halo Transistors):** For the noise modeling, it is now assumed that the transistor is composed of two transistors, channel transistor of length  $L - LH$  and halo transistor of length LH connected in series and

carries same current ( $I_{DS}$ ) as in single transistor configuration. The individual contribution of the halo and channel transistors to overall noise is obtained using small signal analysis and principle of superposition [13] [14].

Total drain current noise PSD becomes,

$$S_{ID} = S_{ID,1} + S_{ID,2} \quad (2.302)$$

$$= S_{ID,h} \left[ \frac{g_{m,ch} + g_{d,ch}}{g_{m,ch} + g_{d,ch} + g_{d,h}} \right]^2 + S_{ID,ch} \left[ \frac{g_{d,h}}{g_{m,ch} + g_{d,ch} + g_{d,h}} \right]^2 \quad (2.303)$$

$$= S_{ID,h} \cdot CF_h + S_{ID,ch} \cdot CF_{ch} \quad (2.304)$$

We refer to the multiplying factors to  $S_{ID,h}$  and  $S_{ID,ch}$  in (2.303) as contribution factors (CF). Where,

$$g_{d,ch} = 2n_q\mu C_{ox} \frac{W}{L - L_h} V_t q_{d,ch} \quad (2.305)$$

$$g_{d,h} = 2n_q\mu C_{ox} \frac{W}{L_h} V_t q_{d,h} \quad (2.306)$$

$$g_{m,ch} = 2\mu C_{ox} \frac{W}{L - L_h} V_t (q_{s,ch} - q_{d,ch}) \quad (2.307)$$

To calculate  $q_{d,h}$  and  $q_{s,ch}$ , the fact that the same current flows in one transistor and two transistor noise equivalent configuration is used,

$$i_h = \frac{I_{DS}}{-2n_q\mu C_{ox} \frac{W}{L_h} V_t^2} = (q_{s,h}^2 + q_{s,h}) - (q_{d,h}^2 + q_{d,h}) \quad (2.308)$$

$$i_{ch} = \frac{I_{DS}}{-2n_q\mu C_{ox} \frac{W}{L-L_h} V_t^2} = (q_{s,ch}^2 + q_{s,ch}) - (q_{d,ch}^2 + q_{d,ch}) \quad (2.309)$$

where  $i_h$  and  $i_{ch}$  are the normalized drain current of halo and channel transistor respectively. Since  $I_{DS}$  is known from DC modeling, the above equations are solved for,

$$q_{d,h} = -\frac{1}{2} + \frac{1}{2} \sqrt{1 + 4(q_{s,h}^2 + q_{s,h} - i_h)} \quad (2.310)$$

$$q_{s,ch} = -\frac{1}{2} + \frac{1}{2} \sqrt{1 + 4(q_{d,ch}^2 + q_{d,ch} + i_{ch})} \quad (2.311)$$

Here we have used the unified model presented in for halo and channel transistors separately, where  $S_{ID}$  is expressed as

$$S_{ID,h} = \frac{kTI_{DS}^2}{\gamma f W L_h^2} \int_0^{L_h} \frac{N_{t,h}^*(E_{F_n})}{N_h^2} dx \quad (2.312)$$

$$S_{ID,ch} = \frac{kTI_{DS}^2}{\gamma f W (L - L_h)^2} \int_{L_h}^L \frac{N_{t,ch}^*(E_{F_n})}{N_{ch}^2} dx \quad (2.313)$$

where apparent trap density  $N_{t,ch(h)}^*(E_{F_n}) = A_{ch(h)} + B_{ch(h)}N_{ch(h)} + C_{ch(h)}N_{ch(h)}^2$ ,  $A$ ,  $B$ ,  $C$  are the noise parameters,  $\gamma$  is the tunneling parameter,  $k$  is the Boltzmann constant and  $T$  is the temperature.

### 2.23.2 Channel Thermal Noise

There are two channel thermal noise models in BSIM6. One is a charge-based model (default model) similar to that used in BSIM3v3.2 and BSIM4.7.0 (TNOIMOD=0). The other is the holistic model similar to BSIM4.7.0 (TNOIMOD=2). These two models can be selected through the model selector TNOIMOD.

**TNOIMOD = 0 (Charge based Model):** The noise current is given by

$$Q_{inv} = |Q_{s,intrinsic} + Q_{d,intrinsic}| \times NFIN_{total} \quad (2.314)$$

$$\overline{i_d^2} = \begin{cases} NTNOI \cdot \frac{4kT\Delta f}{L_{eff}^2} & \text{if RDSMOD} = 0 \\ R_{ds} + \frac{L_{eff}^2}{\mu_{eff}Q_{inv}} & \\ NTNOI \cdot \frac{4kT\Delta f}{L_{eff}^2} \cdot \mu_{eff}Q_{inv} & \text{if RDSMOD} = 1 \end{cases} \quad (2.315)$$

where  $R_{ds}(V)$  is the bias-dependent LDD source/drain resistance, and the parameter NTNOI is introduced for more accurate fitting of short-channel devices.  $Q_{inv}$  is the total inversion charge in the channel.

**TNOIMOD = 1 (Holistic Model):** In this thermal noise model (similar to TNOIMOD = 2 in BSIM4.7.0), all the short-channel effects and velocity saturation effect incorporated in the IV model are automatically included, hence the name "holistic thermal

noise model". In this thermal noise model both the gate and the drain noise are implemented as current noise sources. The drain current noise flows from drain to source; whereas the induced gate current noise flows from the gate to the source. The correlation between the two noise sources is independently controllable and can be tuned using the parameter  $RNOIC$ , although the use of default value 0.395 is recommended when measured data is not available. As illustrated in Fig. 4,  $TNOIMOD=1$  shows good physical behavior in both the weak and strong inversion regions. The white noise gamma factor  $\gamma_{WN} = \frac{S_{Id}}{4kTg_{d0}}$  shows a value of 1 at low  $V_{ds}$ , as expected. At high  $V_{ds}$ , it correctly goes to  $2/3$  for strong inversion and  $1/2$  in sub-threshold [15]. The relevant formulations of  $TNOIMOD=2$  are given below. For more details, see Ph.D. thesis of Darsen Lu and BSIM4 manual.

$$\beta_{tnoi} = RNOIA \cdot \left[ 1.0 + TNOIA \cdot L_{eff} \cdot \left( \frac{q_{ia}}{E_{sat,noi} L_{eff}} \right)^2 \right] \quad (2.316)$$

$$\theta_{tnoi} = RNOIB \cdot \left[ 1.0 + TNOIB \cdot L_{eff} \cdot \left( \frac{q_{ia}}{E_{sat,noi} L_{eff}} \right)^2 \right] \quad (2.317)$$

$$c_{tnoi} = RNOIC \cdot \left[ 1.0 + TNOIC \cdot L_{eff} \cdot \left( \frac{q_{ia}}{E_{sat,noi} L_{eff}} \right)^2 \right] \quad (2.318)$$

$$(2.319)$$

$$S_{id} = 4KT \cdot \mu C_{ox} \frac{W_{eff}}{L_{vsat}} V_t D_{ptwg} M_{oc} \left[ \frac{q_s + q_{def}}{2} \cdot \left( 1 + \frac{\beta_{lowId}^2}{TNOIK2 + q_{ia}} \cdot \frac{V_{dseff}}{V_{dsat}} \right) + (3 \cdot \beta_{tnoi}^2) \cdot \frac{(q_s - q_{def})^2}{12 \left( \frac{1+q_s+q_{def}}{2} \right)} \right] \quad (2.320)$$

$$mig = \frac{1}{12 \cdot NF \cdot W_{eff} \mu_{eff} \cdot D_{ptwg} M_{oc} C_{ox} \cdot V_t} \frac{L_{vsat}^3}{L_{eff}^2} \cdot \left[ \frac{\frac{q_s + q_{def}}{2}}{\left( \frac{1+q_s+q_{def}}{2} \right)^2} - \frac{\left( 6 \left( \frac{q_s + q_{def}}{2} \right) + \frac{1}{2} \right) (q_s - q_{def})^2}{60 \left( \frac{1+q_s+q_{def}}{2} \right)^4} + \frac{(q_s - q_{def})^4}{144 \left( \frac{1+q_s+q_{def}}{2} \right)^5} \right] \cdot \left( \frac{15}{4} \cdot \theta_{tnoi}^2 \right) \quad (2.321)$$

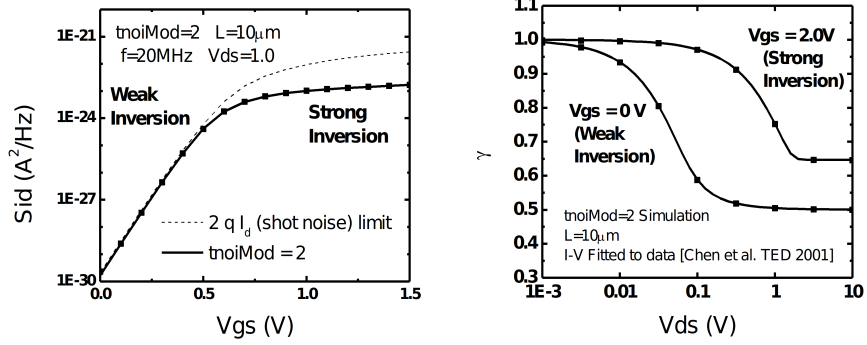


Figure 4: TNOIMOD=1 shows good physical behavior at high and low  $V_{ds}$  from sub-threshold to strong inversion regions.

$$S_{ig} = \frac{4KT \cdot [\omega \cdot C_{ox} \cdot W \cdot NF \cdot L]^2 \cdot mig}{1 + (\omega \cdot C_{0x} \cdot L \cdot W \cdot NF \cdot mig)^2} \quad (2.322)$$

$$S_{ig,id} = -j\omega \cdot 4KT \cdot \mu C_{ox} D_{ptwg} M_{oc} V_t \left( \frac{L_{vsat}}{L_{eff}} \right) \cdot \left[ \frac{(q_s - q_{deff})}{12 \left( \frac{1+q_s+q_{deff}}{2} \right)} - \frac{(q_s - q_{deff})^3}{144 \left( \frac{1+q_s+q_{deff}}{2} \right)^3} \right] \cdot \frac{C_{tnoi}}{0.395} \quad (2.323)$$

$$c = \frac{S_{ig,id}}{\sqrt{S_{ig}} \cdot \sqrt{S_{id}}} \quad (2.324)$$

### 2.23.3 Gate Current Shot Noise

$$\overline{i_{gs}^2} = 2q(I_{gcs} + I_{gs}) \quad (2.325)$$

$$\overline{i_{gd}^2} = 2q(I_{gcd} + I_{gd}) \quad (2.326)$$

$$\overline{i_{gb}^2} = 2qI_{gbinv} \quad (2.327)$$



### 2.23.4 Resistor Noise

The noise associated with each parasitic resistors in BSIM6 are calculated

If  $RDSMOD = 1$  then

$$\frac{\overline{i_{RS}^2}}{\Delta f} = 4kT \cdot \frac{1}{R_{source}} \quad (2.328)$$

$$\frac{\overline{i_{RD}^2}}{\Delta f} = 4kT \cdot \frac{1}{R_{drain}} \quad (2.329)$$

If  $RGATEMOD = 1$  then

$$\frac{\overline{i_{RG}^2}}{\Delta f} = 4kT \cdot \frac{1}{R_{gelltd}} \quad (2.330)$$

## 2.24 Self Heating Model

Effect of self heating is modeled by employing a thermal network consisting of thermal resistance ( $R_{th}$ ) and capacitance ( $C_{th}$ ) as shown in Fig.5. The voltage at thermal node T gives the rise in temperature, which is added to the ambient temperature and all the temperature sensitive variables in the model are updated accordingly [16].

$$R_{th} = \frac{RTH0}{(WTH0 + Weff) \cdot NF}$$

$$C_{th} = CTH0 * (WTH0 + Weff) \cdot NF$$

## 3 Asymmetric MOS Junction Diode Models

### 3.1 Junction Diode IV Model

In BSIM6, there is only one diode model (DIOMOD=2 from BSIM4), which includes resistance and breakdown. BSIM6 models the diode breakdown with current limiting in both forward IJTHSFWD or IJTHDFWD and reverse operations XJBVS, XJBVD, BVS, and BVD.

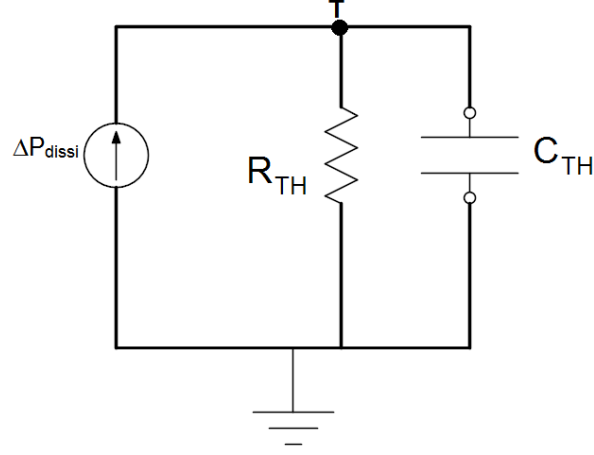


Figure 5: Thermal Network for Self Heating Model.

**Source/Body Junction Diode** The equations for the source-side diode are as follows:

$$I_{bs} = I_{sbs} \left[ \exp\left(\frac{V_{bs}}{NJS \cdot V_t}\right) - 1 \right] \cdot f_{breakdown} + V_{bs} \cdot G_{min} \quad (3.1)$$

where  $I_{sbs}$  is the total saturation current consisting of the components through the gate-edge (Jsswgs) and isolation-edge sidewalls (Jssws) and the bottom junction (Jss),

$$I_{sbs} = A_{seff} J_{ss}(T) + P_{seff} J_{ssws}(T) + W_{effcj} \cdot NF \cdot J_{sswgs}(T) \quad (3.2)$$

where the calculation of the junction area and perimeter is discussed in section Layout-Dependent Parasitics Models, and the temperature-dependent current density model is given in Section Temperature Dependence of Junction Diode IV. The exponential term in equation given below is linearized at both the limiting current IJTHSFWD in the forward-bias mode and the limiting current IJTHSREV in the reverse-bias mode. In (3.1),  $f_{breakdown}$  is given by

$$f_{breakdown} = 1 + XJBVS \cdot \exp\left(-\frac{(BVS + V_{bs})}{NJS \cdot V_t}\right) \quad (3.3)$$

**Drain/Body Junction Diode** The equations for the drain-side diode are as follows:

$$I_{bd} = I_{sbd} \left[ \exp \left( \frac{V_{bd}}{NJD \cdot V_t} \right) - 1 \right] \cdot f_{breakdown} + V_{bd} \cdot G_{min} \quad (3.4)$$

where  $I_{sbs}$  is the total saturation current consisting of the components through the gate-edge (Jsswgs) and isolation-edge sidewalls (Jssws) and the bottom junction (Jss),

$$I_{sbd} = A_{defj} J_{sd}(T) + P_{defj} J_{sswd}(T) + W_{effcj} \cdot NF \cdot J_{sswgd}(T) \quad (3.5)$$

where the calculation of the junction area and perimeter is discussed in Section Layout-Dependent Parasitics Models, and the temperature-dependent current density model is given in Section Temperature Dependence of Junction Diode IV. The exponential term in (3.6) is linearized at both the limiting current IJTHDFWD in the forward-bias mode and the limiting current IJTHDREV in the reverse-bias mode. In (3.1),  $f_{breakdown}$  is given by

$$f_{breakdown} = 1 + XJBVD \cdot \exp \left( - \frac{\cdot(BVD + V_{bd})}{NJD \cdot V_t} \right) \quad (3.6)$$

**Total Junction Source/Drain Diode Including Tunneling** Total diode current including the carrier recombination and trap-assisted tunneling current in the space-charge region is modeled by:

$$\begin{aligned} I_{bs\_totle} &= I_{bs} \\ &- W_{effcj} \cdot NF \cdot J_{tsswgs}(T) \cdot \left[ \exp \left( \frac{-V_{bs}}{NJTSSWG(T) \cdot Vtm0} \cdot \frac{VTSSWGS}{VTSSWGS - V_{bs}} \right) \right] \\ &- P_{s,defj} J_{tssws}(T) \left[ \exp \left( \frac{-V_{bs}}{NJTSSW(T) \cdot Vtm0} \cdot \frac{VTSSWS}{VTSSWS - V_{bs}} \right) - 1 \right] \\ &- A_{s,defj} J_{tss}(T) \left[ \exp \left( \frac{-V_{bs}}{NJTSS(T) \cdot Vtm0} \cdot \frac{VTSS}{VTSS - V_{bs}} \right) - 1 \right] + g_{min} \cdot V_{bs} \quad (3.7) \end{aligned}$$

$$\begin{aligned} I_{bd\_totle} &= I_{bd} \\ &- W_{effcj} \cdot NF \cdot J_{tsswgd}(T) \cdot \left[ \exp \left( \frac{-V_{bd}}{NJTSSWGD(T) \cdot Vtm0} \cdot \frac{VTSSWGD}{VTSSWGD - V_{bd}} \right) \right] \\ &- P_{d,defj} J_{tsswd}(T) \left[ \exp \left( \frac{-V_{bd}}{NJTSSWD(T) \cdot Vtm0} \cdot \frac{VTSSWD}{VTSSWD - V_{bd}} \right) - 1 \right] \\ &- A_{d,defj} J_{tsd}(T) \left[ \exp \left( \frac{-V_{bd}}{NJTSD(T) \cdot Vtm0} \cdot \frac{VTSD}{VTSD - V_{bd}} \right) - 1 \right] + g_{min} \cdot V_{bd} \quad (3.8) \end{aligned}$$

## 3.2 Junction Diode CV Model

Source and drain junction capacitances consist of three components: the bottom junction capacitance, sidewall junction capacitance along the isolation edge, and sidewall junction capacitance along the gate edge. An analogous set of equations are used for both sides but each side has a separate set of model parameters.

**Source/Body Junction Diode** The source-side junction capacitance can be calculated by

$$C_{bs} = A_{seff}C_{jbs} + P_{seff}C_{jbssw} + W_{effcj} \cdot NF \cdot C_{jbsswg} \quad (3.9)$$

where  $C_{jbs}$  is the unit-area bottom S/B junction capacitance,  $C_{jbssw}$  is the unit-length S/B junction sidewall capacitance along the isolation edge, and  $C_{jbsswg}$  is the unit-length S/B junction sidewall capacitance along the gate edge. The effective area and perimeters in (3.9) are given in Section Layout-Dependent Parasitics Models.

Cjbs is calculated by

$$C_{jbs} = \begin{cases} CJS(T) \cdot \left(1 - \frac{V_{bs}}{PBS(T)}\right)^{-MJS} & \text{if } \frac{V_{bs}}{PBS(T)} \leq x_0 \\ CJS(T) \cdot \frac{1}{(1-x_0)^{MJS}} \cdot \left[1 + MJS \left(1 + \frac{\frac{V_{bs}}{PBS} - 1}{1-x_0}\right)\right] & \text{otherwise} \end{cases} \quad (3.10)$$

where the value of  $x_0$  is taken as 0.9.

Cjbssw is calculated by

$$C_{jbssw} = \begin{cases} CJSWS(T) \cdot \left(1 - \frac{V_{bs}}{PBSWS(T)}\right)^{-MJSWS} & \text{if } \frac{V_{bs}}{PBSWS(T)} \leq x_0 \\ CJSWS(T) \cdot \frac{1}{(1-x_0)^{MJSWS}} \cdot \left[1 + MJSWS \left(1 + \frac{\frac{V_{bs}}{PBSWS(T)} - 1}{1-x_0}\right)\right] & \text{otherwise} \end{cases} \quad (3.11)$$

where the value of  $x_0$  is taken as 0.9.

Cjbswg is calculated by

$$C_{jbswg} = \begin{cases} CJSWGS(T) \cdot \left(1 - \frac{V_{bs}}{PBSWGS(T)}\right)^{-MJSWGS} & \text{if } \frac{V_{bs}}{PBSWGS(T)} \leq x_0 \\ CJSWGS(T) \cdot \frac{1}{(1-x_0)^{MJSWGS}} \cdot \left[1 + MJSWGS \left(1 + \frac{\frac{V_{bs}}{PBSWGS(T)} - 1}{1-x_0}\right)\right] & \text{otherwise} \end{cases} \quad (3.12)$$

where the value of  $x_0$  is taken as 0.9.

**Drain/Body Junction Diode** The drain-side junction capacitance can be calculated by

$$C_{bd} = A_{def}C_{jbd} + P_{def}C_{jbdsw} + W_{effej} \cdot NF \cdot C_{jbdswg} \quad (3.13)$$

where  $C_{jbd}$  is the unit-area bottom D/B junction capacitance,  $C_{jbdsw}$  is the unit-length D/B junction sidewall capacitance along the isolation edge, and  $C_{jbdswg}$  is the unit-length D/B junction sidewall capacitance along the gate edge. The effective area and perimeters in (3.13) are given in Section Layout-Dependent Parasitics Models.

Cjbd is calculated by

$$C_{jbd} = \begin{cases} CJD(T) \cdot \left(1 - \frac{V_{bs}}{PBD(T)}\right)^{-MJD} & \text{if } \frac{V_{bs}}{PBD(T)} \leq x_0 \\ CJD(T) \cdot \frac{1}{(1-x_0)^{MJD}} \cdot \left[1 + MJD \left(1 + \frac{\frac{V_{bs}}{PBD(T)} - 1}{1-x_0}\right)\right] & \text{otherwise} \end{cases} \quad (3.14)$$

where the value of  $x_0$  is taken as 0.9.

Cjbdsw is calculated by

$$C_{jbdsw} = \begin{cases} CJSWD(T) \cdot \left(1 - \frac{V_{bs}}{PBSWD(T)}\right)^{-MJSWS} & \text{if } \frac{V_{bs}}{PBSWD(T)} \leq x_0 \\ CJSWD(T) \cdot \frac{1}{(1-x_0)^{MJSWD}} \cdot \left[1 + MJSWD \left(1 + \frac{\frac{V_{bs}}{PBSWD(T)} - 1}{1-x_0}\right)\right] & \text{otherwise} \end{cases} \quad (3.15)$$

where the value of  $x_0$  is taken as 0.9.

Cjbdswg is calculated by

$$C_{jbdswg} = \begin{cases} CJSWGD(T) \cdot \left(1 - \frac{V_{bs}}{PBSWGD(T)}\right)^{-MJSWGD} & \text{if } \frac{V_{bs}}{PBSWGD(T)} > 1 \\ CJSWGD(T) \cdot \frac{1}{(1-x_0)^{MJSWGD}} \cdot \left[1 + MJSWGD \left(1 + \frac{\frac{V_{bs}}{PBSWGD(T)} - 1}{1-x_0}\right)\right] & \text{otherwise} \end{cases} \quad (3.16)$$

where the value of  $x_0$  is taken as 0.9.

## 4 Layout dependent Parasitics Models

### 4.1 Layout-Dependent Parasitics Models

BSIM6 provides a comprehensive and versatile geometry/layout-dependent parasitics model taken from BSIM4. It supports modeling of series (such as isolated, shared, or merged source/ drain) and multi-finger device layout, or a combination of these two configurations. This model has impact on every BSIM6 sub-models except the substrate resistance network model. Note that the narrow-width effect in the per-finger device with multi-finger configuration is accounted for by this model. A complete list of model parameters and selectors can be found at the end.

#### 4.1.1 Geometry Definition

Figure 6 schematically shows the geometry definition for various source/drain connections and source/drain/gate contacts. The layout parameters shown in this figure will be used to calculate resistances and source/drain perimeters and areas.

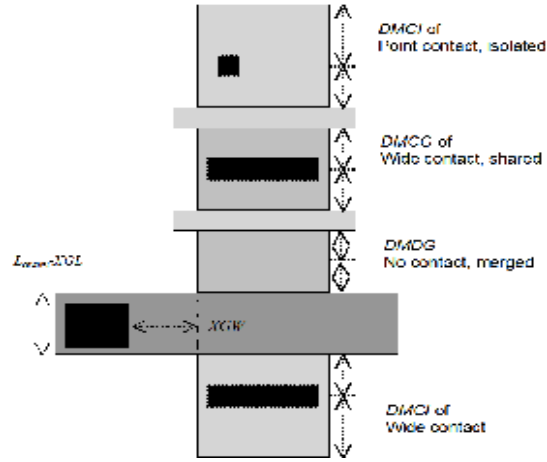


Figure 6: Definition for layout parameters.

#### 4.1.2 Model Formulation and Options

**Effective Junction Perimeter and Area:** In the following, only the source-side case is illustrated. The same approach is used for the drain side. The effective junction perimeter on the source side is calculated by

**If** (PS is given)

if (**perMod**=0)

$$P_{seff} = PS$$

else

**Else**

$P_{seff}$  computed from NF, DWJ, **geoMod**, DMCG, DMCI, DMDG, DMC GT, RSH, and MIN.

The effective junction area on the source side is calculated by

**If** (AS is given)

$$A_{seff} = AS$$

**Else**

$A_{seff}$  computed from NF, DWJ, **geoMod**, DMCG, DMCI, DMDG, DMC GT, RSH, and MIN.

In the above,  $P_{seff}$  and  $A_{seff}$  will be used to calculate junction diode IV and CV.  $P_{seff}$  does not include the gate-edge perimeter.

**Source/Drain Diffusion Resistance:** The source diffusion resistance is calculated by

**If**(number of sources NRS is given)

**ELSE if**(**rgeoMod**=0)

Source diffusion resistance  $R_{sdiff}$  is not generated.

**Else**

$R_{sdiff}$  computed from NF, DWJ, **geoMod**, DMCG, DMCI, DMDG, DMC GT, RSH, and MIN.

where the number of source squares NRS is an instance parameter. Similarly, the drain diffusion resistance is calculated by

**If**(number of sources NRD is given)

**ELSE if**(**rgeoMod**=0)

Drain diffusion resistance  $R_{ddiff}$  is not generated.

**Else**

$R_{ddiff}$  computed from NF, DWJ, **geoMod**, DMCG, DMCI, DMDG, DMC GT, RSH, and MIN.

**Gate Electrode Resistance:** The gate electrode resistance with multi-finger configuration is modeled by

$$R_{geltd} = \frac{RSHG \cdot \left( XGW + \frac{W_{effci}}{3NGCON} \right)}{NGCON \cdot \left( L_{drawn} - XGL \right) \cdot NF} \quad (4.1)$$

**Option for Source/Drain Connections:** Table 1 lists the options for source/drain connections through the model selector **geoMod**. For multi-finger devices, all inside S/D diffusions are assumed shared.

**Option for Source/Drain Contacts:** Table 2 lists the options for source/drain contacts through the model selector **rgeoMod**.



<b>geomod</b>	<b>End Source</b>	<b>End drain</b>	<b>Note</b>
0	isolated	isolated	NF=Odd
1	isolated	shared	NF=Odd, Even
2	shared	shared	NF=Odd, Even
3	shared	isolated	NF=Odd, Even
4	isolated	merged	NF=Odd
5	shared	merged	NF=Odd, Even
6	merged	isolated	NF=Odd
7	merged	shared	NF=Odd, Even
8	merged	merged	NF=Odd
9	sha/iso	shared	NF=Even
10	shared	sha/iso	NF=Even

Table 1: geoMod options.

<b>rgeoMod</b>	<b>End-source contact</b>	<b>End-drain contact</b>
0	No $R_{sdiff}$	No $R_{ddiff}$
1	wide	wide
2	wide	point
3	point	wide
4	point	point
5	wide	merged
6	point	merged
7	merged	wide
8	merged	point

Table 2: rgeoMod options.

## 5 Temperature dependence Models

### 5.1 Temperature Dependence Model

Accurate modeling of the temperature effects on MOSFET characteristics is important to predict circuit behavior over a range of operating temperatures (T). The operating temperature might be different from the nominal temperature (TNOM) at which the BSIM6 model parameters are extracted. This chapter presents the BSIM6 temperature dependence models for threshold voltage, mobility, saturation velocity, source/drain resistance, and junction diode IV and CV.

#### 5.1.1 Length Scaling of Temperature parameters

$$UTE = UTE \cdot \left(1 + UTEL \frac{1}{L_{eff}}\right) \quad (5.1)$$

$$UA1 = UA1 \cdot \left(1 + UA1L \frac{1}{L_{eff}}\right) \quad (5.2)$$

$$UD1 = UD1 \cdot \left(1 + UD1L \frac{1}{L_{eff}}\right) \quad (5.3)$$

$$AT = AT \cdot \left(1 + ATL \frac{1}{L_{eff}}\right) \quad (5.4)$$

$$PTWGT = PTWGT \cdot \left(1 + PTWGTL \frac{1}{L_{eff}}\right) \quad (5.5)$$

$$(5.6)$$

### 5.1.2 Temperature Dependence of Threshold Voltage

The temperature dependence of  $V_{th}$  is modeled by

$$V_{th}(T) = V_{th}(TNOM) + \left( KT1_i + KT2_i \cdot V_{bref} \right) \cdot \left( \left( \frac{T}{TNOM} \right)^{KT1EXP} - 1 \right)$$

$$V_{fb}(T) = V_{fb}(TNOM) - KT1 \cdot \left( \frac{T}{TNOM} - 1 \right) \quad (5.7)$$

$$VFBSDOFF(T) = VFBSDOFF(TNOM) \cdot [1 + TVFBSDOFF \cdot (T - TNOM)]$$

$$NFACTOR(T) = NFACTOR(TNOM) + TFACTOR \cdot \left( \frac{T}{TNOM} - 1 \right) \quad (5.8)$$

$$ETA0(T) = ETA0(TNOM) + TETA0 \left( \frac{T}{TNOM} - 1 \right) \quad (5.9)$$

### 5.1.3 Temperature Dependence of Mobility

$$U0(T) = U0(TNOM) \cdot (T/TNOM)^{UTE} \quad (5.10)$$

$$UA(T) = UA(TNOM)[1 + UA1 \cdot (T - TNOM)] \quad (5.11)$$

$$UC(T) = UC(TNOM)[1 + UC1 \cdot (T - TNOM)] \quad (5.12)$$

$$UD(T) = UD(TNOM) \cdot (T/TNOM)^{UD1} \quad (5.13)$$

$$UCS(T) = UCS(TNOM) \cdot (T/TNOM)^{UCSTE} \quad (5.14)$$

$$(5.15)$$

### 5.1.4 Temperature Dependence of Saturation Velocity

$$VSAT(T) = VSAT(TNOM) \cdot (T/TNOM)^{-AT} \quad (5.16)$$

### 5.1.5 Temperature Dependence of LDD Resistance

$$rdstemp = (T/TNOM)^{PRT} \quad (5.17)$$

$$(5.18)$$

**RDSMOD** = 0 (internal source/drain LDD resistance)

$$RDSW(T) = RDSW(TNOM) \cdot rdstemp \quad (5.19)$$

$$RDSWMIN(T) = RDSWMIN(TNOM) \cdot rdstemp \quad (5.20)$$

**RDSMOD** = 1 (external source/drain LDD resistance)

$$RDW(T) = RDW(TNOM) \cdot rdstemp \quad (5.21)$$

$$RDWMIN(T) = RDWMIN(TNOM) \cdot rdstemp \quad (5.22)$$

$$RSW(T) = RSW(TNOM) \cdot rdstemp \quad (5.23)$$

$$RSWMIN(T) = RSWMIN(TNOM) \cdot rdstemp \quad (5.24)$$

### 5.1.6 Temperature Dependence of Junction Diode IV

- **Source-side diode** The source-side diode is turned off if both  $A_{seff}$  and  $P_{seff}$  are zero. Otherwise, the source-side saturation current is given by

$$I_{sbs} = A_{seff} J_{ss}(T) + P_{seff} J_{ssws}(T) + W_{effcj} \cdot NF \cdot J_{sswgs}(T) \quad (5.25)$$

where

$$J_{ss}(T) = JSS(TNOM) \cdot \exp\left(\frac{\frac{E_g(TNOM)}{v_t(TNOM)} - \frac{E_g(T)}{v_t(T)} + XTIS \cdot \ln\left(\frac{T}{TNOM}\right)}{NJS}\right)$$

$$J_{ssws}(T) = JSSWS(TNOM) \cdot \exp\left(\frac{\frac{E_g(TNOM)}{v_t(TNOM)} - \frac{E_g(T)}{v_t(T)} + XTIS \cdot \ln\left(\frac{T}{TNOM}\right)}{NJS}\right)$$

$$J_{sswgs}(T) = JSSWGS(TNOM) \cdot \exp\left(\frac{\frac{E_g(TNOM)}{k_b \cdot TNOM} - \frac{E_g(T)}{k_b \cdot T} + XTIS \cdot \ln\left(\frac{T}{TNOM}\right)}{NJS}\right) \quad (5.26)$$

where  $E_g$  is given in Temperature Dependences of  $E_g$  and  $n_i$ .

- **Drain-side diode** The drain-side diode is turned off if both  $A_{seff}$  and  $P_{seff}$  are zero. Otherwise, the drain-side saturation current is given by

$$I_{sbd} = A_{def} J_{sd}(T) + P_{def} J_{sswd}(T) + W_{efcj} \cdot NF \cdot J_{sswgd}(T) \quad (5.27)$$

where

$$\begin{aligned} J_{sd}(T) &= JSD(TNOM) \cdot \exp\left(\frac{\frac{E_g(TNOM)}{k_b \cdot TNOM} - \frac{E_g(T)}{k_b \cdot T} + XTID \cdot \ln\left(\frac{T}{TNOM}\right)}{NJD}\right) \\ J_{sswd}(T) &= JSSWD(TNOM) \cdot \exp\left(\frac{\frac{E_g(TNOM)}{k_b \cdot TNOM} - \frac{E_g(T)}{k_b \cdot T} + XTID \cdot \ln\left(\frac{T}{TNOM}\right)}{NJD}\right) \\ J_{sswgd}(T) &= JSSWGD(TNOM) \cdot \exp\left(\frac{\frac{E_g(TNOM)}{k_b \cdot TNOM} - \frac{E_g(T)}{k_b \cdot T} + XTID \cdot \ln\left(\frac{T}{TNOM}\right)}{NJD}\right) \end{aligned} \quad (5.28)$$

### 5.1.7 Temperature Dependence of Junction Diode CV

- Source-side diode: The temperature dependences of zero-bias unit-length/area junction capacitances on the source side are modeled by

$$CJS(T) = CJS(TNOM) + TCJ \cdot (T - TNOM) \quad (5.29)$$

$$CJSWS(T) = CJSWS(TNOM) + TCJSW \cdot (T - TNOM) \quad (5.30)$$

$$CJSWGS(T) = CJSWGS(TNOM) + TCJSWG \cdot (T - TNOM) \quad (5.31)$$

The temperature dependences of the built-in potentials on the source side are modeled by

$$PBS(T) = PBS(TNOM) - TPB \cdot (T - TNOM) \quad (5.32)$$

$$PBSWS(T) = PBSWS(TNOM) - TPBSW \cdot (T - TNOM) \quad (5.33)$$

$$PBSWGS(T) = PBSWGS(TNOM) - TPBSWG \cdot (T - TNOM) \quad (5.34)$$

- Drain-side diode: The temperature dependences of zero-bias unit-length/area junction capacitances on the drain side are modeled by

$$CJS(T) = CJS(TNOM)[1 + TCJ \cdot (T - TNOM)] \quad (5.35)$$

$$CJSWS(T) = CJSWS(TNOM) + TCJSW \cdot (T - TNOM) \quad (5.36)$$

$$CJSWGS(T) = CJSWGS(TNOM)[1 + TCJSWG \cdot (T - TNOM)] \quad (5.37)$$

The temperature dependences of the built-in potentials on the drain side are modeled by

$$PBD(T) = PBD(TNOM) - TPB \cdot (T - TNOM) \quad (5.38)$$

$$PBSD(T) = PBSD(TNOM) - TPBSW \cdot (T - TNOM) \quad (5.39)$$

$$PBSWGD(T) = PBSWGD(TNOM) - TPBSWG \cdot (T - TNOM) \quad (5.40)$$

• trap-assisted tunneling (TAT) and recombination current

$$\begin{aligned}
J_{tsswgs}(T) &= J_{tsswgs}(TNOM) \cdot \left( \sqrt{\frac{JTWEFF}{W_{effcj}}} + 1 \right) \\
&\cdot \exp \left[ \frac{-E_g(TNOM)}{k_b T} \cdot X_{tsswgs} \cdot \left( 1 - \frac{T}{TNOM} \right) \right] \quad (5.41)
\end{aligned}$$

$$J_{tssws}(T) = J_{tssws}(TNOM) \cdot \exp \left[ \frac{-E_g(TNOM)}{k_b T} \cdot X_{tssws} \cdot \left( 1 - \frac{T}{TNOM} \right) \right]$$

$$J_{tss}(T) = J_{tss}(TNOM) \cdot \exp \left[ \frac{-E_g(TNOM)}{k_b T} \cdot X_{tss} \cdot \left( 1 - \frac{T}{TNOM} \right) \right]$$

$$\begin{aligned}
J_{tsswgd}(T) &= J_{tsswgd}(TNOM) \cdot \left( \sqrt{\frac{JTWEFF}{W_{effcj}}} + 1 \right) \\
&\cdot \exp \left[ \frac{-E_g(TNOM)}{k_b T} \cdot X_{tsswgd} \cdot \left( 1 - \frac{T}{TNOM} \right) \right] \quad (5.42)
\end{aligned}$$

$$J_{tsd}(T) = J_{tsd}(TNOM) \cdot \exp \left[ \frac{-E_g(TNOM)}{k_b T} \cdot X_{tsd} \cdot \left( 1 - \frac{T}{TNOM} \right) \right]$$

$$NJTSSWG(T) = NJTSSWG(TNOM) \cdot \left[ 1 + TNJTSSWG \left( \frac{T}{TNOM} - 1 \right) \right]$$

$$NJTSSW(T) = NJTSSW(TNOM) \cdot \left[ 1 + TNJTSSW \left( \frac{T}{TNOM} - 1 \right) \right]$$

$$NJTS(T) = NJTS(TNOM) \cdot \left[ 1 + TNJTS \left( \frac{T}{TNOM} - 1 \right) \right]$$

$$NJTSSWGD(T) = NJTSSWGD(TNOM) \cdot \left[ 1 + TNJTSSWGD \left( \frac{T}{TNOM} - 1 \right) \right]$$

$$NJTSSWD(T) = NJTSSWD(TNOM) \cdot \left[ 1 + TNJTSSWD \left( \frac{T}{TNOM} - 1 \right) \right]$$

$$NJTSSWD(T) = NJTSSWD(TNOM) \cdot \left[ 1 + TNJTSSWD \left( \frac{T}{TNOM} - 1 \right) \right]$$

$$NJTSD(T) = NJTSD(TNOM) \cdot \left[ 1 + TNJTSD \left( \frac{T}{TNOM} - 1 \right) \right]$$

(5.43)

### 5.1.8 Temperature Dependences of $E_g$ and $n_i$

- Energy-band gap of channel ( $E_g$ ): The temperature dependence of  $E_g$  is modeled by

$$E_{g0} = BG0SUB - \frac{TBGASUB \times Tnom^2}{Tnom + TBGBSUB} \quad (5.44)$$

$$E_g = BG0SUB - \frac{TBGASUB \times T^2}{T + TBGBSUB} \quad (5.45)$$

- Intrinsic carrier concentration of non-silicon channel ( $n_i$ )

$$n_i = NI0SUB \times \left( \frac{T}{Tnom} \right)^{(3/2)} \times \exp\left( \frac{Eg}{2 \frac{kTnom}{q}} - \frac{Eg}{2 \frac{kT}{q}} \right) \quad (5.46)$$

## 6 Stress effect Model Development

### 6.1 Stress Effect Model

CMOS feature size aggressively scaling makes shallow trench isolation(STI) very popular active area isolation process in advanced technologies. Recent years, strain channel materials have been employed to achieve high device performance. The mechanical stress effect induced by these process causes MOSFET performance function of the active area size(OD: oxide definition) and the location of the device in the active area. And the necessity of new models to describe the layout dependence of MOS parameters due to stress effect becomes very urgent in advance CMOS technologies. Influence of stress on mobility has been well known since the 0.13um technology. The stress influence on saturation velocity is also experimentally demonstrated. Stress-induced enhancement or suppression of dopant diffusion during the processing is reported. Since the doping profile may be changed due to different STI sizes and stress, the threshold voltage shift and changes of other second-order effects, such as DIBL and body effect, were shown in process integration. BSIM4 considers the influence of stress on mobility, velocity saturation, threshold voltage, body effect, and DIBL effect.



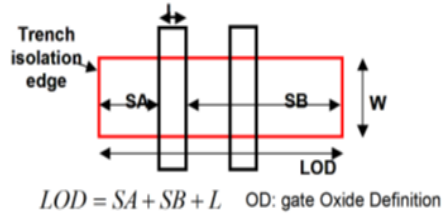


Figure 7: the typical layout of a MOSFET

### 6.1.1 Stress Effect Model Development

Experimental analysis show that there exist at least two different mechanisms within the influence of stress effect on device characteristics. The first one is mobility-related and is induced by the band structure modification. The second one is  $V_{th}$ -related as a result of doping profile variation. Both of them follow the same  $1/LOD$  trend but reveal different L and W scaling. We have derived a phenomenological model based on these findings by modifying some parameters in the BSIM model. Note that the following equations have no impact on the iteration time because there are no voltage-controlled components in them.

**Mobility-related Equations:** This model introduces the first mechanism by adjusting the  $U_0$  and  $V_{sat}$  according to different W, L and OD shapes. Define mobility relative change due to stress effect as :

$$\rho_{\mu_{eff}} = \Delta\mu_{eff}/\mu_{effo} = (\mu_{eff} - \mu_{effo})/\mu_{effo} = \frac{\mu_{eff}}{\mu_{effo}} - 1 \quad (6.1)$$

So,

$$\frac{\mu_{eff}}{\mu_{effo}} = 1 + \rho_{\mu_{eff}} \quad (6.2)$$

Figure 7 shows the typical layout of a MOSFET on active layout surrounded by STI isolation. SA, SB are the distances between isolation edge to Poly from one and the other side, respectively. 2D simulation shows that stress distribution can be expressed by a simple function of SA and SB. Assuming that mobility relative change is proportional to stress distribution. It can be described as function of SA, SB(LOD effect), L, W, and

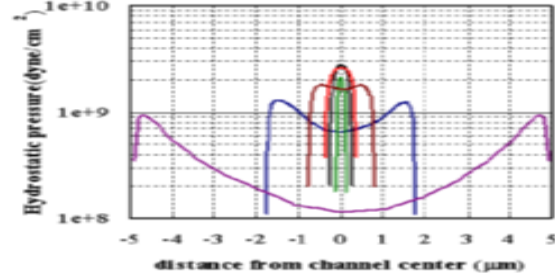


Figure 8: Stress distribution within MOSFET channel using 2D simulation

T dependence:

$$\rho_{\mu_{eff}} = \frac{KU0}{Kstress_{u0}} \cdot (Inv_{sa} + Inv_{sb}) \quad (6.3)$$

where:

$$Inv_{sa} = \frac{1}{SA + 0.5 \cdot L_{drawn}} \quad (6.4)$$

$$Inv_{sb} = \frac{1}{SB + 0.5 \cdot L_{drawn}} \quad (6.5)$$

$$Kstress_{u0} = \left( 1 + \frac{LKU0}{(L_{drawn} + XL)^{LLODKU0}} + \frac{WKU0}{(W_{drawn} + XW + WLOD)^{WLODKU0}} + \frac{PKU0}{(L_{drawn} + XL)^{LLODKU0} \cdot (W_{drawn} + XW + WLOD)^{WLODKU0}} \right) \times \left( 1 + TKU0 \cdot \left( \frac{Temperature}{TNOM} - 1 \right) \right) \quad (6.6)$$

So that:

$$\mu_{eff} = \frac{1 + \rho_{\mu_{eff}}(SA, SB)}{1 + \rho_{\mu_{eff}}(SA_{ref}, SB_{ref})} \mu_{effo} \quad (6.7)$$

$$v_{sattemp} = \frac{1 + KVSAT \cdot \rho_{\mu_{eff}}(SA, SB)}{1 + KVSAT \cdot \rho_{\mu_{eff}}(SA_{ref}, SB_{ref})} v_{sattempo} \quad (6.8)$$

and  $SA_{ref}$ ,  $SB_{ref}$  are reference distances between OD edge to poly from one and the other side.

**Vth-related Equations:**  $V_{th0}$  (threshold voltage without stress effect),  $K_2$  and  $ETA_0$  are modified to cover the doping profile change in the devices with different LOD. They use the same  $1/LOD$  formulas as shown in earlier sections, but different equations for  $W$  and  $L$  scaling:

$$\begin{aligned}
V_{TH0} &= V_{TH0_{original}} + \frac{KV_{TH0}}{K_{stress\_vth0}} \cdot (Inv\_sa + Inv\_sb - Inv\_sa_{ref} - Inv\_sb_{ref}) \\
K_2 &= K_{2_{original}} + \frac{STK_2}{K_{stress\_vth0}^{LODK_2}} \cdot (Inv\_sa + Inv\_sb - Inv\_sa_{ref} - Inv\_sb_{ref}) \\
ETA_0 &= ETA_{0_{original}} + \frac{STETA_0}{K_{stress\_vth0}^{LODETA_0}} \cdot (Inv\_sa + Inv\_sb - Inv\_sa_{ref} - Inv\_sb_{ref})
\end{aligned} \tag{6.9}$$

where:

$$Inv\_sa_{ref} = \frac{1}{SA_{ref} + 0.5 \cdot L_{drawn}} \tag{6.10}$$

$$Inv\_sb_{ref} = \frac{1}{SB_{ref} + 0.5 \cdot L_{drawn}} \tag{6.11}$$

$$\begin{aligned}
K_{stress\_vth0} &= \left( 1 + \frac{LKV_{TH0}}{(L_{drawn} + XL)^{LLODKVTH}} \right. \\
&\quad + \frac{WKV_{TH0}}{(W_{drawn} + XW + WLOD)^{WLODKVTH}} \\
&\quad \left. + \frac{PKV_{TH0}}{(L_{drawn} + XL)^{LLODKVTH} \cdot (W_{drawn} + XW + WLOD)^{WLODKVTH}} \right) \tag{6.12}
\end{aligned}$$

**Multiple Finger Device:** For multiple finger device, the total LOD effect is the average of LOD effect to every finger. That is (see Figure 9) for the layout for multiple

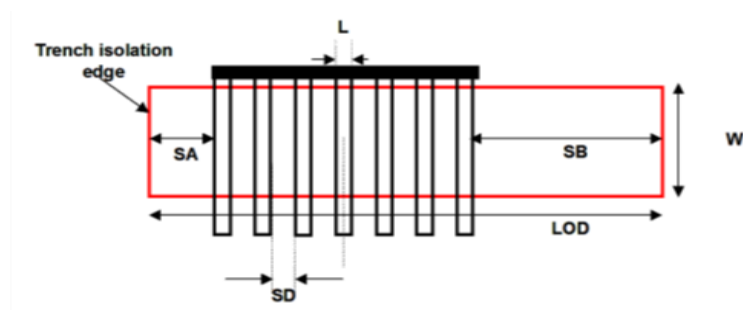


Figure 9: Layout of multiple finger MOSFET

finger device):

$$Inv_{sa} = \frac{1}{NF} \sum_{i=0}^{NF-1} \frac{1}{SA + 0.5 \cdot L_{drawn} + i \cdot (SD + L_{drawn})} \quad (6.13)$$

$$Inv_{sb} = \frac{1}{NF} \sum_{i=0}^{NF-1} \frac{1}{SB + 0.5 \cdot L_{drawn} + i \cdot (SD + L_{drawn})} \quad (6.14)$$

$$(6.15)$$

### 6.1.2 Effective SA and SB for Irregular LOD

General MOSFET has an irregular shape of active area shown in Figure 10. To fully describe the shape of OD region will require additional instance parameters. However, this will result in too many parameters in the net lists and would massively increase the read-in time and degrade the readability of parameters. One way to overcome this difficulty is the concept of effective SA and SB similar to [17]. Stress effect model as described earlier allows an accurate and efficient layout extraction of effective SA and

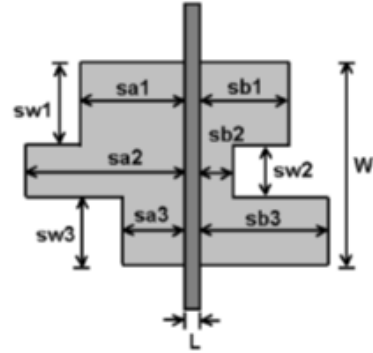


Figure 10: A typical layout of MOS devices with more instance parameters ( $sw_i$ ,  $sa_i$  and  $sb_i$ ) in addition to the traditional  $L$  and  $W$

SB while keeping fully compatibility of the LOD model. They are expressed as:

$$\frac{1}{SA_{eff} + 0.5 \cdot L_{drawn}} = \sum_{i=1}^n \frac{sw_i}{W_{drawn}} \cdot \frac{1}{sa_i + 0.5 \cdot L_{drawn}} \quad (6.16)$$

$$\frac{1}{SB_{eff} + 0.5 \cdot L_{drawn}} = \sum_{i=1}^n \frac{sw_i}{W_{drawn}} \cdot \frac{1}{sb_i + 0.5 \cdot L_{drawn}} \quad (6.17)$$

$$(6.18)$$

**Stress Model for EDGEFET:** Same stress model is implemented for the EDGEFET. New parameters are **SAEDGE**, **SBEDGE**, **KVTH0EDGE**, **STK2EDGE**, **STETA0EDGE**.

## 7 Well Proximity Effect Model

## 8 Well Proximity Effect Model

Retrograde well profiles have several key advantages for highly scaled bulk complementary metal oxide semiconductor (CMOS) technology. With the advent of high-energy implanters and reduced thermal cycle processing, it has become possible to provide a

relatively heavily doped deep nwell and pwell without affecting the critical device-related doping at the surface. The deep well implants provide a low resistance path and suppress parasitic bipolar gain for latchup protection, and can also improve soft error rate and noise isolation. A deep buried layer is also key to forming triple-well structures for isolated-well NMOSFETs. However, deep buried layers can affect devices located near the mask edge. Some of the ions scattered out of the edge of the photoresist are implanted in the silicon surface near the mask edge, altering the threshold voltage of those devices [18]. It is observed a threshold voltage shifts of up to 100 mV in a deep boron retrograde pwell, a deep phosphorus retrograde nwell, and also a triple-well implementation with a deep phosphorus isolation layer below the pwell over a lateral distance on the order of a micrometer [18]. This effect is called well proximity effect. BSIM6 considers the influence of well proximity effect on threshold voltage, mobility, and body effect. This well proximity effect model is developed by the Compact Model Council [19].

## 8.1 Well Proximity Effect Model

Experimental analysis [18] shows that well proximity effect is strong function of distance of FET from mask edge, and electrical quantities influenced by it follow the same geometrical trend. A phenomenological model based on these findings has been developed by modifying some parameters in the BSIM model. Note that the following equations have no impact on the iteration time because there are no voltage controlled components in them. Well proximity affects threshold voltage, mobility and the body effect of the device. The effect of the well proximity can be described through the following equations :

If SCA, SCB, SCC are given then WPE is given by (8.1), otherwise it is given by (8.2)

$$\begin{aligned}
 V_{th0} &= V_{th0_{org}} + KV_{TH0WE} \cdot (SCA + WEB \cdot SCB + WEC \cdot SCC) \\
 K2 &= K2_{org} + K2WE \cdot (SCA + WEB \cdot SCB + WEC \cdot SCC) \\
 \mu_{eff} &= \mu_{eff,org} \cdot (1 + KU0WE \cdot (SCA + WEB \cdot SCB + WEB \cdot SCC)) \quad (8.1)
 \end{aligned}$$

$$\begin{aligned}
W_{drn} &= W/NF \\
T1 &= SC + W_{drn} \\
T2 &= 1.0/SCREF \\
T3 &= \exp(-10.0 \cdot SC \cdot T2) \\
T4 &= \exp(-10.0 \cdot T1 \cdot T2) \\
T5 &= \exp(-20.0 \cdot SC \cdot T2) \\
T6 &= \exp(-20.0 \cdot T1 \cdot T2) \\
LOCAL_{SCA} &= \frac{SCREF \cdot SCREF}{SC \cdot T1} \\
LOCAL_{SCB} &= \frac{(0.1 \cdot SC + 0.01 \cdot SCREF) \cdot T3 - (0.1 \cdot T1 + 0.01 \cdot SCREF) \cdot T4}{W_{drn}} \\
LOCAL_{SCC} &= \frac{(0.05 \cdot SC + 0.0025 \cdot SCREF) \cdot T5 - (0.05 \cdot T1 + 0.0025 \cdot SCREF) \cdot T6}{W_{drn}} \\
Vth0 &= Vth0_{org} + KVTH0WE \cdot (LOCAL_{SCA} + WEB \cdot LOCAL_{SCB} + WEC \cdot LOCAL_{SCC}) \\
K2 &= K2_{org} + K2WE \cdot (LOCAL_{SCA} + WEB \cdot LOCAL_{SCB} + WEC \cdot LOCAL_{SCC}) \\
\mu_{eff} &= \mu_{eff,org} \cdot (1 + KU0WE \cdot (LOCAL_{SCA} + WEB \cdot LOCAL_{SCB} + WEB \cdot LOCAL_{SCC}))
\end{aligned} \tag{8.2}$$

where SCA, SCB, SCC are instance parameters that represent the integral of the first/second/third distribution function for scattered well dopant. The guidelines for calculating the instance parameters SCA, SCB, SCC have been developed by the Compact Model Council which can be found at the CMC website [19].

## 9 C-V Model

**Inversion Charge :** Total inversion charge (excluding velocity saturation, CLM and poly depletion) can be expressed explicitly in terms of normalized charge densities at source and drain sides as follows,

$$Q_I = W \cdot \int_0^L Q_i dx \quad (9.1)$$

$$= -WL \cdot C_{ox} \cdot V_t \int_0^1 2 \cdot n_q \cdot q d\xi \quad (9.2)$$

$$-\frac{Q_I}{WL \cdot C_{ox} V_t} = q_I = 2 \cdot n_q \cdot \int_0^1 q d\xi \quad (9.3)$$

Here  $\xi = \frac{x}{L}$ . Inversion charge density is normalized to  $-2 \cdot n_q \cdot C_{ox} \cdot V_t$  and voltages to  $V_t$ . From (2.222),

$$I_{ds} = -2 \cdot n_q \cdot \mu_{eff} \cdot \frac{W_{eff}}{L_{eff}} \cdot C_{ox} \cdot nV_t^2 \cdot (2q + 1) \frac{dq}{d\xi} \quad (9.4)$$

Normalizing current with  $2 \cdot n_q \cdot \mu_{eff} \cdot \frac{W_{eff}}{L_{eff}} \cdot C_{ox} \cdot nV_t^2$ ,

$$i = -(2q + 1) \frac{dq}{d\xi} \quad (9.5)$$

which gives  $d\xi = -\frac{(2q+1)}{i} dq = -\frac{(2q+1)}{(q_s - q_d)(1 + q_s + q_d)}$ . Substituting in (9.3)

$$q_I = -\frac{2n_q}{(q_s - q_d)(1 + q_s + q_d)} \int_{q_s}^{q_d} q(2q + 1) dq \quad (9.6)$$

$$= -\frac{2n_q}{(q_s - q_d)(1 + q_s + q_d)} \left[ \frac{2}{3}(q_d^3 - q_s^3) + \frac{1}{2}(q_d^2 - q_s^2) \right] \quad (9.7)$$

on rearranging,

$$q_I = n_q \cdot \left[ q_s + q_d + \frac{1}{3} \cdot \frac{(q_s - q_d)^2}{1 + q_s + q_d} \right] \quad (9.8)$$

**Bulk Charge:** Bulk charge density is given as

$$Q_b = -C_{ox} \cdot (V_G - V_{FB} - \psi_S) - Q_i \quad (9.9)$$

$$(9.10)$$



using charge linearization

$$Q_b = -C_{ox} \cdot (V_G - V_{FB} - \psi_P) - Q_i \left(1 - \frac{1}{n_q}\right) \quad (9.11)$$

Total bulk charge,

$$Q_B = W \cdot \int_0^L Q_b dx \quad (9.12)$$

$$= -WL \cdot C_{ox} \cdot \left[ V_G - V_{FB} - \psi_P + \left(1 - \frac{1}{n_q}\right) \cdot \int_0^1 \frac{Q_i}{C_{ox}} d\xi \right] \quad (9.13)$$

Normalizing the bulk charge to  $-W.L.C_{ox}.V_t$ ,

$$q_B = v_g - v_{fb} - \psi_p - 2(n_q - 1) \cdot \int_0^1 q d\xi \quad (9.14)$$

We know that  $i_{ds} = -(2q + 1) \frac{dq}{d\xi}$  with  $i_{ds}$  given by (2.230). Thus  $d\xi = -\frac{-(2q+1)}{i_{ds}} dq$ ,

$$q_B = v_g - v_{fb} - \psi_p + \frac{2(n_q - 1)}{i_{ds}} \cdot \int_{q_s}^{q_d} q(2q + 1) dq \quad (9.15)$$

$$= v_g - v_{fb} - \psi_p + \frac{2(n_q - 1)}{(q_s - q_d)(1 + q_s + q_d)} \int_{q_s}^{q_d} \left[ \frac{2q^3}{3} + \frac{q^2}{2} \right] \quad (9.16)$$

$$= v_g - v_{fb} - \psi_p + \frac{2(n_q - 1)}{(q_s - q_d)(1 + q_s + q_d)} \left[ \frac{2}{3} \cdot (q_d - q_s)(q_d^2 + q_s^2 + q_s \cdot q_d) + \frac{1}{2} \cdot (q_d - q_s)(q_d + q_s) \right] \quad (9.17)$$

which on rearrangement becomes,

$$q_B = v_g - v_{fb} - \psi_p - (n_q - 1) \left[ q_s + q_d + \frac{1}{3} \cdot \frac{(q_s - q_d)^2}{1 + q_s + q_d} \right] \quad (9.18)$$

Bulk charge with poly depletion effect :

$$q_B = A + B + \frac{1}{3} \cdot \frac{\Delta q^2}{C^3} \cdot \left[ \frac{4}{8} \cdot \left( C^2 + P \cdot Q \right) \cdot \frac{1}{1 + q_s + q_d} + \frac{2}{\gamma_g^2} \right] - n_q \cdot \left[ q_s + q_d + \frac{1}{3} \cdot \frac{(q_s - q_d)^2}{1 + q_s + q_d} \right] \quad (9.19)$$

where

$$P = \sqrt{\frac{1}{4} + \frac{v_g - v_{fb} - \psi_p + 2.q_s}{\gamma_g^2}} \quad (9.20)$$

$$Q = \sqrt{\frac{1}{4} + \frac{v_g - v_{fb} - \psi_p + 2.q_d}{\gamma_g^2}} \quad (9.21)$$

$$A = \frac{v_g - v_{fb} - \psi_p + 2.q_s}{1 + 2 \cdot \sqrt{\frac{1}{4} + \frac{v_g - v_{fb} - \psi_p + 2.q_s}{\gamma_g^2}}} \quad (9.22)$$

$$B = \frac{v_g - v_{fb} - \psi_p + 2.q_d}{1 + 2 \cdot \sqrt{\frac{1}{4} + \frac{v_g - v_{fb} - \psi_p + 2.q_d}{\gamma_g^2}}} \quad (9.23)$$

$$C = \sqrt{\frac{1}{4} + \frac{v_g - v_{fb} - \psi_p + 2.q_s}{\gamma_g^2}} + \sqrt{\frac{1}{4} + \frac{v_g - v_{fb} - \psi_p + 2.q_d}{\gamma_g^2}} \quad (9.24)$$

Bulk charge with poly depletion effect, CLM and Velocity Saturation effects :

$$d_{qgeff} = (v_g - v_{fb} - \psi_p + 2.q_d) \left[ \frac{2\sqrt{\frac{1}{4} + \frac{v_g - v_{fb} - \psi_p + 2.q_d}{\gamma_g^2}} - 1}{2\sqrt{\frac{1}{4} + \frac{v_g - v_{fb} - \psi_p + 2.q_d}{\gamma_g^2}} + 1} \right] \quad (9.25)$$

$$q_{beff} = \left[ (v_g - v_{fb} - \psi_p) - 2(n_q - 1)q_d + d_{qgeff} \right] \quad (9.26)$$

$$q_B = \frac{1}{MDL} \left[ A + B + \frac{1}{3} \cdot \frac{\Delta q^2}{C^3} \cdot \left( \frac{4}{8} \cdot (C^2 + P \cdot Q) \cdot \frac{1}{1 + q_s + q_d} + \frac{2}{\gamma_g^2} \right) - n_q \cdot \left( q_s + q_d + \frac{1}{3} \cdot \frac{(q_s - q_d)^2}{1 + q_s + q_d} \right) \right] + (MDL - 1)q_{beff} \quad (9.27)$$

where

$$P = \sqrt{\frac{1}{4} + \frac{v_g - v_{fb} - \psi_p + 2 \cdot q_s}{\gamma_g^2}} \quad (9.28)$$

$$Q = \sqrt{\frac{1}{4} + \frac{v_g - v_{fb} - \psi_p + 2 \cdot q_d}{\gamma_g^2}} \quad (9.29)$$

$$A = \frac{v_g - v_{fb} - \psi_p + 2 \cdot q_s}{1 + 2 \cdot \sqrt{\frac{1}{4} + \frac{v_g - v_{fb} - \psi_p + 2 \cdot q_s}{\gamma_g^2}}} \quad (9.30)$$

$$B = \frac{v_g - v_{fb} - \psi_p + 2 \cdot q_d}{1 + 2 \cdot \sqrt{\frac{1}{4} + \frac{v_g - v_{fb} - \psi_p + 2 \cdot q_s}{\gamma_g^2}}} \quad (9.31)$$

$$C = \sqrt{\frac{1}{4} + \frac{v_g - v_{fb} - \psi_p + 2 \cdot q_s}{\gamma_g^2}} + \sqrt{\frac{1}{4} + \frac{v_g - v_{fb} - \psi_p + 2 \cdot q_d}{\gamma_g^2}} \quad (9.32)$$

### Source and Drain Charges

$$Q_s = \frac{n_q}{3} \left[ 2 \cdot q_s + q_{def} + \frac{1}{2} \cdot \left( 1 + \frac{4}{5} \cdot q_s + \frac{6}{5} \cdot q_{def} \right) \left( \frac{q_s - q_{def}}{1 + q_s + q_{def}} \right)^2 \right] \quad (9.33)$$

$$Q_d = \frac{n_q}{3} \left[ q_s + 2 \cdot q_{def} + \frac{1}{2} \cdot \left( 1 + \frac{6}{5} \cdot q_s + \frac{4}{5} \cdot q_{def} \right) \left( \frac{q_s - q_{def}}{1 + q_s + q_{def}} \right)^2 \right] \quad (9.34)$$

### Source and Drain Charges with CLM and Velocity Saturation Model

$$Q_i = \frac{n_q}{MDL} \left[ (q_s + q_{def}) + \frac{1}{3} (q_s - q_{def})^2 \frac{DVSAT}{MDL \cdot (1 + q_s + q_{def})} + 2n_q(MDL - 1)q_{def} \right] \quad (9.35)$$

$$Q_d = \frac{n_q}{3 \cdot MDL^2} \left[ q_s + 2 \cdot q_{def} + \frac{1}{2} \cdot \left( \frac{1}{5} \cdot (q_s - q_{def}) + \frac{MDL}{DVSAT} \cdot (1 + q_s + q_{def}) \right) \left( \frac{q_s - q_{def}}{1 + q_s + q_{def}} \right)^2 \left( \frac{DVSAT}{MDL} \right)^2 \right] + n_q \left[ MDL - \frac{1}{MDL} \right]$$

$$Q_s = Q_i - Q_d \quad (9.36)$$

$$(9.37)$$

## Quantum Mechanical Effect

$$X_{DC}^{inv} = \frac{ADOS \cdot (1.9 \cdot 10^{-9})}{1 + \left[ \frac{Q_i + ETAQM \cdot Q_B}{QMO} \right]^{0.7 * BDOS}} \quad (9.38)$$

$$C_{ox}^{inv} = \frac{3.9 \cdot \epsilon_0}{TOXP \cdot \frac{3.9}{EPSROX} + \frac{X_{DC}^{inv}}{\epsilon_{ratio}}} \quad (9.39)$$

Intrinsic Charge expressions:

$$WLCOXVt_{inv} = NF \cdot Wact \cdot Lact \cdot C_{ox}^{inv} \cdot nVt \quad (9.40)$$

$$QBi = -NF \cdot Wact \cdot Lact \cdot \left( \frac{\epsilon_0 \cdot EPSROX}{TOXP} \right) \cdot nVt \cdot Qb \quad (9.41)$$

$$QSi = -WLCOXVt_{inv} \cdot Qs \quad (9.42)$$

$$QDi = -WLCOXVt_{inv} \cdot Qd \quad (9.43)$$

$$QGi = QSi + QDi + QBi \quad (9.44)$$

## Bias-dependent overlap capacitance model

An accurate overlap capacitance model is essential. This is especially true for the drain side where the effect of the capacitance is amplified by the transistor gain. The overlap capacitance changes with gate to source and gate to drain biases. In LDD MOSFETs a substantial portion of the LDD region can be depleted, both in the vertical and lateral directions. This can lead to a large reduction of the overlap capacitance. This LDD region can be in accumulation or depletion. We use a single equation for both regions by using such smoothing parameters as  $V_{gs,overlap}$  and  $V_{gd,overlap}$  for the source and drain side, respectively. Unlike the case with the intrinsic capacitance, the overlap capacitances are reciprocal. In other words,  $C_{gs,overlap} = C_{sg,overlap}$  and  $C_{gd,overlap} = C_{dg,overlap}$ .

The bias-dependent overlap capacitance model in BSIM6 is adopted from BSIM4. The overlap charge is given by:

$$\frac{Q_{gs,ov}}{NF \cdot W_{effCV}} = CGSO \cdot V_{gs} + CGSL \cdot \left[ V_{gs} - V_{fbsd} - V_{gs,overlap} - \frac{CKAPPAS}{2} \left( \sqrt{1 - \frac{4V_{gs,overlap}}{CKAPPAS}} - 1 \right) \right] \quad (9.45)$$

$$\frac{Q_{gd,ov}}{NF \cdot W_{effCV}} = CGDO \cdot V_{gd} + CGDL \cdot \left[ V_{gd} - V_{fbsd} - V_{gd,overlap} - \frac{CKAPPAD}{2} \left( \sqrt{1 - \frac{4V_{gd,overlap}}{CKAPPAD}} - 1 \right) \right] \quad (9.46)$$

$$V_{gs,overlap} = \frac{1}{2} \left[ V_{gs} - V_{fbsd} + \delta_1 - \sqrt{(V_{gs} - V_{fbsd} + \delta_1)^2 + 4\delta_1} \right] \quad (9.47)$$

$$V_{gd,overlap} = \frac{1}{2} \left[ V_{gd} - V_{fbsd} + \delta_1 - \sqrt{(V_{gd} - V_{fbsd} + \delta_1)^2 + 4\delta_1} \right] \quad (9.48)$$

$$\delta_1 = 0.02V \quad (9.49)$$

### Outer Fringing Capacitance

The fringing capacitance consists of a bias-independent outer fringing capacitance and a bias-dependent inner fringing capacitance. Only the bias-independent outer fringing capacitance is modeled. If CF is not given then outer fringe capacitance is calculated as

$$CF = \frac{2 \cdot EPSROX \cdot \epsilon_0}{\pi} \cdot \ln[CFRcoeff \cdot (1 + \frac{0.4e-6}{TOX})] \quad (9.50)$$

## 10 Parameter Extraction Procedure

The objective of this section is to provide guidelines for the extraction of the main model parameters. The procedure is structured in such a way that parameters linked to specific psychical phenomena are extracted from analyses where these effects are prominent. Although parameter extraction is not always a straight-forward procedure, the aim is to minimize the effort invested and the number of the essential loops performed.

If all the steps of the described procedure are followed then a global model card is obtained which means that the model can be used across the entire width/length plane of the technology. If a local fitting is targeted, then only the parameters of Section 10.1 need to be extracted for each DUT. However, in that case binning is necessary if the model card is to be used for the entire geometry range of the technology. Irrespectively of the choice between global and local fitting, different model cards should be extracted for nmos and pmos devices or for different technologies.

Before proceeding to the extraction of any parameter, it is very important that **TNOM** is set to the value of the temperature at which the measurements were carried out. Also, it is recommended that if they are available, the values of the process parameters are provided. The most common process parameters are shown in Table 3.

Parameter Name	Physical Description
<b>EPSROX</b>	Relative Gate Dielectric Constant
<b>EPSRSUB</b>	Relative Dielectric Constant of the Channel
<b>TOXE</b>	Electrical Gate Equivalent Oxide Thickness
<b>TOXP</b> or <b>DTOX</b>	Physical Gate Equivalent Oxide Thickness
<b>NDEP</b>	Channel Doping Concentration
<b>NGATE</b>	Gate Doping Concentration
<b>NSD</b>	S/D Doping Concentration
<b>XJ</b>	S/D Junction Depth
<b>XW/XL</b>	Channel W/L Offset due to Mask/Etch Effect

Table 3: Process parameters which are recommended to be provided before parameter extraction.

## 10.1 Extraction of Geometry Independent Parameters

The first part of the model parameter extraction procedure is to extract the parameters that are related to the main physical phenomena, which define transistor's behavior, and are also geometry independent. For that, a wide and long channel device should be chosen. At this point, **WWIDE** and **LLONG** parameters must be assigned to the values of the width and length of this large chosen DUT. This ensures that once the behavior of the long/wide channel device is fitted, it cannot be further affected by the values scaling parameters that will be extracted in the next steps.

### 10.1.1 Gate Capacitance $C_{GG}$ vs. $V_G$ Analysis @ $V_S = 0 V$ , $V_D = 0 V$ & $V_B = 0 V$

At this step process parameters and parameters related to quantum mechanical effect are extracted. Even if values have been already assigned to process parameters, a fine tuning should be made in order to fit accurately the electrical behavior of the device. From  $C_{GG}$  vs.  $V_G$  analysis the following process parameters can be extracted: **NDEP**, **TOXE**, **VFB** and **NGATE**. Each of these parameters affects a different region or in a different way the  $C_{GG}$  capacitance, so they should be extracted accordingly. More specifically:

- **VFB** is defining the flat-band voltage of the device and it can be extracted by studying the region from depletion till the onset of strong-inversion.
- **NDEP** is affecting  $C_{GG}$  in the depletion region. If possible, **NDEP**, which defines the doping level, is better to be extracted from  $C_{GB}$  vs.  $V_G$  analysis (S and D terminals are grounded).
- **TOXE** is affecting the deep accumulation and strong-inversion regions.
- **NGATE** is related to the poly-silicon depletion effect, so it affects the slope of  $C_{GG}$  in the strong-inversion region.

Furthermore, the value of  $C_{OX}$  is affected by the Quantum Mechanical effect. So, the parameters: **ADOS**, **BDOS**, **QM0** and **ETAQM** are also extracted from  $C_{GG}$  vs.  $V_G$  analysis, when focusing at the slope of  $C_{GG}$  at the onset of the strong-inversion region.

### 10.1.2 Drain Current $I_D$ vs. $V_G$ Analysis @ $V_D = [V_{D,lin}, V_{D,sat}]$ , $V_S = 0$ V & $V_B = 0$ V

In this step, the  $V_G$  dependence of the drain current -  $I_D$ , is extracted. Different parameters are extracted in two different regions of operation, namely *linear mode* (i.e.  $V_D \ll V_G - V_{TH}$ ) and *saturation* (i.e.  $V_D \gg V_G - V_{TH}$ ). It is very important that during extraction in this step, both  $I_D$  and the transconductance -  $g_m$  (even  $g'_m$  and  $g''_m$ ) are extracted at once.

#### Linear Mode

- Focusing in *weak-inversion* region ( $I_D$  vs.  $V_G$  characteristic when y-axis is in logarithmic scale), **NFACTOR**, which is related to the sub-threshold slope of the  $I_D$ , can be extracted. Furthermore, a fine tuning of the **NDEP** and **VFB** parameters is performed. In case the values of **NDEP** and **VFB** obtained during the fitting of  $I_D$  vs.  $V_G$  characteristic differ much from those obtained during the fitting of  $C_{GG}$  vs.  $V_G$  characteristic (Section 10.1.1), parameters **NDEPCV** and **VFBCV** can be used for dynamic operation (CV) and **NDEP** and **VFB** for static operation (IV). In general, using different values for **NDEP** and **NDEPCV** for IV and CV operation is not recommended unless necessary.
- From *strong-inversion* region, the mobility **U0**, the parameter for the effective field **ETAMOB**, the parameters related to the effect of mobility reduction due to vertical field **UA** and **EU** and the parameters for the coulomb scattering effect **UD** and **UCS**, are extracted. Furthermore, the parameters for S/D series resistances are also extracted under the same bias conditions. If **RDSMOD = 0** (internal S/D series resistances), **RDSW** is extracted. Otherwise, **RSW** and **RDW** are extracted.

#### Saturation

- From *weak-inversion* region ( $I_D$  vs.  $V_G$  characteristic when y-axis is in logarithmic scale), **CDSCD** parameter, which is linked to the dependence of the sub-threshold slope on drain bias, is extracted.
- Focusing in *strong-inversion* region, the parameters that are connected to the velocity saturation effect, namely **VSAT**, **PSAT**, **PTWG** and **PSATX**, can be extracted. **PSATX** does need to be changed.



Finally, from *accumulation* to *depletion* region, in both *linear mode* and *saturation*, the parameters related to GIDL effect are extracted. First, the selector **GIDLMOD** should be set to 1 to activate GIDL/GILS currents and then the parameters **AGIDL**, **BGIDL**, **CGIDL** and **EGIDL** are extracted. Ideally GIDL and GILS currents should be equal, so it is sufficient to extract **AGIDL**, **BGIDL**, **CGIDL** and **EGIDL** parameters. But in case GIDL and GILS currents differ, then parameters **AGISL**, **BGISL**, **CGISL** and **EGISL** can also be used.

### 10.1.3 Gate Current $I_G$ vs. $V_G$ Analysis @ various $V_D$ , $V_S = 0 V$ & $V_B = 0 V$

From  $I_G$  vs.  $V_G$  analysis, parameters related to the gate current can be extracted. First, the tunneling components should be activated by setting to 1 the selectors **IGCMOD** and **IGBMOD**. Different parameters are extracted in different regions of operation and more specifically:

Accumulation to weak-inversion Region

- **AIGBACC**, **BIGBACC**, **CIGBACC** and **NIGBACC**, which are linked to the gate-to-substrate current component determined by ECB.
- **AIGS**, **BIGS** and **CIGS**, which are linked to the tunneling current between the gate and the source diffusion region and **AIGD**, **BIGD** and **CIGD**, which are linked to the tunneling current between the gate and the drain diffusion region.
- **DLCIG** and **DLCIGD**, which are linked to the S/D overlap length for  $I_{GS}$  and  $I_{GD}$  respectively.

Weak to strong-inversion Region

- **AIGBINV**, **BIGBINV**, **CIGBINV**, **EIGBINV** and **NIGBINV**, which are linked to the gate-to-substrate current component determined by EVB.
- **AIGC**, **BIGC**, **CIGC**, **NIGC** and **PIGCD**, which are linked to the gate-to-channel current. **PIGCD** is expressing the  $V_D$  dependence of gate-to-channel current.

#### 10.1.4 Drain Current $I_D$ vs. $V_D$ Analysis @ various $V_G$ , $V_S = 0 V$ & $V_B = 0 V$

In this step, both  $I_D$  vs.  $V_D$  and output conductance -  $g_{ds}$  (even  $g'_{ds}$ ) vs.  $V_D$  characteristics are studied at once. Different effects impact both the characteristics, so the parameters related to those effects are extracted. In detail,

- **DELTA**, which is a smoothing factor for the transition between  $V_{DS}$  and  $V_{DS,sat}$ .
- **PDITS** and **PDITS D**, linked to DITS effect.
- **PCLM**, **PCLMG** and **FPROUT** linked to the CLM effect.
- **PDIBLC**, linked to the impact of DIBL effect on  $R_{out}$ .
- **PVAG**, linked to the  $V_G$  dependence on Early voltage.

#### 10.1.5 Gate Capacitance $C_{GG}$ vs. $V_G$ Analysis @ $V_{DS} \neq 0 V$ & $V_B = 0 V$

Velocity saturation (VS) and channel length modulation (CLM) effects not only affect the static behavior of the transistor but the dynamic as well. The extraction of **VSAT** and **PCLM** from  $I_D$  vs.  $V_G$  and  $I_D$  vs.  $V_D$  characteristics should be sufficient in order to capture these effects for CV operation. To verify that,  $C_{GG}$  vs.  $V_G$  characteristic for different  $V_{DS} \neq 0 V$ , from linear mode to saturation must be studied. If different values for **VSAT** and **PCLM** are necessary for accurate fitting of the CV behavior at different  $V_D$  biases, then **VSATCV** and **PCLMCV** can be used.

#### 10.1.6 Drain Current $I_D$ vs. $V_G$ Analysis @ $V_D = [V_{D,lin}, V_{D,sat}]$ & various $V_B$

In this step almost the same procedure as in Section 10.1.2 will be repeated in order to extract the parameters that are linked to the body effect. Similar to Section 10.1.2, it is also very important that during the extraction in this step both  $I_D$  and  $g_m$  are studied at once.

Linear Mode

- Focusing in *weak-inversion* region, **CDSCB**, which is linked to the  $V_B$  (or  $V_S$ ) dependence of the sub-threshold slope, is extracted. Also **K2**, which is linked to the  $V_{TH}$  shift due to vertical non-uniform doping, is extracted in the same region.

- In *strong-inversion* region, **UC**, which is linked to the  $V_B$  (or  $V_S$ ) dependence of mobility, is extracted. The parameter for  $V_B$  (or  $V_S$ ) dependence of S/D series resistances, **PRWB**, is also extracted under the same bias conditions.

Saturation

- In *strong-inversion* region, the parameter that is connected to  $V_B$  (or  $V_S$ ) dependence of the velocity saturation effect, i.e. **PSATB**, is extracted.

In order to validate that the values of the parameters, which are linked to  $V_B$  (or  $V_S$ ) dependencies, are correctly extracted, it is useful to check  $I_D$  vs.  $V_D$  and  $g_{ds}$  vs.  $V_D$  characteristics @ various  $V_G$  &  $V_B \neq 0 V$  (or  $V_S \neq 0 V$ ) and, if needed, to fine tune the values of the parameters.

### 10.1.7 Fitting Verification

When all the extraction steps of this part have been performed, the fitting of the model should be checked for all the analyses carried out up to this point. Parameters can be fine tuned for better fitting in all regions.

## 10.2 Extraction of Short Channel Effects & Length Scaling Parameters

Once the behavior of the wide/long channel device has been accurately modeled, the next step is the extraction of the parameters that are either related to short channel effects or express the different length dependencies. So at this part, devices across the entire length range of the technology, from the shortest to the longest one, are studied simultaneously. In order to avoid the impact of narrow channel effects or of the width dependencies these devices should have the same **wide** channel. The extraction that is carried out follows the same flow as in Section 10.1, but now a set of devices with constant **wide** channel but different channel lengths is used.

### 10.2.1 Gate Capacitance $C_{GG}$ vs. $V_G$ Analysis @ $V_S = 0 V$ , $V_D = 0 V$ & $V_B = 0 V$

In this step, parameters related to overlap and fringing capacitances as well as those that are linked to the length dependence of doping concentration and flat-band voltage are extracted. More specifically:

- **NDEPL1**, **NDEPLEXP1**, **NDEPL2** and **NDEPLEXP2**, which are the length scaling parameters for the doping concentration, are extracted from  $C_{GG}$  in the depletion region. If possible, it is recommended that those parameters are extracted from  $C_{GB}$  vs.  $V_G$  analysis (S and D terminals are grounded).
- Extraction of parameters related to overlap and fringing capacitances is carried out by studying the entire range of  $V_G$  bias of  $C_{GG}$  vs.  $V_G$  characteristic. These parameters are: **CGSO**, **CGDO**, **CGBO**, **CGSL**, **CGDL**, **CKAPPAS**, **CKAPPAD** and **CF**. If possible, it is recommended that **CGSO**, **CGDO**, **CGBO** and **CF** are extracted from  $C_{GD}$  vs.  $V_G$  at low  $V_B$  (when S and D terminals are connected together and B terminal is grounded), while **CGSL**, **CGDL**, **CKAPPAS** and **CKAPPAD** are extracted from  $C_{GD}$  vs.  $V_G$  at high  $V_B$  (when S, D and B terminals are connected together).
- **DLC**, which is the channel-length offset parameter for the CV model, is extracted in the strong-inversion region of  $C_{GG}$ .
- **VFBCVL** and **VFBCVLEXP**, which express the length dependence of flat-band voltage at CV, are extracted from depletion region till the onset of strong-inversion. In order to be able to use **VFBCVL** and **VFBCVLEXP** parameters, **VFBCV** must be  $\neq 0$ .

### 10.2.2 Drain Current $I_D$ vs. $V_G$ Analysis @ $V_D = [V_{D,lin}, V_{D,sat}]$ , $V_S = 0 V$ & $V_B = 0 V$

In this step, parameters related to short channel effects or to length dependencies of  $I_D$  vs.  $V_G$ , are extracted. Similar to the procedure described in Section 10.1.2, the parameters are divided in two groups, those which are extracted in *linear mode* (i.e.  $V_D \ll V_G - V_{TH}$ ) and those which are extracted in *saturation* (i.e.  $V_D \gg V_G - V_{TH}$ ). It is very important that during the extraction both  $I_D$  and  $g_m$  of all the devices are studied at once.

## Linear Mode

- Focusing in *weak-inversion* region ( $I_D$  vs.  $V_G$  characteristic when y-axis is in logarithmic scale), **NFACTORL** and **NFACTORLEXP**, which are related to the length dependence of the sub-threshold slope of  $I_D$  vs.  $V_G$ , can be extracted. Furthermore, **LINT**, which is the channel length offset parameter, is used to fit both the sub-threshold slope and the  $V_{TH}$ . For fitting the  $V_{TH}$  of the devices also **DVTP0** and **UD** can prove to be useful. **UD** should be used only for fine tuning because it mainly affects the region above threshold. It is recommended that the parameters **NDEPL1**, **NDEPLEXP1**, **NDEPL1** and **NDEPLEXP1** keep the values extracted from the  $C_{GG}$  vs.  $V_G$  analysis (Section 10.2.1). But, if the fitting of the  $V_{TH}$  across the entire length range cannot be achieved without changing the values of **NDEPL1**, **NDEPLEXP1**, **NDEPL1** and **NDEPLEXP1**, then these parameters are used for static operation (IV) and **NDEPCVL1**, **NDEPCVLEXP1**, **NDEPCVL1** and **NDEPCVLEXP1** parameters are used for dynamic operation (CV).
- In *strong-inversion* region, the parameters related to the length dependence of: i) the mobility; **U0L** and **U0LEXP**, ii) the effect of mobility reduction due to vertical field; **UAL**, **UALEXP**, **EUL** and **EULEXP** and iii) the coulomb scattering effect; **UDL** and **UDLEXP**, are extracted. Furthermore, parameters for the length dependence of S/D series resistances, namely **RDSWL** and **RDSWLEXP** (when **RDSMOD** = 0) or **RSWL**, **RSWLEXP**, **RDWL** and **RDWLEXP** (when **RDSMOD** = 1), are also extracted under the same bias conditions.

## Saturation

- In *weak-inversion* region ( $I_D$  vs.  $V_G$  characteristic when y-axis is in logarithmic scale), **CDSCDL** and **CDSCDLEXP** parameters, which are linked to the length dependence of the sub-threshold slope dependence on drain bias, are extracted. Moreover, parameters for DIBL effect, which control  $V_{TH}$  when  $V_{DS} \neq 0$ , namely **ETA0** and **DSUB**, are also extracted in the same region.
- Focusing in *strong-inversion* region, the length scaling parameters linked to the velocity saturation effect, i.e **VSATL**, **VSATLEXP**, **PSATL**, **PSATLEXP**, **PTWGL** and **PTWGLEXP**, can be extracted.

Finally, from *accumulation* to *depletion* region, in both *linear mode* and *saturation*, the parameters **AGIDLL/AGISLL**, which are related the length dependence of GIDL effect (GIDL/GISL currents), are extracted.

### 10.2.3 $I_G$ vs. $V_G$ Analysis @ various $V_D$ , $V_S = 0 V$ & $V_B = 0 V$

From  $I_G$  vs.  $V_G$  analysis, parameters related to the length dependence of gate current are extracted. These parameters are: **AIGCL**, **AIGSL**, **AIGDL** and **PIGCDL**.

### 10.2.4 $I_D$ vs. $V_D$ Analysis @ various $V_G$ , $V_S = 0 V$ & $V_B = 0 V$

In this step, both  $I_D$  vs.  $V_D$  and  $g_{ds}$  vs.  $V_D$  characteristics should be studied at once. Similar to the procedure described in Section 10.2.4 the parameters that are extracted are:

- **DELTA** and **DELTALEXP**, which are related to the length dependence of the smoothing factor for the transition between  $V_{DS}$  and  $V_{DS,sat}$ .
- **PDITSL**, linked to the length dependence of DITS effect.
- **PCLML**, **PCLMLEXP**, **FPROUTL** and **FPROUTLEXP** linked to the length dependence of CLM effect.
- **PDIBLCL** and **PDIBLCLEXP**, linked to the length dependence of the impact of DIBL effect on  $R_{out}$ .

It is very important to be mentioned here, that if the slope of  $g_{ds}$  vs.  $V_D$  characteristic at low levels of inversion is steeper than the measurements, then **ETA0** should be decreased and **DVTP1** can be used to achieve an accurate fit for the  $V_{TH}$  in *saturation*.

### 10.2.5 $C_{GG}$ vs. $V_G$ Analysis @ $V_{DS} \neq 0 V$ & $V_B = 0 V$

The extraction of the length scaling parameters of **VSAT** and **PCLM** from  $I_D$  vs.  $V_G$  and  $I_D$  vs.  $V_D$  characteristics (Steps 10.2.2 and 10.2.4) should be sufficient in order to capture VS and CLM effects for CV operation. To verify that,  $C_{GG}$  vs.  $V_G$  characteristic of all devices, for different  $V_{DS} \neq 0 V$ , from linear mode to saturation, must be studied. If different values for **VSATL**, **VSATLEXP**, **PCLML** and **PCLMLEXP** are necessary

for accurate fitting of the CV behavior across L, then **VSATCVL**, **VSATCVLEXP**, **PCLMCVL** and **PCLMCVLEXP** can be used.

### 10.2.6 $I_D$ vs. $V_G$ Analysis @ $V_D = [V_{D,lin}, V_{D,sat}]$ & various $V_B$ (or various $V_S$ )

In this step almost the same procedure as in Section 10.1.6 will be repeated in order to extract the length scaling parameters that are linked to the body effect. Similar to Section 10.1.6, it is also very important that during the extraction in this step both  $I_D$  and  $g_m$  of all devices are studied at once.

Linear Mode

- Focusing in *weak-inversion* region, **K2L** and **K2LEXP**, which are linked to the length dependence  $V_{TH}$  shift due to vertical non-uniform doping, are extracted.
- In *strong-inversion* region, **UCL** and **UCLEXP**, which are linked to the length dependence of mobility reduction with  $V_B$  (or  $V_S$ ) bias, are extracted. The parameters for the length dependence of S/D series resistances with  $V_B$  (or  $V_S$ ) bias, namely **PRWBL** and **PRWBLEXP**, are also extracted under the same bias conditions.

Saturation

- In *weak-inversion* region ( $I_D$  vs.  $V_G$  characteristic when y-axis is in logarithmic scale), the parameters related to length dependence of DIBL effect dependence on  $V_B$  (or  $V_S$ ) bias, namely **ETAB** and **ETABEXP**, are extracted.

In order to validate that the values of the length scaling parameters, which are linked to  $V_B$  (or  $V_S$ ) dependencies, are correctly extracted, it is useful to check  $I_D$  vs.  $V_D$  and  $g_{ds}$  vs.  $V_D$  characteristics @ various  $V_G$  &  $V_B \neq 0 V$  (or  $V_S \neq 0 V$ ) and, if needed, to fine tune the values of the parameters.

### 10.2.7 Fitting Verification

When all the steps for the extraction of short channel effects and length scaling parameters have been performed, the fitting of the model should be checked for all the analyses carried out in Section 10.2 and parameters can be fine tuned for better fitting.

## 10.3 Extraction of Narrow Channel Effects & Width Scaling Parameters

The next step in the parameter extraction procedure is the extraction of the parameters that are either related to narrow channel effects or express the different width dependencies. So at this part, devices across the entire width range of the technology, from the narrowest to the widest one, are studied simultaneously. In order to avoid the impact of short channel effects or of the length dependencies these devices should have the same **long** channel. The extraction that is carried out follows the same flow as in Section 10.2, but now a set of devices with constant **long** channel but different channel widths is used.

### 10.3.1 Gate Capacitance $C_{GG}$ vs. $V_G$ Analysis @ $V_S = 0 V$ , $V_D = 0 V$ & $V_B = 0 V$

In this step, parameters related to the width dependencies of the CV behavior of the device, e.g. width dependence of the doping concentration and flat-band voltage, are extracted. More specifically:

- **NDEPW** and **NDEPWEXP**, which are the width scaling parameters for the doping concentration, are extracted from  $C_{GG}$  in the depletion region. If possible, it is recommended that those parameters are extracted from  $C_{GB}$  vs.  $V_G$  analysis (S and D terminals are grounded).
- **DWC**, which is the channel-width offset parameter for the CV model, is extracted in the strong-inversion region of  $C_{GG}$ .
- **VFBCVW** and **VFBCVWEXP**, which express the width dependence of flat-band voltage at CV, are extracted along the entire  $V_G$  bias range of  $C_{GG}$  characteristic. In order to be able to use **VFBCVW** and **VFBCVWEXP** parameters, **VFBCV** must be  $\neq 0$ .

### 10.3.2 Drain Current $I_D$ vs. $V_G$ Analysis @ $V_D = [V_{D,lin}, V_{D,sat}]$ , $V_S = 0 V$ & $V_B = 0 V$

In this step, parameters related to width dependencies of  $I_D$  vs.  $V_G$ , are extracted. Similar to the procedure described in Section 10.1.2, the parameters are divided in two



groups, those which are extracted in *linear mode* (i.e.  $V_D \ll V_G - V_{TH}$ ) and those which are extracted in *saturation* (i.e.  $V_D \gg V_G - V_{TH}$ ). It is very important that during the extraction both  $I_D$  and  $g_m$  of all the devices are studied at once.

#### Linear Mode

- Focusing in *weak-inversion* region ( $I_D$  vs.  $V_G$  characteristic when y-axis is in logarithmic scale), **NFACTORW** and **NFACTORWEXP**, which are related to the width dependence of the sub-threshold slope of  $I_D$  vs.  $V_G$ , can be extracted. Furthermore, **WINT**, which is the channel width offset parameter, is used to fit both the sub-threshold slope and the  $V_{TH}$  across  $W$ . It is recommended that the parameters **NDEPW** and **NDEPWEXP** keep the values extracted from the  $C_{GG}$  vs.  $V_G$  analysis (Section 10.3.1). But, if the fitting of the  $V_{TH}$  across the entire width range cannot be achieved without changing the values of **NDEPW** and **NDEPWEXP**, then these parameters are used for static operation (IV) and **NDEPCVW** and **NDEPCVWEXP** parameters are used for dynamic operation (CV).
- In *strong-inversion* region, the parameters related to the width dependence of mobility reduction due to vertical field effect, namely **UAW**, **UAWEXP**, **EUW** and **EUWEXP**, are extracted.

#### Saturation

- Focusing in *strong-inversion* region, the width scaling parameters linked to the velocity saturation effect, i.e. **VSATW** and **VSATWEXP**, can be extracted.

Finally, from *accumulation to depletion* region, in both *linear mode* and *saturation*, the parameters **AGIDLW/AGISLW**, which are related the width dependence of GIDL effect (GIDL/GISL currents), are extracted.

In order to validate that the values of the width scaling parameters are correctly extracted, it is useful to check  $I_D$  vs.  $V_D$  and  $g_{ds}$  vs.  $V_D$  characteristics @ various  $V_G$ ,  $V_S = 0 V$  &  $V_B = 0 V$  (or  $V_S \neq 0 V$ ) and, if needed, to fine tune the values of the parameters.

### 10.3.3 Gate Current $I_G$ vs. $V_G$ Analysis @ various $V_D$ , $V_S = 0 V$ & $V_B = 0 V$

From  $I_G$  vs.  $V_G$  analysis, parameters related to the width dependence of gate current are extracted. These parameters are: **AIGCW**, **AIGSW** and **AIGDW**.

### 10.3.4 Gate Capacitance $C_{GG}$ vs. $V_G$ Analysis @ $V_{DS} \neq 0 V$ & $V_B = 0 V$

The extraction of the width scaling parameters of **VSATW** and **VSATWEXP** from  $I_D$  vs.  $V_G$  and  $I_D$  vs.  $V_D$  characteristics (Step 10.3.2) should be sufficient in order to capture VS for CV operation. To verify that,  $C_{GG}$  vs.  $V_G$  characteristic of all devices, for different  $V_{DS} \neq 0 V$ , from linear mode to saturation, must be studied. If different values for **VSATW** and **VSATWEXP** are necessary for accurate fitting of the CV behavior across W, then **VSATCVW** and **VSATCVWEXP** can be used.

### 10.3.5 Drain Current $I_D$ vs. $V_G$ Analysis @ $V_D = [V_{D,lin}, V_{D,sat}]$ & various $V_B$ (or various $V_S$ )

In this step, from *weak-inversion* region of *linear mode*, **K2W** and **K2WEXP**, which are linked to the width dependence  $V_{TH}$  shift due to vertical non-uniform doping, can be extracted. For validation purposes, it is useful to check: i)  $I_D$  vs.  $V_G$  and  $g_m$  vs.  $V_G$  characteristics in *weak* and *strong-inversion* and for both *linear mode* and *saturation*, and ii)  $I_D$  vs.  $V_D$  and  $g_{ds}$  vs.  $V_D$  characteristics @ various  $V_G$  &  $V_B \neq 0 V$  (or  $V_S \neq 0 V$ ) and, if needed, extract **K2W** and **K2WEXP** to fit both (i) and (ii).

### 10.3.6 Fitting Verification

When all the extraction steps for the width scaling have been performed, the fitting of the model should be checked for all the analyses carried out in Section 10.3 and parameters can be further tuned for better fitting.

## 10.4 Extraction of Parameters for Narrow/Short Channel Devices

The final part in the parameter extraction procedure from a geometrical point of view, is the extraction of the parameters for narrow/short channel devices. These devices have the minimum dimensions so it is more difficult to capture their behavior. Since the narrow/short channel device parameters can affect the already performed fitting across length and width, it is recommended that two different sets of devices are studied simultaneously, i.e. one set with a constant **short** channel but different channel widths

(from narrowest to widest) and one set with a constant **narrow** channel but different channel lengths (from the shortest to the longest one).

#### 10.4.1 Gate Capacitance $C_{GG}$ vs. $V_G$ Analysis @ $V_S = 0 V$ , $V_D = 0 V$ & $V_B = 0 V$

In this step, geometry dependent parameters for modeling the CV behavior of the narrow/short channel devices, are extracted. More specifically:

- **NDEPWL** and **NDEPWLEXP**, which are used to fit the doping concentration of small channel devices, are extracted from  $C_{GG}$  in the depletion region. If possible, it is recommended that those parameters are extracted from  $C_{GB}$  vs.  $V_G$  analysis (S and D terminals are grounded).
- **LWLC** and **WWLC**, which are coefficients of length/width dependencies for CV model, are extracted in the strong-inversion region of  $C_{GG}$ .
- **VFBCVWL** and **VFBCVWLEXP**, which are used to fit the flat-band voltage at CV, are extracted from depletion till the onset of strong-inversion region of  $C_{GG}$  characteristic. In order to be able to use **VFBCVWL** and **VFBCVWLEXP** parameters, **VFBCV** must be  $\neq 0$ .

#### 10.4.2 Drain Current $I_D$ vs. $V_G$ Analysis @ $V_D = [V_{D,lin}, V_{D,sat}]$ , $V_S = 0 V$ & $V_B = 0 V$

In this step, geometry dependent parameters for modeling  $I_D$  of the narrow/short channel devices, are extracted. Similar to the procedure described in Section 10.1.2, the parameters are divided in two groups, those which are extracted in *linear mode* (i.e.  $V_D \ll V_G - V_{TH}$ ) and those which are extracted in *saturation* (i.e.  $V_D \gg V_G - V_{TH}$ ). It is very important that during the extraction both  $I_D$  and  $g_m$  of all the devices are studied at once.

Linear Mode

- Focusing in *weak-inversion* region ( $I_D$  vs.  $V_G$  characteristic when y-axis is in logarithmic scale), **NFACTORWL** and **NFACTORWLEXP**, which are used to fit

the sub-threshold slope of  $I_D$  vs.  $V_G$  for small channel devices, can be extracted. It is recommended that the parameters **NDEPWL** and **NDEPWLEXP** keep the values extracted from the  $C_{GG}$  vs.  $V_G$  analysis (Section 10.4.1). But, if the fitting of the  $V_{TH}$  for both sets of devices cannot be achieved without changing the values of **NDEPWL** and **NDEPWLEXP**, then these parameters are used for static operation (IV) and **NDEPCVWL** and **NDEPCVWLEXP** parameters are used for dynamic operation (CV).

- In *strong-inversion* region, the parameters which are used to model the effect of mobility reduction due to vertical field in small channel devices, namely **UAWL**, **UAWLEXP**, **EUWL** and **EUWLEXP**, are extracted.

Saturation

- Focusing in *strong-inversion* region, the parameters which are used to model to the velocity saturation effect in small channel devices, i.e. **VSATWL** and **VSATWLEXP**, can be extracted.

In order to validate that the values of the parameters, modeling the behavior of narrow/short channel devices, are correctly extracted, it is useful to check  $I_D$  vs.  $V_D$  and  $g_{ds}$  vs.  $V_D$  characteristics @ various  $V_G$ ,  $V_S = 0$  V &  $V_B = 0$  V and, if needed, to fine tune the values of the parameters.

#### 10.4.3 $C_{GG}$ vs. $V_G$ Analysis @ $V_{DS} \neq 0$ V & $V_B = 0$ V

The extraction of the parameters, which are used to model to the velocity saturation effect in small channel devices, **VSATWL** and **VSATWLEXP**, from  $I_D$  vs.  $V_G$  and  $I_D$  vs.  $V_D$  characteristics (Step 10.4.2) should be sufficient in order to capture VS for CV operation. To verify that,  $C_{GG}$  vs.  $V_G$  characteristic of all devices, for different  $V_{DS} \neq 0$  V, from linear mode to saturation, must be studied. If different values for **VSATWL** and **VSATWLEXP** are necessary for accurate fitting of the CV behavior for both sets of devices, then **VSATCVWL** and **VSATCVWLEXP** can be used.

#### 10.4.4 Drain Current $I_D$ vs. $V_G$ Analysis @ $V_D = [V_{D,lin}, V_{D,sat}]$ & various $V_B$ (or various $V_S$ )

In this step, from *weak-inversion* region of *linear mode*, **K2WL** and **K2WLEXP**, which are linked to the  $V_{TH}$  shift due to vertical non-uniform doping in small channel

devices, can be extracted. For validation purposes, it is useful to check: i)  $I_D$  vs.  $V_G$  and  $g_m$  vs.  $V_G$  characteristics in *weak* and *strong-inversion* and for both *linear mode* and *saturation*, and ii)  $I_D$  vs.  $V_D$  and  $g_{ds}$  vs.  $V_D$  characteristics @ various  $V_G$  &  $V_B \neq 0 V$  (or  $V_S \neq 0 V$ ) and, if needed, extract **K2WL** and **K2WLEXP** to fit both (i) and (ii).

### 10.4.5 Fitting Verification

When all the steps for narrow/short channel devices have been performed, the fitting of the model should be checked for all the analyses carried out in Section 10.4 and parameters can be fine tuned for better fitting.

## 10.5 Extraction of Temperature Dependence Parameters

Up to this point of the parameter extraction procedure, the temperature dependence of the parameters has been ignored since all the parameters were extracted at **TNOM**. In this part, the parameters that are related to the impact of temperature on the behavior of devices are extracted, and for that, data across the temperature range of the technology are necessary. The behavior of devices is studied with the same geometrical sequence as the previous steps, while the temperature dependence parameters are extracted in the same regions of operation as the parameters of the corresponding physical effects.

### 10.5.1 Wide & Long Channel Devices

The first step, in the extraction of temperature dependence parameters, is to extract the behavior of a long and wide channel device @ **different T** and for different analyses. It is recommended that the same device as the one in Section 10.1 is used. In detail:

$I_D$  vs.  $V_G$  analysis @  $V_D = V_{D,lin}$ ,  $V_S = 0 V$  &  $V_B = 0 V$

- From *weak-inversion* region ( $I_D$  vs.  $V_G$  characteristic when y-axis is in logarithmic scale), the parameters **TBGASUB** and **TBGBSUB**, which control the temperature dependence of  $E_g$ , are extracted. Also, **TNFACTOR** is extracted in order to fit the sub-threshold slope of  $I_D$  in different T, while **KT1** and **KT1EXP** are extracted for fitting the  $V_{TH}$  across T.

- From *strong-inversion* region, the mobility temperature exponent, **UTE** and the temperature coefficients: i) for mobility reduction due to vertical field effect, namely **UA1** and **UD1**, ii) for coulomb scattering effect, **UCSTE** and iii) for S/D series resistances, **PRT**, are extracted.

$I_D$  vs.  $V_G$  analysis @  $V_D = V_{D,sat}$ ,  $V_S = 0 V$  &  $V_B = 0 V$

- From *strong-inversion* region, the parameters that are used to model to the temperature dependence of velocity saturation effect, i.e. **AT** and **PTWGT**, are extracted.

It is very important that in the above analyses both  $I_D$  and  $g_m$  of all the devices are studied at once. Furthermore, from *accumulation* to *depletion* region, in both *linear mode* and *saturation* of  $I_D$  vs.  $V_G$  analysis, the parameter **TGIDL**, which controls the temperature dependence of GIDL effect, is extracted.

$I_D$  vs.  $V_D$  Analysis @ various  $V_G$ ,  $V_S = 0 V$  &  $V_B = 0 V$

From  $I_D$  vs.  $V_D$  analysis in different temperatures, **TDELTA**, which is related to the temperature dependence of the smoothing factor for the transition between  $V_{DS}$  and  $V_{DS,sat}$ , is extracted.

$I_D$  vs.  $V_G$  Analysis @  $V_D = V_{D,lin}$  & various  $V_B$  (or various  $V_S$ )

- From weak-inversion region ( $I_D$  vs.  $V_G$  characteristic when y-axis is in logarithmic scale) **KT2**, which is linked to the temperature dependence of  $V_{TH}$  shift due to vertical non-uniform doping with  $V_B$ (or  $V_S$ ) bias, is extracted.
- From *strong-inversion* region, the temperature coefficient for mobility reduction with  $V_B$ (or  $V_S$ ) bias, namely **UC1**, is extracted.

For validation purposes, it is useful to check: i)  $I_D$  vs.  $V_G$  and  $g_m$  vs.  $V_G$  characteristics in *weak* and *strong-inversion* and for both *linear mode* and *saturation*, and ii)  $I_D$  vs.  $V_D$  and  $g_{ds}$  vs.  $V_D$  characteristics @ various  $V_G$  &  $V_B \neq 0 V$  (or  $V_S \neq 0 V$ ) and, if needed, extract **KT2** and **UC1** to fit both (i) and (ii).

## 10.5.2 Length Scaling of Wide Channel Devices

The following step in the extraction of temperature dependence parameters, is to study the temperatures dependences across L. For this, data @ **different T** of a set of devices with constant **wide** channel but different channel lengths are used.

$I_D$  vs.  $V_G$  analysis @  $V_D = V_{D,lin}$ ,  $V_S = 0 V$  &  $V_B = 0 V$

- From *weak-inversion* region ( $I_D$  vs.  $V_G$  characteristic when y-axis is in logarithmic scale), the parameter **KT1L** is extracted for fitting the  $V_{TH}$  across L, at different T.
- From *strong-inversion* region, the length scaling parameters for: i) mobility temperature exponent, **UTEL** and for the temperature coefficients or mobility reduction due to vertical field effect, namely **UA1L** and **UD1L**, are extracted.

$I_D$  vs.  $V_G$  analysis @  $V_D = V_{D,sat}$ ,  $V_S = 0 V$  &  $V_B = 0 V$

- From *weak-inversion* region ( $I_D$  vs.  $V_G$  characteristic when y-axis is in logarithmic scale), the parameter **TETA0**, which is related to the temperature dependence of DIBL effect and thus is controlling the  $V_{TH}$  in saturation, is extracted.
- From *strong-inversion* region, the parameters that are used to model the temperature dependence of velocity saturation effect across L, i.e. **ATL** and **PTWGTL**, are extracted.

It is very important that in the above analyses both  $I_D$  and  $g_m$  of all the devices are studied at once. For validating that the values of length scaling parameters for temperature dependence parameters are extracted correctly, it is useful to check also  $I_D$  vs.  $V_D$  and  $g_{ds}$  vs.  $V_D$  characteristics and, if needed, to fine tune their value by repeating Step 10.5.2.

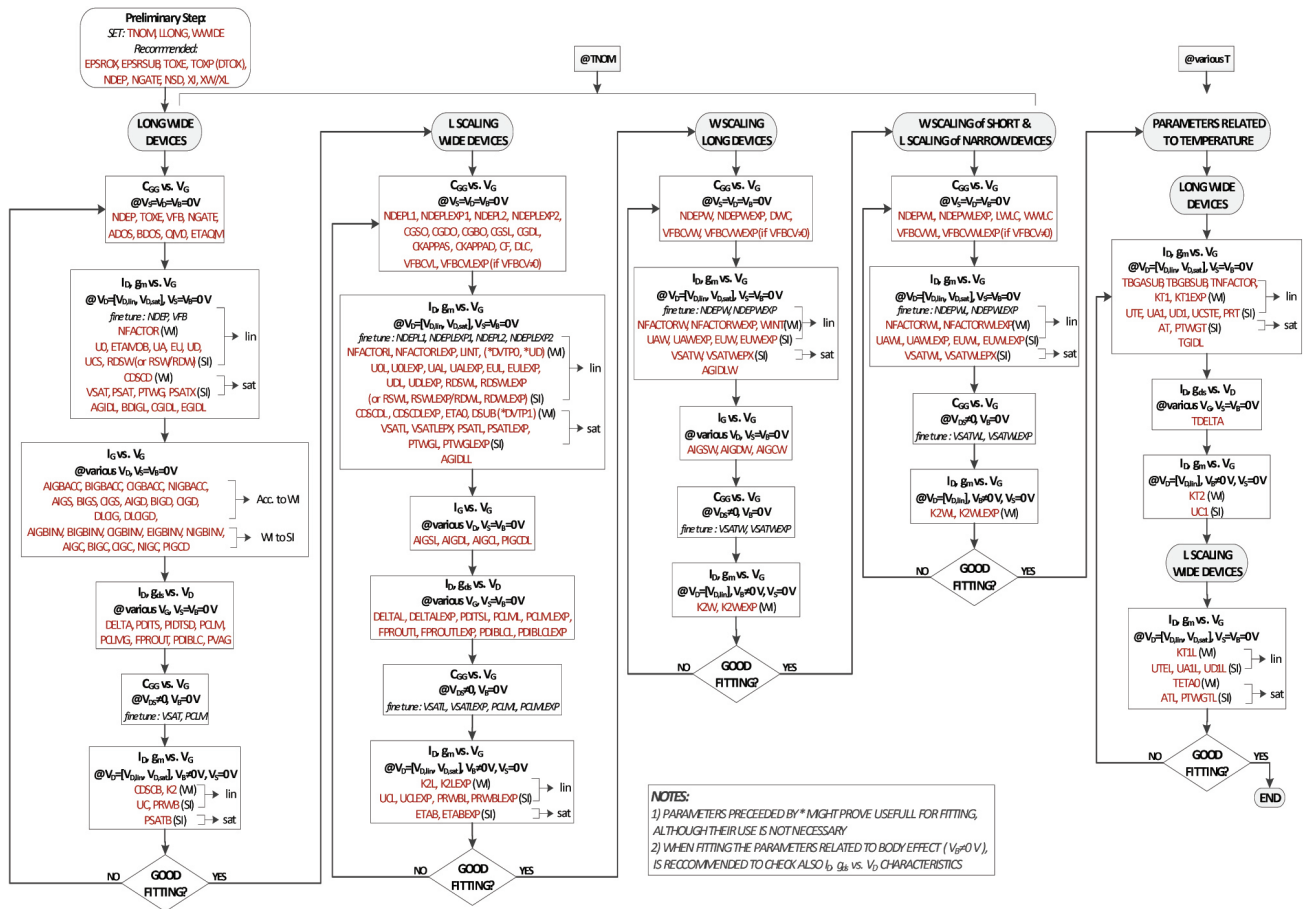


Figure 11: Parameters Extraction Procedure.



## 11 Instance Parameters

Name	Unit	Default	Min	Max	Description
L	$m$	10u	-	-	Designed Gate Length
W	$m$	10u	-	-	Designed Gate Width (per finger)
NF	-	1	1	-	Number of fingers
NRS	-	1	-	-	Number of source diffusion squares
NRD	-	1	-	-	Number of drain diffusion squares
VFBSDOFF	$V$	0	-	-	Source-Drain flat band offset
MINZ	-	0	0	1	Minimize either no. of drain or source ends
XGW	$m$	0	0	-	Distance from gate contact center to dev edge
NGCON	-	1	1	2	Number of gate contacts
RGATEMOD	-	0	0	2	Gate resistance model selector
RBODYMOD	-	0	0	2	Substrate resistance network model selector
GEOMOD	-	0	0	10	Geometry-dependent parasitic model selector-specifying how the end S/D diffusion are connected
RGEOMOD	-	0	0	8	Bias independent parasitic resistance model selector
RBPB	Ohm	50	1mV	-	Resistance between bNodePrime and bNode
RBPD	Ohm	50	1mV	-	Resistance between bNodePrime and dbNode
RBPS	Ohm	50	1mV	-	Resistance between bNodePrime and sbNode
RBDB	Ohm	50	1mV	-	Resistance between dbNode and bNode
RBSB	Ohm	50	1mV	-	Resistance between sbNode and bNode
SA	$m$	0	0	-	Distance between OD edge from Poly from one side
SB	$m$	0	0	-	Distance between OD edge from Poly from other side
SD	$m$	0	0	-	Distance between neighboring fingers
SCA	-	0	0	-	Integral of the first distribution function for scatted well dopant
SCB	-	0	0	-	Integral of second distribution function for scattered well dopant

SCC	-	0	0	-	Integral of third distribution function for scattered well dopant
SC	$m$	0	0	-	Distance to a single well edge
AS	$m^2$	0	0	-	Source to Substrate Junction Area
AD	$m^2$	0	0	-	Drain to Substrate Junction Area
PS	$m$	0	0	-	Source to Substrate Junction Perimeter
PD	$m$	0	0	-	Drain to Substrate Junction Perimeter

## 12 Model Controllers and Process Parameters

Note: binnable parameters are marked as: <sup>(b)</sup>

Name	Unit	Default	Min	Max	Description and Scaling Parameters
TYPE	-	1	-1	1	NMOS=1, PMOS=-1
CVMOD	-	0	0	1	IV-CV: Consistent:0, Different:1
GEOMOD	-	0	0	10	For description, please refer Table 1
RGEOMOD	-	0	0	8	Bias independent parasitic resistance model selector, refer Table 2
RGATEMOD	-	0	0	2	Gate resistance Model selector
ASYMMOD	-	0	0	1	Asymmetry model will be ON or OFF
MOBSCALE	-	0	0	1	Two different models for mobility.
RBODYMOD	-	0	0	2	Substrate resistance network model selector
RDSMOD	-	0	0	2	0: Bias dependent internal, independent external, 1: External RDS, 2: Internal RDS
COVMOD	-	0	0	1	Bias-independent overlap capacitance:0, Bias-dependent overlap capacitance:1
GIDLMOD	-	0	0	1	Turn off GIDL model:0, Turn-on GIDL model:1
SHMOD	-	0	0	1	Turn off Self Heating model:0, Turn-on :1
PERMOD	-	1	0	1	Whether PS/PD (when given) includes the gate-edge perimeter 1: (including the gate-edge perimeter)

					0: (not including the gate-edge perimeter)
TNOIMOD	-	0	0	1	Thermal noise model selector
FNOIMOD	-	1	0	1	Flicker noise model selector
BINUNIT	-	1	0	1	Binning unit selector
XL	$m$	0	-	-	L offset for channel length due to mask/etch effect
XW	$m$	0	-	-	W offset for channel length due to mask/etch effect
LINT <sup>(b)</sup>	$m$	0	-	-	Length reduction parameter (dopant diffusion effect)
WINT <sup>(b)</sup>	$m$	0	-	-	Width reduction parameter (dopant diffusion effect)
DLC <sup>(b)</sup>	$m$	0	-	-	Length reduction parameter for CV (dopant diffusion effect)
DWC <sup>(b)</sup>	$m$	0	-	-	Width reduction parameter for CV (dopant diffusion effect)
TOXE	$m$	3.0n	-	-	$SiO_2$ equivalent gate dielectric thickness
TOXP	$m$	=TOXE	-	-	Physical dielectric thickness
DTOX	$m$	0.0	-	-	Difference between effective dielectric thickness and physical thickness
NDEP <sup>(b)</sup>	$m^{-3}$	1e24	-	-	channel (body) doping concentration. Global Scaling Parameters - NDEPL1, NDEPLEXP1, NDEPL2, NDEPLEXP2, NDEPW, NDEPWEXP, NDEPWL, NDEPWLEXP
NSD <sup>(b)</sup>	$m^{-3}$	1e26	2e25	1e27	S/D doping concentration
EASUB	$eV$	4.05	-	-	Electron affinity of substrate
NGATE <sup>(b)</sup>	$m^{-3}$	5e25	-	-	parameter for Poly Gate doping. Set $NGATE = 0$ for metal gates
VFB <sup>(b)</sup>	$V$	-0.5	-	-	Flat band Voltage
EPSROX	-	3.9	1	-	relative dielectric constant of the gate insulator
EPSRSUB	-	11.9	1	-	relative dielectric constant of the channel material

NIOSUB	$m^{-3}$	1.1e16	-	-	intrinsic carrier concentration of channel at 300.15K
XJ <sup>(b)</sup>	$m$	1.5e-7	-	-	S/D junction depth
DMCG		0	0	-	Distance of Mid-Contact to Gate edge
DMCI		DMCG	0	-	Distance of Mid-Contact to Isolation
DMDG		0	0	-	Distance of Mid-Diffusion to Gate edge
DMCGT		0	0	-	Distance of Mid-Contact to Gate edge in Test

## 13 Basic Model Parameters

Note: binnable parameters are marked as: <sup>(b)</sup>

Name	Unit	Default	Min	Max	Description
LLONG	$m$	$10\mu m$	-	-	Length of extracted long channel device
WWIDE	$m$	$10\mu m$	-	-	Width of extracted long channel device
CIT <sup>(b)</sup>	$F/m^2$	0	-	-	Interface trap capacitance
NFACTOR <sup>(b)</sup>		0	-	-	Subthreshold Swing factor. Global Scaling Parameters - NFACTORL, NFACTORLEXP, NFACTORW, NFACTORWEXP, NFACTORWL
CDSCD <sup>(b)</sup>	$F/m^2/V$	1e-9	-	-	Drain-bias sensitivity of Subthreshold Swing. Global Scaling Parameters - CDSCDL, CDSCDLEXP
CDSCB <sup>(b)</sup>	$F/m^2/V$	1e-9	-	-	Drain-bias sensitivity of Subthreshold Swing. Global Scaling Parameters - CDSCBL, CDSCBLEXP
CDSCBR <sup>(b)</sup>	$F/m^2/V$	CDSCD	0.0	-	Reverse-mode drain-bias sensitivity. Global Scaling Parameter - CDSCDLR
CDSCDR <sup>(b)</sup>	$F/m^2/V$	1e-9	-	-	Drain-bias sensitivity of Subthreshold Swing. Global Scaling Parameters - CDSCDR, LCDSCDR
DVTP0 <sup>(b)</sup>	$m$	1e-10	-	-	Coefficient of drain-induced $V_{th}$ shift for long channel devices with pocket implant
DVTP1 <sup>(b)</sup>	$1/V$	0	-	-	Coefficient of drain-induced $V_{th}$ shift for long channel devices with pocket implant
DVTP2 <sup>(b)</sup>	$m * V$	0	-	-	Coefficient of drain-induced $V_{th}$ shift for long channel devices with pocket implant
DVTP3 <sup>(b)</sup>	-	0	-	-	Coefficient of drain-induced $V_{th}$ shift for long channel devices with pocket implant

DVTP4 <sup>(b)</sup>	1/V	0	-	-	Coefficient of drain-induced $V_{th}$ shift for long channel devices with pocket implant
DVTP5 <sup>(b)</sup>	V	0	-	-	Coefficient of drain-induced $V_{th}$ shift for long channel devices with pocket implant
PHIN <sup>(b)</sup>	V	0.045	-	-	Vertical nonuniform doping effect on surface potential
K2 <sup>(b)</sup>	V	0	-	-	Vth shift due to nonuniform vertical doping. Global Scaling Parameters - K2L, K2LEXP, K2W, K2WEXP
K1 <sup>(b)</sup>	$V^{0.5}$	0	-	-	Vth shift due to nonuniform vertical doping. Global Scaling Parameters - K1L, K1LEXP, K1W, K1WL, K1WEXP, K1WLEXP
ETA0 <sup>(b)</sup>	-	0.08	-	-	DIBL coefficient
ETA0R <sup>(b)</sup>	-	0.08	-	-	DIBL coefficient
DSUB <sup>(b)</sup>	-	0.375	> 0	-	DIBL exponent coefficient
ETAB <sup>(b)</sup>	1/V	-0.07	-	-	Body bias sensitivity to DIBL effect. Global Scaling Parameters - ETABEXP
U0 <sup>(b)</sup>	$m^2/V/s$	67e-3	-	-	Low field mobility. Global Scaling Parameters - U0L, U0LEXP
ETAMOB	-	1.0	-	-	effective field parameter
UA <sup>(b)</sup>	$(m/V)^{EU}$	0.001	> 0.0	-	Phonon / surface roughness scattering parameter. Global Scaling Parameters - UAL, UALEXP, UAW, UAWEXP, UAWL
EU <sup>(b)</sup>	-	1.5	> 0.0	-	Phonon / surface roughness scattering parameter. Global Scaling Parameters - EUL, EULEXP, EUW, EUWEXP, EUWL
UD <sup>(b)</sup>	-	0.001	> 0.0	-	Columbic scattering parameter. Global Scaling Parameters - UDL, UDLEXP
UCS <sup>(b)</sup>	-	2.0	1	2	Columbic scattering parameter.

UC <sup>(b)</sup>	$(m/V)^{EU}/V$	0.0	-	-	Body-bias sensitivity on mobility. Global Scaling Parameters - UCL, UCLEXP
VSAT <sup>(b)</sup>	$m/s$	1e6	-	-	Saturation velocity. Global Scaling Parameters - VSATL, VSALEXP, VSATW, VSATWEXP
VSATR <sup>(b)</sup>	$m/s$	1e6	-	-	Saturation velocity. Global Scaling Parameters - VSATR, LVSATR, WVSATR, PVSATR
DELTA <sup>(b)</sup>	-	0.125	> 0	0.5	Smoothing factor for Vds to Vdsat. Global Scaling Parameters - DELTAL, DELTALEXP
AVDSX	-	0.16	> 0	-	Smoothing factor for Vdsx calculation.
PSAT <sup>(b)</sup>	-	1.0	0.25	1.0	Velocity saturation exponent. Global Scaling Parameters - PSATL, PSATLEXP
PTWG <sup>(b)</sup>	-	0	-	-	Correction factor for velocity saturation in forward mode. Global Scaling Parameters - PTWGL, PTWGLEXP
PTWGR <sup>(b)</sup>	-	PTWG	-	-	Correction factor for velocity saturation in reverse mode. Global Scaling Parameters - PTWGLR, PTWGLEXPR
A1 <sup>(b)</sup>	$V^{-2}$	0.0	-	-	Non-saturation effect parameter in strong inversion region.
A2 <sup>(b)</sup>	$V^{-1}$	0.0	-	-	Non-saturation effect parameter in moderate inversion region.
PSATX	-	1	0.25	4	Fine tuning of PTWG effect
PSATB <sup>(b)</sup>	$1/V$	0	-	-	Velocity saturation exponent for non-zero $V_{bs}$
PCLM <sup>(b)</sup>	-	0.00	-	-	Channel Length Modulation (CLM) parameter. Global Scaling Parameters - PCLML, PCLMLEXP
PCLMG	$V$	0	-	-	Gate bias dependent parameter for channel Length Modulation (CLM)

PSCBE1 <sup>(b)</sup>	$V/m$	4.24e8	–	-	Substrate current body-effect coefficient
PSCBE2 <sup>(b)</sup>	$m/V$	1.0e-8	–	-	Substrate current body-effect coefficient
PDITS <sup>(b)</sup>	$1/V$	0	–	-	Drain-induced Vth shift
PDITSL	$1/m$	0	–	-	L dependence of Drain-induced Vth shift
PDITSD <sup>(b)</sup>	$1/V$	0	–	-	VDS dependence of Drain-induced Vth shift
RSWMIN <sup>(b)</sup>	$\Omega m^{WR}$	0.0	0.0	-	source extension resistance per unit width at high $V_{gs}$
RSW <sup>(b)</sup>	$\Omega m^{WR}$	10	0.0	-	Zero bias source extension resistance per unit width. Global Scaling Parameters - RSWL, RSWLEXP
RDWMIN <sup>(b)</sup>	$\Omega m^{WR}$	0.0	0.0	-	Drain extension resistance per unit width at high $V_{gs}$
RDW <sup>(b)</sup>	$\Omega m^{WR}$	10	0.0	-	Zero bias drain extension resistance per unit width. Global Scaling Parameters - RDWL, RDWLEXP
RDSWMIN <sup>(b)</sup>	$\Omega m^{WR}$	0.0	0.0	-	LDD resistance per unit width at high $V_{gs}$ for $RDSMOD = 0$
RDSW <sup>(b)</sup>	$\Omega m^{WR}$	10	0.0	-	Zero bias LDD resistance per unit width for $RDSMOD=0$ . Global Scaling Parameters - RDSWL, RDSWLEXP
PRWG <sup>(b)</sup>	$V^{-1}$	1	0	-	gate bias dependence of S/D extension resistance
PRWB <sup>(b)</sup>	$V^{-1}$	0	0	-	body bias dependence of S/D extension resistance. Global Scaling Parameters - PRWBL, PRWBLEXP
WR <sup>(b)</sup>	-	1.0	-	-	W dependence parameter of S/D extension resistance
RSH	$\Omega$	0	0	-	Sheet resistance



PDIBLC <sup>(b)</sup>	-	2e-4	0	-	DIBL effect on Rout. Global Scaling Parameters - PDIBLCL, PDIBLCLEXP
PDIBLCB <sup>(b)</sup>	1/V	0	0	-	Body-bias sensitivity on DIBL
PVAG <sup>(b)</sup>	-	1	-	-	V <sub>gs</sub> dependence on early voltage
FPROUT <sup>(b)</sup>	V/m <sup>0.5</sup>	0	0	-	g <sub>ds</sub> degradation factor due to pocket implant. Global Scaling Parameters - FPROUTL, FPROUTLEXP
AGIDL <sup>(b)</sup>	V/m	0	-	-	Pre-exponential coefficient for GIDL. Global Scaling Parameters - AGIDLL, AGIDLW
BGIDL <sup>(b)</sup>	V/m	2.3e-9	-	-	exponential coefficient for GIDL
CGIDL <sup>(b)</sup>	V/m	0.5	-	-	exponential coefficient for GIDL
EGIDL <sup>(b)</sup>	V	0.8	-	-	band bending parameter for GIDL
AGISL <sup>(b)</sup>	V/m	0	-	-	Pre-exponential coefficient for GISL (AGISL < 0 means GISL parameters will same as GIDL parameters). Global Scaling Parameters - AGISLL, AGISLW
BGISL <sup>(b)</sup>	V/m	2.3e-9	-	-	exponential coefficient for GISL
CGISL <sup>(b)</sup>	V/m	0.5	-	-	exponential coefficient for GISL
EGISL <sup>(b)</sup>	V	0.8	-	-	band bending parameter for GISL
ALPHA0 <sup>(b)</sup>	m/V	0.0	-	-	First parameter of impact ionization current. Global Scaling Parameters - ALPHA0L, ALPHA0LEXP
BETA0 <sup>(b)</sup>	1/V	0.0	-	-	First V <sub>ds</sub> dependent parameter of impact ionization current
AIGC <sup>(b)</sup>	(Fs <sup>2</sup> /g) <sup>0.5</sup> /m	1.36e-2 (NMOS) and 9.8e-3 (PMOS)	-	-	Parameter for I <sub>gcs</sub> and I <sub>gcd</sub> . Global Scaling Parameters - AIGCL, AIGCW

BIGC <sup>(b)</sup>	$(Fs^2/g)^{0.5}/m/V$	1.71e-3 (NMOS) and 7.59e-4 (PMOS)	-	-	Parameter for $I_{gcs}$ and $I_{gcd}$
CIGC <sup>(b)</sup>	$1/V$	0.075 (NMOS) and 0.03 (PMOS)	-	-	Parameter for $I_{gcs}$ and $I_{gcd}$
AIGS <sup>(b)</sup>	$(Fs^2/g)^{0.5}/m$	1.36e-2 (NMOS) and 9.8e-3 (PMOS)	-	-	Parameter for $I_{gs}$ . Global Scaling Parameters - AIGSL, AIGSW
BIGS <sup>(b)</sup>	$(Fs^2/g)^{0.5}/m/V$	1.71e-3 (NMOS) and 7.59e-4 (PMOS)	-	-	Parameter for $I_{gs}$
CIGS <sup>(b)</sup>	$1/V$	0.075 (NMOS) and 0.03 (PMOS)	-	-	Parameter for $I_{gs}$
DLCIG <sup>(b)</sup>	$m$	LINT	-	-	Source/Drain overlap length for $I_{gs}$
AIGD <sup>(b)</sup>	$(Fs^2/g)^{0.5}m$	1.36e-2 (NMOS) and 9.8e-3 (PMOS)	-	-	Parameter for $I_{gd}$ . Global Scaling Parameters - AIGDL, AIGDW
BIGD <sup>(b)</sup>	$(Fs^2/g)^{0.5}m/V$	1.71e-3 (NMOS) and 7.59e-4 (PMOS)	-	-	Parameter for $I_{gd}$

CIGD <sup>(b)</sup>	1/V	0.075 (NMOS) and 0.03 (PMOS)	-	-	Parameter for $I_{gd}$
DLCIGD <sup>(b)</sup>	$m$	DLCIG	-	-	Source/Drain overlap length for $I_{gd}$
POXEDGE <sup>(b)</sup>	-	1.0	-	-	Factor for the gate oxide thickness in source/drain overlap regions
PIGCD <sup>(b)</sup>	-	1.0	-	-	$V_{ds}$ dependence of $I_{gcs}$ and $I_{gcd}$ . Global Scaling Parameters - PIGCDL, PIGCDLEXP
NTOX <sup>(b)</sup>	-	1.0	-	-	Exponent for the gate oxide ratio
TOXREF	m	3.0e-9	-	-	Nominal gate oxide thickness for gate dielectric tunneling current model only
VFBSDOFF <sup>(b)</sup>	V	0.0	-	-	Flatband Voltage Offset Parameter
NDEPCV <sup>(b)</sup>	$m^{-3}$	NDEP	-	-	channel (body) doping concentration for CV. Global Scaling Parameters - NDEPCVL1, NDEPCVLEXP1, NDEPCVL2, NDEPCVLEXP2, NDEPCVW, NDEPCVWEXP, NDEPCVWL, NDEPCVWLEXP
VFBCV <sup>(b)</sup>	V	VFB	-	-	channel (body) doping concentration for CV. Global Scaling Parameters - VFBCVL, VFBCVLEXP, VFBCVW, VFBCVWEXP, VFBCVWL, VFBCVWLEXP
VSATCV <sup>(b)</sup>	$m/s$	VSAT	-	-	Saturation velocity for CV. Global Scaling Parameters - VSATCVL, VSATCVLEXP, VSATCVW, VSATCVWEXP
PCLMCV <sup>(b)</sup>	-	PCLM	-	-	Channel Length Modulation (CLM) parameter for CV. Global Scaling Parameters - PCLMCVL, PCLMCVLEXP
CF <sup>(b)</sup>	$F/m$	0	0.0	-	Outer fringe cap
CFRCOEFF <sup>(b)</sup>	$F/m$	1	1	-	Outer fringe cap coefficient

CGSO	$F/m$	calculated	0.0	-	Non LDD region source-gate overlap capacitance per unit channel width
CGDO	$F/m$	calculated	0.0	-	Non LDD region drain-gate overlap capacitance per unit channel width
CGSL <sup>(b)</sup>	$F/m$	0	0.0	-	Overlap capacitance between gate and lightly-doped source region
CGDL <sup>(b)</sup>	$F/m$	0	0.0	-	Overlap capacitance between gate and lightly-doped drain region
CKAPPAS <sup>(b)</sup>	$V$	0.6	0.02	-	Coefficient of bias-dependent overlap capacitance for the source side
CKAPPAD <sup>(b)</sup>	$V$	0.6	0.02	-	Coefficient of bias-dependent overlap capacitance for the drain side
CGBO	$F/m$	0	0.0	-	Gate-substrate overlap capacitance per unit channel length
ADOS	-	0	0	-	Quantum mechanical effect prefactor cum switch in inversion
BDOS	-	1.0	0	-	Charge centroid parameter - slope of CV curve under QME in inversion
K0 <sup>(b)</sup>	-	0	0	-	Non-saturation effect parameter for strong inversion region
M0 <sup>(b)</sup>	-	1.0	0	-	Offset of non-saturation effect parameter for strong inversion region
QM0	-	1e-3	> 0.0	-	Charge centroid parameter - starting point for QME in inversion
ETAQM	-	0.0	0	-	Bulk charge coefficient for charge centroid in inversion
DLBIN	-	0.0	-	-	Length reduction parameter for binning
DWBIN	-	0.0	-	-	Width reduction parameter for binning
LMLT	-	1.0	> 0.0	-	Length shrinking factor
WMLT	-	1.0	> 0.0	-	Width shrinking factor

## 14 Both model and instance parameters

Name	Unit	Default	Min	Max	Description
DTEMP	$K$	0.0	-	-	Offset of Device Temperature
MULU0	$m^2/V/s$	1.0	-	-	Multiplication factor for low field mobility
DELVTO	$V$	0	-	-	Zero bias threshold voltage variation
IDSOMULT	-	1.0	-	-	Variability in drain current for miscellaneous reasons

## 15 High-Speed/RF Model Parameters

Name	Description	Default
XRCRG1 (b)	Parameter for distributed channel-resistance effect for both intrinsic-input resistance and charge-deficit NQS models(Warning message issued if binned $XRCRG1 \leq 0.0$ ) distributed channel-resistance effect for both intrinsic-input resistance and charge-deficit NQS models(Warning message issued if binned $XRCRG1 \leq 0.0$ )	12.0
XRCRG2 (b)	Parameter to account for the excess channel diffusion resistance for both intrinsic input resistance and charge-deficit NQS models	1.0
RBPB (Also an instance parameter)	Resistance connected between bNodePrime and bNode	50.0ohm
RBPD (Also an instance parameter)	Resistance connected between bNodePrime and dbNode (If less than 1.0e-3ohm, reset to 1.0e-3ohm )	50.0ohm
RBPS (Also an instance parameter)	Resistance connected between bNodePrime and sbNode (If less than 1.0e-3ohm, reset to 1.0e-3ohm)	50.0ohm
RBDB (Also an instance parameter)	Resistance connected between dbNode and bNode	50.0ohm

RBSB (Also an instance parameter)	Resistance connected between sbNode and bNode	50.0ohm
GBMIN	Conductance in parallel with each of the five substrate resistances to avoid potential numerical instability due to unreasonably too large a substrate resistance (Warning message issued if less than 1.0e-20 mho )	1.0e-12mho
RBPS0	Scaling prefactor for RBPS	50 Ohms
RBPSL	Length Scaling parameter for RBPS	0.0
RBPSW	Width Scaling parameter for RBPS	0.0
RBPSNF	Number of fingers Scaling parameter for RBPS	0.0
RBPD0	Scaling prefactor for RBPD	50 Ohms
RPDL	Length Scaling parameter for RBPD	0.0
RPDW	Width Scaling parameter for RBPD	0.0
RPDNF	Number of fingers Scaling parameter for RBPD	0.0
RPBX0	Scaling prefactor for RPBX	100 Ohms
RPBXL	Length Scaling parameter for RPBX	0.0
RPBXW	Width Scaling parameter for RPBX	0.0
RPBXNF	Number of fingers Scaling parameter for RPBX	0.0
RPBY0	Scaling prefactor for RPBYP	100 Ohms
RPBYL	Length Scaling parameter for RPBYP	0.0
RPBYW	Width Scaling parameter for RPBYP	0.0
RPBYNF	Number of fingers Scaling parameter for RPBYP	0.0
RBSBX0	Scaling prefactor for RBSBX	100 Ohms
RBSBY0	Scaling prefactor for RBSBY	100 Ohms
RBDBX0	Scaling prefactor for RBDBX	100 Ohms
RDBY0	Scaling prefactor for RDBY	100 Ohms
RBSDBXL	Length Scaling parameter for RBSBX and RBDBX	0.0

RBSDBXW	Width Scaling parameter for RBSBX and RBDBX	0.0
RBSDBXNF	Number of fingers Scaling parameter for RBSBX and RBDBX	0.0
RBSDBYL	Length Scaling parameter for RSBY and RBDBY	0.0
RBSDBYW	Width Scaling parameter for RSBY and RBDBY	0.0
RBSDBYNF	Number of fingers Scaling parameter for RSBY and RBDBY	0.0

## 16 Flicker and Thermal Noise Model Parameters

Parameter Name	Description	Default Value
NOIA	Flicker noise parameter A	$6.25e41(eV)^{-1}s^{1-EF}m^{-3}$ for NMOS; $6.188e40(eV)^{-1}s^{1-EF}m^{-3}$ for PMOS
NOIB	Flicker noise parameter B	$3.125e26(eV)^{-1}s^{1-EF}m^{-1}$ for NMOS; $1.5e25(eV)^{-1}s^{1-EF}m^{-1}$ for PMOS
NOIC	Flicker noise parameter C	$8.75(eV)^{-1}s^{1-EF}m$
NOIA2	Flicker noise parameter A for Halo model	$6.25e41(eV)^{-1}s^{1-EF}m^{-3}$ for NMOS; $6.188e40(eV)^{-1}s^{1-EF}m^{-3}$ for PMOS
NOIB2	Flicker noise parameter B for Halo model	$3.125e26(eV)^{-1}s^{1-EF}m^{-1}$ for NMOS; $1.5e25(eV)^{-1}s^{1-EF}m^{-1}$ for PMOS
NOIC2	Flicker noise parameter C for Halo model	$8.75(eV)^{-1}s^{1-EF}m$
EM	Saturation field	4.1e7V/m
AF	Flicker noise exponent	1.0
EF	Flicker noise frequency exponent	1.0
KF	Flicker noise coefficient	$0.0^{A2-EF}s^{1-EF}$
LINTNOI	Length Reduction Parameter Offset	0.0 m
NTNOI	Noise factor for short-channel devices for TNOIMOD=0 only	1.0
TNOIA	Coefficient of channel-length dependence of total channel thermal noise	1.5
TNOIB	Channel-length dependence parameter for channel thermal noise partitioning	3.5
TNOIC	Length dependent parameter for Correlation Coefficient	0
RNOIA	Thermal Noise Coefficient	0.577
RNOIB	Thermal Noise Coefficient	0.5164



RNOIC	Correlation Coefficient parameter	0.395
RNOIK	Exponential coeff. for enhanced correlated thermal noise	0.0
TNOIK	Empirical parameter for Leff trend of Sid at low Ids	0.0
TNOIK2	Empirical parameter for sensitivity of RNOIK	0.1

## 17 Layout-Dependent Parasitic Model Parameters

Parameter Name	Description	Default Value
DMCG	Distance from S/D contact center to the gate edge	0.0m
DMCI	Distance from S/D contact center to the isolation edge in the channel-length direction	DMCG
DMDG	Same as DMCG but for merged device only	0.0m
DMCGT	DMCG of test structures	0.0m
NF (instance parameter only)	Number of device fingers (Fatal error if less than one )	1
DWJ	Offset of the S/D junction width	DWC (in CVmodel)
MIN (instance parameter only)	Whether to minimize the number of drain or source diffusions for even-number fingered device	0 (minimize the drain diffusion number)
XGW(Also an instance parameter)	Distance from the gate contact to the channel edge	0.0m
XGL	Offset of the gate length due to variations in patterning	0.0m
XL	Channel length offset due to mask/ etch effect	0.0m
XW	Channel width offset due to mask/etch effect	0.0m
NGCON(Also an instance parameter)	Number of gate contacts (Fatal error if less than one; if not equal to 1 or 2, warning message issued and reset to 1 )	1

## 18 Asymmetric Source/Drain Junction Diode Model Parameters

Parameter Name (separate for source and drain side as indicated in the names)	Description	Default Value
IJTHSREV IJTHDREV	Limiting current in reverse bias region	IJTHSREV = 0.1A, IJTHDREV = IJTHSREV
IJTHSFWD IJTHDFWD	Limiting current in forward bias region	IJTHSFWD = 0.1A, IJTHDFWD = IJTHSFWD
XJBVS XJBVD	Fitting parameter for diode breakdown	XJBVS = 1.0, XJBVD = XJBVS
BVS BVD	Breakdown voltage (If not positive, reset to 10.0V )	BVS = 10.0V, BVD = BVS
JSS JSD	Bottom junction reverse saturation current density	JSS= 1.0e-4A/m <sup>2</sup> , JSD = JSS
JSWS JSWD	Isolation-edge sidewall reverse saturation current density	JSWS = 0.0A/m, JSWD = JSWS
JSWGS JSWGD	Gate-edge sidewall reverse saturation current density	JSWGS = 0.0A/m, JSWGD = JSWGS
JTSS JTSD	Bottom trap-assisted saturation current density	JTSS = 0.0A/m JTSD = JTSS
JTSSWS JTSSWD	STI sidewall trap-assisted saturation current density	JTSSWS = 0.0A/m <sup>2</sup> JTSSWD = JTSSWS
JTSSWGS JTSSWGD	Gate-edge sidewall trap-assisted saturation current density	JTSSWGS = 0.0A/m JTSSWGD = JTSSWGS
JTWEFF	Trap-assistant tunneling current density width dependence	0.0
NJTS NJTSD	Non-ideality factor for JTSS and JTSD	NJTS = 20.0 NJTSD = NJTS

NJTSSW NJTSSWD	Non-ideality factor for JTSSWS and JTSSWD	NJTSSW = 20.0 NJTSSWD = NJTSSW
NJTSSWG NJTSSWGD	Non-ideality factor for JTSSWGS and JTSSWGD	NJTSSWG = 20.0 NJTSSWGD = NJTSSWG
XTSS, XTSD	Power dependence of JTSS, JTSD on temperature	XTSS = 0.02 XTSD = 0.02
XTSSWS, XTSSWD	Power dependence of JTSSWS, JTSSWD on temperature	XTSSWS = 0.02 XTSSWD = 0.02
XTSSWGS, XTSSWGD	Power dependence of JTSSWGS, JTSSWGD on temperature	XTSSWGS = 0.02 XTSSWGD = 0.02
VTSS VTSD	Bottom trap-assisted voltage dependent parameter	VTSS = 10V VTSD = VTSS
VTSSWS VTSSWD	STI sidewall trap-assisted voltage dependent parameter	VTSSWS = 10V VTSSWD = VTSSWS
VTSSWGS VTSSWGD	Gate-edge sidewall trap-assisted voltage dependent parameter	VTSSWGS = 10V VTSSWGD = VTSSWGS
TNJTS TNJTSD	Temperature coefficient for NJTS and NJTSD	TNJTS = 0.0 TNJTSD = TNJTS
TNJTSSW TNJTSSWD	Temperature coefficient for NJTSSW and NJTSSWD	TNJTSSW = 0.0 TNJTSSWD = TNJTSSW
TNJTSSWG TNJTSSWGD	Temperature coefficient for NJTSSWG and NJTSSWGD	TNJTSSWG = 0.0 TNJTSSWGD = TNJTSSWG
CJS CJD	Bottom junction capacitance per unit area at zero bias	CJS = 5.0e-4 F/m <sup>2</sup> CJD = CJS
MJS MJD	Bottom junction capacitance grading coefficient	MJS = 0.5 MJD = MJS
MJSWS MJSWD	Isolation-edge sidewall junction capacitance grading coefficient	MJSWS = 0.33 MJSWD = MJSWS
CJSWS CJSWD	Isolation-edge sidewall junction capacitance per unit area	CJSWS = 5.0e-10 F/m CJSWD = CJSWS
CJSWGS CJSWGD	Gate-edge sidewall junction capacitance per unit length	CJSWGS = CJSWS CJSWGD = CJSWS

MJSWGS MJSWGD	Gate-edge sidewall junction capacitance grading coefficient	MJSWGS =MJSWS MJSWGD =MJSWS
PBS	Source-side bulk junction built-in potential	1.0V
PBD	Drain-side bulk junction built-in potential	PBD=PBS
PBSWS    PB- SWD	Isolation-edge sidewall junction built-in potential	PBSWS =1.0V PBSWD =PBSWS
PBSWGS    PB- SWGD	Gate-edge sidewall junction built-in potential	PBSWGS =PBSWS PB- SWGD =PBSWS

## 19 Temperature Dependence and Self Heating Parameters

Parameter Name	Description	Default Value
TNOM	Temperature at which parameters are extracted	27 <sup>0</sup> C
DTEMP	Variability handle for temperature	0
UTE (b)	Mobility temperature exponent	-1.5
UCSTE(b)	Temperature coefficient of coulombic mobility	-4.775e-3
TDELTA	Temperature coefficient for DELTA	0.0
TGIDL (b)	Temperature coefficient for GIDL/GISL	0.0
IIT (b)	Temperature coefficient for BETA0	0.0
KT1 (b)	Temperature coefficient for threshold voltage	-0.11V
KT1EXP	Temperature exponent for threshold voltage	1.0
KT1L (b)	Channel length dependence of the temperature coefficient for threshold voltage	0.0Vm
KT2(b)	Body-bias coefficient of Vth temperature effect	0.022
UA1 (b)	Temperature coefficient for UA	1.0e-9m/V
UC1 (b)	Temperature coefficient for UC	0.0561/K for MOBMOD=1; 0.056e-91/K for MOBMOD=0 and 2
UD1 (b)	Temperature coefficient for UD	0.0(1/m) <sup>2</sup>
AT (b)	Temperature coefficient for saturation velocity	3.3e4m/s
PTWGT	Temperature coefficient for PTWG	0.0K
PRT (b)	Temperature coefficient for Rds	0.0
NJS, NJD	Emission coefficients of junction for source and drain junctions, respectively	NJS=1.0; NJD=NJS
XTIS, XTID	Junction current temperature exponents for source and drain junctions, respectively	XTIS=3.0; XTID=XTIS
TPB	Temperature coefficient of PB	0.0V/K
TPBSW	Temperature coefficient of PBSW	0.0V/K

TPBSWG	Temperature coefficient of PBSWG	0.0V/K
TCJ	Temperature coefficient of CJ	0.0K-1
TCJSW	Temperature coefficient of CJSW	0.0K-1
TCJSWG	Temperature coefficient of CJSWG	0.0K-1
TVFBSDOFF	Temperature coefficient of VFBSDOFF	0.0K-1
TNFACTOR(b)	Temperature coefficient of NFACTOR	0.0
TETA0	Temperature coefficient of ETA0	0.0
RTH0	Thermal resistance for self-heating calculation	$0.0K * m/W$
CTH0	Thermal capacitance for self-heating calculation	$1.0E-5W * s/m/K$
WTH0	Width-dependence coefficient for self heating calculation	$0.0m$

## 20 Stress Effect Model Parameters

Parameter Name	Description	Default Value
SA (Instance Parameter)	Distance between OD edge to Poly from one side (If not given or( $\leq 0$ ), stress effect will be turned off)	0.0m
SAEDGE	SA parameter for EDGEFET	SA
SB (Instance Parameter)	Distance between OD edge to Poly from other side (If not given or( $\leq 0$ ), stress effect will be turned off)	0.0m
SBEDGE	SB parameter for EDGEFET	SB
SD (Instance Parameter)	Distance between neighbouring fingers (For $NF > 1$ :If not given or( $\leq 0$ ), stress effect will be turned off)	0.0m
SAref	Reference distance between OD and edge to poly of one side ( $> 0.0$ )	1E-06[m]
SBref	Reference distance between OD and edge to poly of the other side ( $> 0.0$ )	1E-06[m]
WLOD	Width parameter for stress effect	0.0[m]
KU0	Mobility degradation/enhancement coefficient for stress effect	0.0[m]
KVSAT	Saturation velocity degradation/ enhancement parameter for stress effect ( $1 \leq kvsat \leq 1$ )	0.0[m]
TKU0	Temperature coefficient of KU0	0.0
LKU0	Length dependence of ku0	0.0
WKU0	Width dependence of ku0	0.0
PKU0	Cross-term dependence of ku0	0.0
LLODKU0	Length parameter for u0 stress effect ( $> 0$ )	0.0
WLODKU0	Width parameter for u0 stress effect ( $> 0$ )	0.0
KVTH0	Threshold shift parameter for stress effect	0.0[Vm]
KVTH0EDGE	KVTH0 parameter for EDGEFET	KVTH0[Vm]
LKVTH0	Length dependence of kvth0	0.0
WKVTH0	Width dependence of kvth0	0.0
PKVTH0	Cross-term dependence of kvth0	0.0



LLODVTH	Length parameter for Vth stress effect (>0)	0.0
WLODVTH	Width parameter for Vth stress effect (>0)	0.0
STK2	K2 shift factor related to Vth0 change	0.0[m]
STK2EDGE	STK2E parameter for EDGEFET	STK2[m]
LODK2	K2 shift modification factor for stress effect (>0)	0.0
STETA0	eta0 shift factor related to Vth0 change	0.0[m]
STETA0EDGE	STETA0 parameter for EDGEFET	STETA0[m]
LODETA0	eta0 shift modification factor for stress effect (>0)	1.0

## 21 Well-Proximity Effect Parameters

Parameter Name	Description	Default Value
SCA (Instance Parameter)	Integral of the first distribution function for scattered well dopant (If not given , calculated)	0.0
SCB (Instance Parameter)	Integral of the second distribution function for scattered well dopant (If not given , calculated)	0.0
SCC (Instance Parameter)	Integral of the third distribution function for scattered well dopant (If not given , calculated)	0.0
SC (Instance Parameter)	Distance to a single well edge (If not given or $\leq 0.0$ , turn off WPE)	0.0[m]
WEB	Coefficient for SCB ( $>0.0$ )	0.0
WEC	Coefficient for SCC ( $>0.0$ )	0.0
KVTH0WE(b)	Threshold shift factor for well proximity effect	0.0
K2WE (b)	K2 shift factor for well proximity effect	0.0
KU0WE (b)	Mobility degradation factor for well proximity effect	0.0
SCREF	Reference distance to calculate SCA, SCB and SCC ( $<0$ )	1e-6[m]

## 22 Parameters for Edge FET and Sub-Surface Leakage Current

Note: binnable parameters are marked as: <sup>(b)</sup>

Name	Unit	Default	Min	Max	Description
EDGEFET		1	-	-	Edge FET model Flag: 0: Disable 1: Enable
WEDGE	$m$	$10e^{-9}$	$1e^{-9}$	-	Edge FET Width
DGAMMA		0	-	-	Different in body-bias coefficient between Edge-FET and Main-FET
DGAMMAL		0	-	-	L dependence parameter for DGAMMA
DGAMMALEXP		1.0	-	-	Exponent of L dependence parameter for DGAMMA
DVTEDGE		0.0	-	-	Vth shift for Edge FET
NFACTOREDGE <sup>(b)</sup>		NFACTOR	-	-	NFACTOR for Edge FET
CITEDGE <sup>(b)</sup>	$F/m^2$	CIT	-	-	CIT for Edge FET
CDSCDEGE <sup>(b)</sup>	$F/m^2/V$	CDSCD	-	-	CDSCD for edge FET
CDSCBEDGE <sup>(b)</sup>	$F/m^2/V$	CDSCB	-	-	CDSCB for edge FET
ETA0EDGE <sup>(b)</sup>	-	ETA0	-	-	DIBL parameter for edge FET
ETABEDGE <sup>(b)</sup>	$1/V$	ETAB	-	-	ETAB for edge FET
K2EDGE	$V$	K2	-	-	Vth shift due to body bias
KT1EDGE <sup>(b)</sup>	$V$	KT1	-	-	Temperature dependence parameter of threshold voltage for edge FET
KT1LEDGE <sup>(b)</sup>	$V * m$	KT1L	-	-	Temperature dependence parameter of threshold voltage for edge FET
KT2EDGE <sup>(b)</sup>	-	KT2	-	-	Temperature dependence parameter of threshold voltage for edge FET
KT1EXPEDGE	-	KT1EXP	-	-	Temperature dependence parameter of threshold voltage for edge device
TNFACTOREDGE <sup>(b)</sup>		TNFACTOR	-	-	Temperature dependence parameter of sub-threshold slope factor for edge
TETA0EDGE	-	TETA0	-	-	Temperature dependence parameter of DIBL parameter for edge FET

DVT0EDGE	-	2.2	-	-	First coefficient of SCE effect on Vth for Edge FET
DVT1EDGE	-	0.53	-	-	Second coefficient of SCE effect on Vth for Edge FET
DVT2EDGE	$1/V$	0.0	-	-	Body-bias coefficient for SCE effect for Edge FET
SSLMOD		1	-	-	Sub-Surface Leakage Drain Current, 0: Turn off 1: Turn on
SSL0	$A/m$	400	-	-	
SSL1	$1/m$	3.36E8	-	-	
SSL2	-	0.185	-	-	
SSL3	$V$	0.3	-	-	
SSL4	$1/V$	1.4	-	-	
SSLEXP1		0.490	-	-	
SSLEXP2		1.42	-	-	

## 23 Parameter equivalence between BSIM-BULK & BSIM4

The equivalent parameters are the closest match between two models. There values may be different in two models.

Region	BSIM6 Parameter Name	BSIM4 Parameter Name	Comment
Core Parameters	GEOMOD RGEOMOD RDSMOD COVMOD L W XL XW LINT WINT DLC DWC TOXE TOXP NF NDEP  NGATE VFB, VFBCV	GEOMOD RGEOMOD RDSMOD COVMOD L W XL XW LINT WINT DLC DWC TOXE TOXP NF NDEP VTH0/VTHO NGATE VFB, VFBCV	or
Material properties	EASUB  NI0SUB EPSRSUB EPSROX	-  - - -	Corresponds  to BSIM4 mtrlmod=1
Threshold Voltage	NDEPL1, NDEPLEXP1, NDEPL2, NDEPLEXP2	DVT0, DVT1, DVT2, LPE0	Length scaling

	NDEPW, NDEP- WEXP, NDEPWL, NDEPWLEXP K2W DVTP0, DVTP1, DVTP2, DVTP3, DVTP4, DVTP5 PHIN ETA0 ETAB DSUB K2 K2L, L2LEXP	DVT0W, DVT1W, DVT2W, K3, W0  K3B same as BSIM4  PHIN ETA0 ETAB DSUB K2 K1, LPEB	Width and Narrow-short Scaling
Subthreshold Swing	CIT  NFACTOR CDSCD CDSCB NFACTOR	CIT  CDSC CDSCD CDSCB NFACTOR	
Drain Saturation Voltage	VSAT, DELTA	VSAT, DELTA	
Mobility Model	U0  ETAMOB  U0L U0LEXP UA EU UD UCS UC	U0  -  UP LPA UA EU UD UCS UC	BSIM6 uses MOBMOD=3 from BSIM4 default value of 1 corresponds to BSIM4
Channel Length Modulation and DITS	PCLM	PCLM	

	PCLMG PSCBE1 PSCBE2 PDITS PDITSL PDITSD		PCLMG PSCBE1 PSCBE2 PDITS PDITSL PDITSD	
Velocity Saturation	VSAT  PTWG PSAT PSATX PSATB		VSAT  - - - -	
Rs, Rd parameter	XJ  VFBSDOFF NRS/NRD MINZ NSD RSH PRWG PRWB WR RDSWMIN RSWMIN RDWMIN RDSW RSW RDW DMCG DMCI DMDG DMCGT		XJ  VFBSDOFF NRS/NRD MINZ NSD RSH PRWG PRWB WR RDSWMIN RSWMIN RDWMIN RDSW RSW RDW DMCG DMCI DMDG DMCGT	BSIM6 uses RDSMOD=1 from BSIM4
Impact Ionization	ALPHA0, ALPHA0L, ALPHA0LEXP BETA0	AL- AL-	ALPHA0, ALPHA1  BETA0	

GIDL/GISL	AGIDL BGIDL CGIDL EGIDL AGISL BGISL CGISL EGISL	AGIDL BGIDL CGIDL EGIDL AGISL BGISL CGISL EGISL	
C-V Model	CF CFRCOEFF  CFI CGSO CGDO CGBO CGSL CGDL CKAPPAS CKAPPAD ADOS, BDOS, QM0, ETAQM	CF -  - CGSO CGDO CGBO CGSL CGDL CKAPPAS CKAPPAD ADOS, BDOS	Taken from BSIMSOI



## 24 Appendix A : Smoothing Function

### 24.1 Polynomial Smoothing

The polynomial smoothing is used for a smooth transition between boundaries, maintaining exact values at all the corner points. Consider the function

$$f(x) = x \quad \text{if } x > \frac{\Delta x}{2} \quad (24.1)$$

$$= k \quad \text{if } x < \frac{-\Delta x}{2} \quad (24.2)$$

where  $k$  is some constant. The function is undefined for the region  $-\frac{\Delta x}{2} < x < \frac{\Delta x}{2}$ . If this region is approximated by a polynomial function, the complete function and even derivatives can be made continuous. Now consider the more generalized case

$$f(x) = x \quad \text{if } x > x_1 \quad (24.3)$$

$$= k \quad \text{if } x < x_2 \quad (24.4)$$

To express (24.4) in the form of (24.2),  $x$  is linearly transformed into  $z$ . Defining

$$x_0 = \frac{x_1 + x_2}{2} \quad (24.5)$$

$$\Delta x = x_1 - x_2 \quad (24.6)$$

then the boundary points becomes

$$x_1 = x_0 + \frac{\Delta x}{2} \quad (24.7)$$

$$x_2 = x_0 - \frac{\Delta x}{2} \quad (24.8)$$

Let  $z = \frac{x-x_0}{\Delta x}$ . Thus the above boundary points in  $z$  domain becomes,

$$z_1 = \frac{x_1 - x_0}{\Delta x} = \frac{1}{2} \quad (24.9)$$

$$z_2 = \frac{x_2 - x_0}{\Delta x} = -\frac{1}{2} \quad (24.10)$$

so that the function becomes

$$f(z) = z.\Delta x - x_0 \quad \text{if } z > \frac{1}{2} \quad (24.11)$$

$$= k \quad \text{if } z < -\frac{1}{2} \quad (24.12)$$

the region  $-\frac{1}{2} \leq z \leq \frac{1}{2}$  is modeled by the polynomial function whose order depends on the number of boundary conditions. For example, to have continuous derivatives upto third order, we need seventh order polynomial as there are 8 boundary conditions.

$$f(z) = a.z^7 + b.z^6 + c.z^5 + d.z^4 + e.z^3 + f.z^2 + g.z + 1 \quad (24.13)$$

Then boundary conditions can be applied to derivatives to determine the polynomial coefficients. For the case of continuous third order derivatives, we found that

$$f(x) = x_0 + \Delta x. \left[ \frac{5}{64} + \frac{z}{2} + z^2. \left[ \frac{15}{16} - z^2. \left( \frac{5}{4} - z^2 \right) \right] \right] \quad (24.14)$$

while for continuous second order derivative

$$f(x) = x_0 + \Delta x. \left[ \frac{3}{32} + \frac{z}{2} + z^2. \left[ \frac{3}{4} - z^2. \left( \frac{3}{4} - \frac{z^2}{2} \right) \right] \right] \quad (24.15)$$

with  $z = \frac{x-x_0}{\Delta x}$ . Figure 12 illustrate the concept of polynomial smoothing.

**An Example :** Let the function be given as

$$f(x) = x \quad \text{if } x > -90 \quad (24.16)$$

$$= -100 \quad \text{if } x < -110 \quad (24.17)$$

with the condition that third derivative to exist. From (24.6)

$$x_0 = -100 \quad (24.18)$$

$$\Delta x = 20 \quad (24.19)$$

$$z = \frac{x + 100}{20} \quad (24.20)$$

and function becomes,

$$f(z) = 20.z + 100 \quad \text{if } z > \frac{1}{2} \quad (24.21)$$

$$= -100 \quad \text{if } z < -\frac{1}{2} \quad (24.22)$$

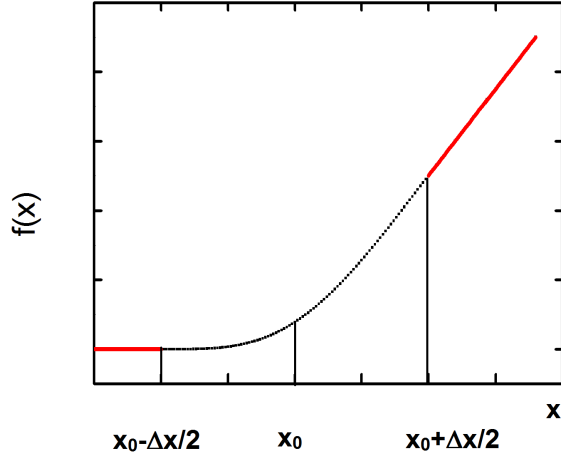


Figure 12: Illustration of Polynomial Smoothing

Boundary Conditions

$$f\left(\frac{1}{2}\right) = -90, f\left(-\frac{1}{2}\right) = -100 \quad (24.23)$$

$$f'\left(\frac{1}{2}\right) = 20, f'\left(-\frac{1}{2}\right) = 0 \quad (24.24)$$

$$f''\left(\frac{1}{2}\right) = 0, f''\left(-\frac{1}{2}\right) = 0 \quad (24.25)$$

$$f'''\left(\frac{1}{2}\right) = 0, f'''\left(-\frac{1}{2}\right) = 0 \quad (24.26)$$

We have 8 boundary conditions. So let

$$f(z) = a.z^7 + b.z^6 + c.z^5 + d.z^4 + e.z^3 + f.z^2 + g.z + 1 \quad (24.27)$$

Now we have 8 equations and 8 unknowns and hence all the coefficients can be derived. By substituting (24.23-24.26) in (24.27) we get

$$a = 0, b = 20, c = 0 \quad (24.28)$$

$$d = -25, e = 0, f = \frac{75}{4} \quad (24.29)$$

$$g = 10, h = -\frac{6300}{64} \quad (24.29)$$

Thus

$$f(z) = 20.z^6 - 25.z^4 + \frac{75}{4}.z^2 + 10.z - \frac{6300}{64} \quad (24.30)$$

Figure:13 shows the above function. As can be seen that due to polynomial nature, the

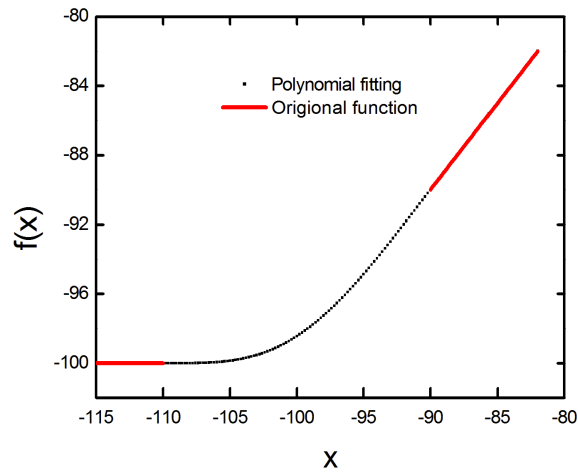


Figure 13: Polynomial Smoothing Function

approximated function undergoes smooth transitions around the boundary points.

## References

- [1] Y. S. Chauhan, S. Venugopalan, M.-A. Chalkiadaki, M. Karim, H. Agarwal, S. Khandelwal, N. Paydavosi, J. Duarte, C. Enz, A. Niknejad, and C. Hu, “BSIM6: Analog and RF Compact Model for Bulk MOSFET,” *IEEE Trans. Electron Devices*, vol. 61, no. 2, pp. 234–244, 2014.
- [2] Y. Tsvividis, *Operation and Modeling of the MOS Transistor 2nd ed.* Oxford, 1999.
- [3] Y. S. Chauhan, M. A. Karim, S. Venugopalan, S. Khandelwal, P. Thakur, N. Paydavosi, A. Sachid, A. B. and Niknejad, and C. Hu, “BSIM6: Symmetric Bulk MOSFET Model,” *Workshop on Compact Modeling, Santa Clara, USA*, June 2012.
- [4] J.-M. Sallese, M. Bucher, F. Krummenacher, and P. Fazan, “Inversion charge linearization in mosfet modeling and rigorous derivation of the ekv compact model,” *Solid-State Electronics*, vol. 47, no. 4, pp. 677–683, April 2003.
- [5] F. Pregaldiny, F. Krummenacher, B. Diagne, F. Pecheux, J.-M. Sallese, and C. Lallement, “Explicit modeling of the double-gate mosfet with vhdl-ams,” *International Journal of Numerical Modelling: Electronic Networks, Devices and Fields*, vol. 19, no. 3, pp. 239–256, May 2006.
- [6] *BSIM4 user manual*. [Online]. Available: <http://www-device.eecs.berkeley.edu/bsim/>
- [7] C. C. Hu, *Modern Semiconductor Devices for Integrated Circuits*. Pearson Education, 2010.
- [8] *MOS Model 11 manual*. [Online]. Available: <http://www.nxp.com/models/simkit/mos-models/model-11.html>
- [9] H. Agarwal, C. Gupta, P. Kushwaha, C. Yadav, J. P. Duarte, S. Khandelwal, C. Hu, and Y. S. Chauhan, “Analytical Modeling and Experimental Validation of Threshold Voltage in BSIM6 MOSFET Model,” *IEEE Journal of the Electron Devices Society*, vol. 3, no. 3, pp. 240–243, 2015.
- [10] S. Khandelwal and H. Agarwal and J. P. Duarte and K. Chan and S. Dey and Y. S. Chauhan and C. Hu, “Modeling STI Edge Parasitic Current for Accurate Circuit Simulations,” *IEEE Transactions on Computer-Aided Design of Integrated Circuits and Systems*, vol. 34, no. 8, pp. 1291–1294, 2015.

- [11] Y. K. Lin, S. Khandelwal, A. Medury, H. Agarwal, H. C. Chang, Y. S. Chauhan, and C. Hu, "Modeling of Sub-surface Leakage Current in Low  $V_{th}$  Short Channel MOSFET at Accumulation Bias," *appearin in IEEE Transactions on Electron Devices*, 2016.
- [12] K. K. Hung, P. Ko, and Y. C. Cheng, "A physics-based mosfet noise model for circuit simulator," *IEEE Transaction on Electron Devices*, vol. 37, no. 5, pp. 1323–1333, 1990.
- [13] H. Agarwal, S. Khandelwal, S. Dey, C. Hu, and Y. S. Chauhan, "Analytical modeling of flicker noise in halo implanted mosfets," *IEEE Journal of the Electron Devices Society*, vol. 3, no. 4, pp. 355–360, July 2015.
- [14] H. Agarwal, C. Gupta, S. Khandelwal, C. Hu, S. Dey, K. Chan, and Y. S. Chauhan, "Analysis and modeling of low frequency noise in presence of doping non-uniformity in mosfets," in *International Conference on Emerging Electronics (ICEE)*. IEEE, 2016.
- [15] A. J. Scholten, R. Langevelde, L. F. Tiemeijer, and D. B. M. Klaassen, "Compact modeling of noise in cmos," in *CICC*, 2006.
- [16] H. Agarwal, S. Venugopalan, M.-A. Chalkiadaki, N. Paydavosi, J. P. Duarte, S. Agnihotri, C. Yadav, P. Kushwaha, Y. S. Chauhan, C. C. Enz, A. Niknejad, and C. Hu, "Recent enhancements in BSIM6 bulk MOSFET model," in *IEEE Simulation of Semiconductor Processes and Devices*, 2013.
- [17] R. A. Bianchi, G. Bouche, and O. Roux-ditBuisson, "Accurate modeling of trench isolation induced mechanical stress effect on mosfet electrical performance," in *2007 Symposium on VLSI Technology*, 2007.
- [18] T. Hook, J. Brown, P. Cottrell, E. Adler, D. Hoyniak, J. Johnson, and R. Mann, "Lateral ion implant straggle and mask proximity effect," *IEEE Transaction on Electron Devices*, vol. 50, no. 9, pp. 1946–1951, 2003.
- [19] *Compact Model Council*. [Online]. Available: <http://www.geia.org/index.asp?bid=597>

## 25 Acknowledgements

We deeply appreciate the feedback we received from (in alphabetical order):

Shantanu Agnihotri(IIT Kanpur)

Maria Anna Chalkiadaki(EPFL)

Kaiman Chan (TI)

Brian Chen (Accelicon)

Sergey Cherepko (ADI)

Geoffrey Coram (ADI)

Krishnanshu Dandu (TI)

Anupam Dutta (IBM)

Christian Enz (EPFL)

Keith Green (TI)

Andre Juge (ST)

Tracey Krakowski (TI)

Francois Krummenacher (EPFL)

Pragya Kushwaha (IIT Kanpur)

Waikit Lee (TSMC)

Samuel Mertens (Agilent)

Saurabh Sirohi (IBM)

Jing Wang (IBM)

Joddy Wang (Synopsys)

Wenli Wang (Cadence)

Josef Watts (IBM)

Richard Williams (IBM)

Weimin Wu (TI)

Jane Xi (Synopsys)

Jushan Xie (Cadence)

Chandan Yadav(IIT Kanpur)

Fang Yu (Synopsys)  
Fulong Zaho (Cadence)

**Manual created: June 29, 2017**